Electronic Supplementary Material (ESI) for Chemical Communications.


# Supporting information

## Development of Anthrazoline Photocatalyst for Promoting Amination and Amidation Reactions via Photoredox/Nickel Dual Catalysis

Table of Contents

# General Information

*Reagents and solvents*

In general, all compounds were commercially available (Sigma Aldrich/Merck, Alfa Aesar，Energy chemical and Bidepharm) and used as received unless otherwise stated. *N*,*N*-dimethylformamide was d alcohol was purchased from Sigma Aldrich and saturated with $N_2$ and dried over 4 Å sieves before use. Solvents for extractions and columns such as dichloromethane, methanol, n-hexane and ethyl acetate were technical grade. Deuterated solvents were purchased from Cambridge Stable Isotopes and used as received.

***Experimental techniques***

Unless otherwise stated, all reaction work-ups were carried out in air. The term 'under reduced pressure' refers to use of a rotary evaporator, and '*in vacuo*' indicates use of a high vacuum pump attached to a Schlenk line. Flash chromatography was carried out using silica gel (200-300 mesh). The photocatalysis experiments were performed using two blue LED light (12 W).

***Characterization***

All $^{1}H$ and $^{13}C\{^{1}H\}$ spectra were recorded on a Bruker 400 or 500 MHz ($^{1}H$) spectrometer. $^{1}H$ and $^{13}C\{^{1}H\}$ NMR chemical shifts were referenced internally using the residual solvent resonance ($CDCl_3$: $\delta$H = 7.26 ppm, $\delta$C = 77.00 ppm). Unless otherwise stated, spectra were recorded at 298 K, and chemical shifts (δ), are quoted in parts per million (ppm). Multiplicity is abbreviated as: s (singlet); d (doublet); t (triplet); q (quartet); m (multiplet) and br (broad).

UV-vis absorption measurements were carried out in spectrophotometric grade solvent on a Cary 3500 UV-Vis spectrophotometer from Agilent Technologies. Emission spectra and the absolute quantum yield were carried out on Horiba FluoroMax Plus spectrofluorometer. The quantum yield was measured once for each sample, with an estimated instrumental error of ± 5%. Emission lifetimes were acquired on an Edinburgh FLS980 spectrophotometer.

Cyclic voltammetry (CV) measurements were a CHI760E instrument. CV experiments of the small molecules were conducted on a 0.5 mM solution in degassed DMF containing 0.05 M TBAPF6 as supporting electrolyte. A typical three-electrode cell was used having a polished glassy carbon (with 4 mm diameter) electrode as the working electrode, a Pt-wire as the counter electrode, and Ag/AgCl as the reference electrode.

# Experimental procedures

**Synthesis of 4,6-diphenyl-1,9-anthrazolines (1a-1d)**.

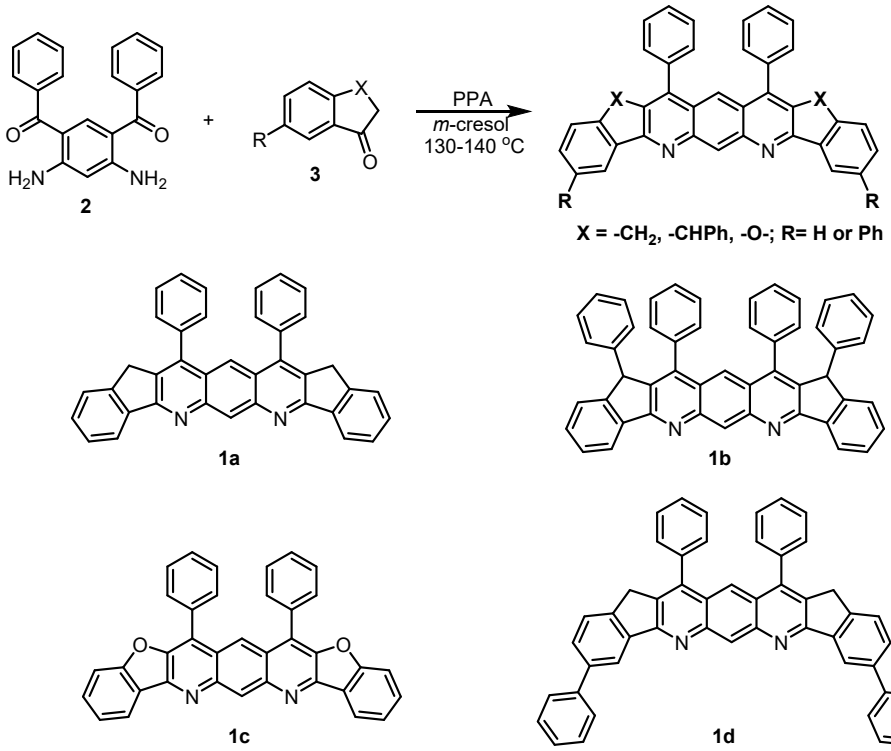


**2** **3** **1a** **1b** **1c** **1d**

**Scheme S1**. Synthetic route of anthrazolines.

*General procedures:*

A mixture of 4,6-dibenzoyl-1,3-phenylenediamine (0.5 mmol), benzofuran- 3(2*H*)-one (1.1 mmol), polyphosphoric acid (PPA) (1.0 g), and *m*-cresol (5 mL) was heated to 130-140 °C for 24 hours. The reaction mixture was then poured into 1.0 M potassium hydroxide solution and stirred for 3 hours. The precipitate was collected by filtration and washed with hot water. The crude product was purified by column chromatography (silica gel, $CH_2Cl_2$/MeOH = 20:1) to afford the pure product. Samples were prepared in $CDCl_3$ by adding one drop of trifluoroacetice acid (TFA) for NMR analyses.

**13,15-Diphenyl-12,16-dihydroindeno[1,2-b] indeno[2',1':5,6]pyrido[3,2-g]quinoline (1a)**.

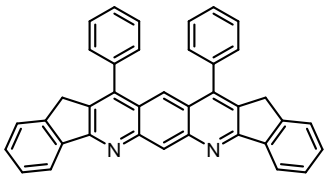

Yellow solid 183 mg was obtained, yield 72 %. $^1$H NMR (400 MHz, $CDCl_3$) $\delta$ 9.60 (s, 1H), 8.65 (d, $J$ = 7.6 Hz, 2H), 8.52 (s, 1H), 7.84 (t, $J$ = 7.6 Hz, 2H), 7.75-7.67(m, 4H), 7.59-7.56 (m, 6H), 7.40-7.44 (m, 4H), 4.17 (s, 4H). $^{13}$C NMR (100 MHz, $CDCl_3$ and TFA) $\delta$ 154.0, 150.2, 137.6, 137.3, 135.8, 131.8, 131.3, 131.2, 130.3, 129.9, 129.5, 128.8, 126.6, 125.8, 125.5, 111.2, 34.8. Elemental analysis calcd. (%) for $C_{38}H_{24}N_2$: C, 89.74; H, 4.76; N, 5.51, found C, 89.54; H, 4.78; N, 5.31. HRMS (ESI) calcd. for $C_{38}H_{24}N_2^+$ $[M+H]^+$ = 509.2012, found 509.2013.

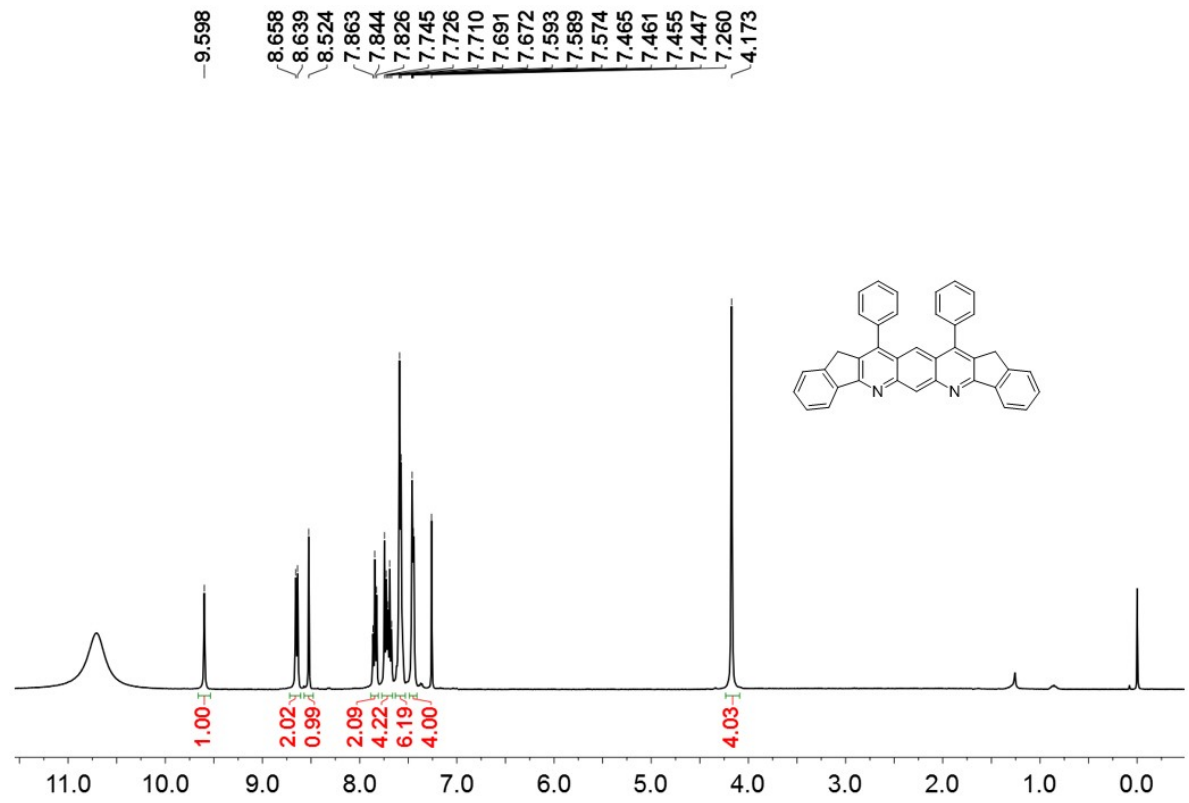


**Fig. S1** $^{1}$H NMR of photocatalyst **1a**.

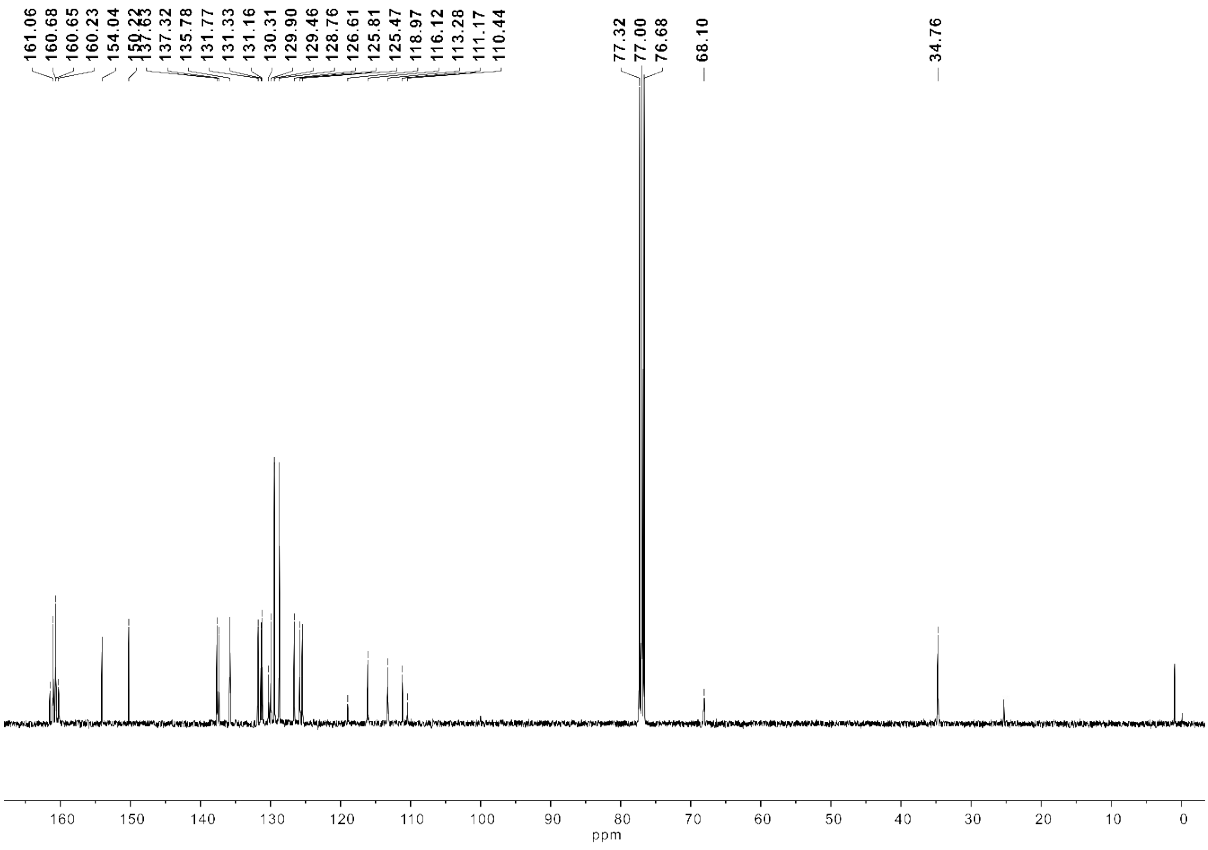


**Fig. S2** $^{13}$C NMR of photocatalyst **1a**.

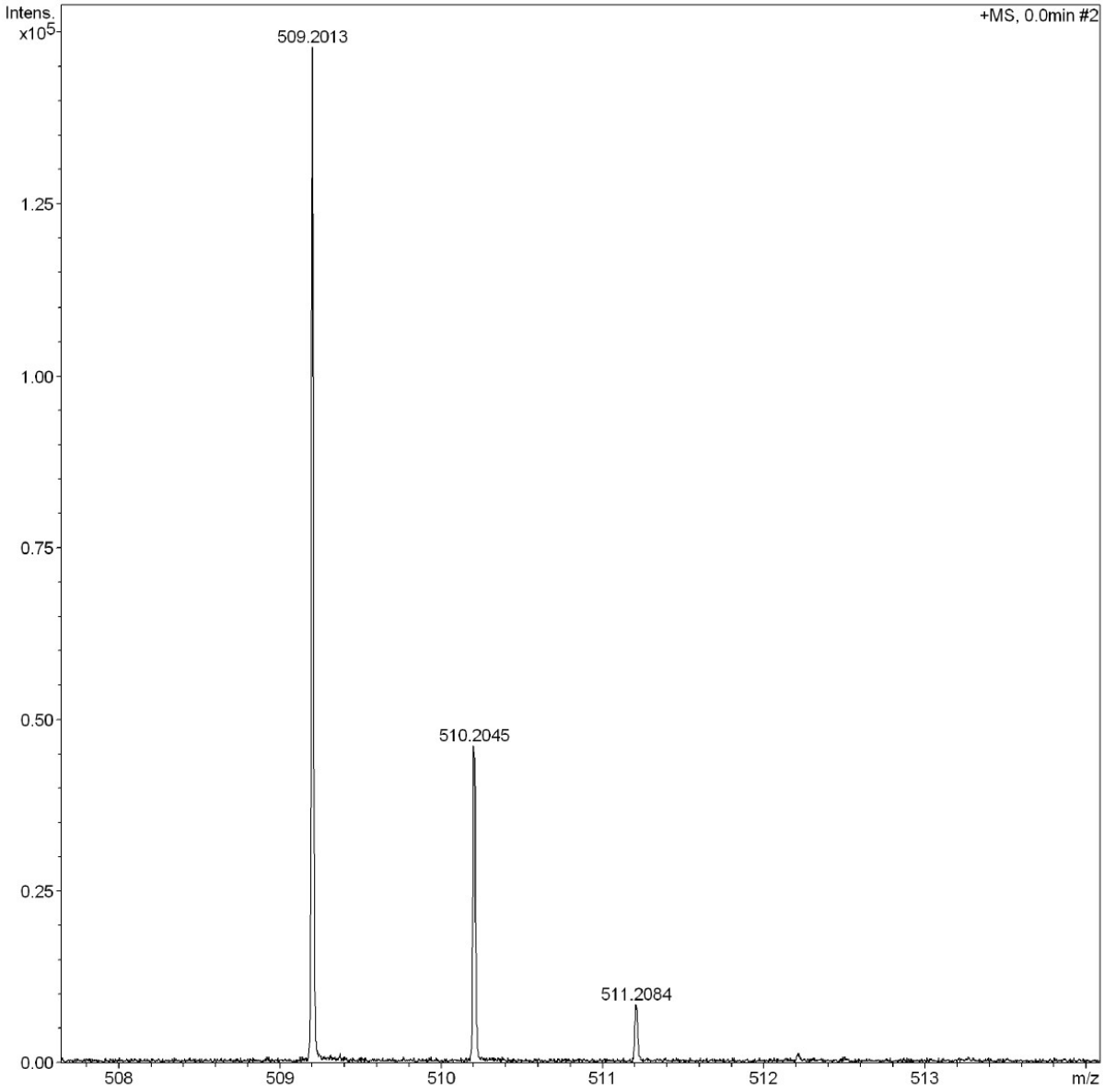


**Fig. S3** HRMS of photocatalyst **1a**

**12,13,15,16-Tetraphenyl-12,16-dihydroindeno[1,2-b]indeno[2',1':5,6]pyrido[3,2-g]quinoline (1b)**.

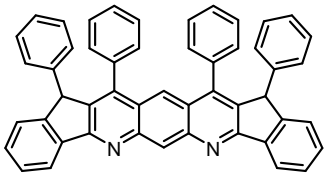

Yellow solid 261 mg was obtained, yield 79%, diastereomer ratio: 54:46. $^{1}$H NMR (400 MHz, $CDCl_3$) $\delta$ 9.64 (s, 1H), 8.70 (d, $J$ = 8.0 Hz, 2H), 8.12 (s, 1H, major), 8.04 (s, 1H, major), 7.97-7.70 (m, 4H), 7.49-7.30 (m, 8H), 7.08-6.85 (m, 8H), 6.52 (t, $J$ = 7.2 Hz, 1H), 6.43 (d, $J$ = 7.6 Hz, 1H), 6.29 (d, $J$ = 7.6 Hz, 1H), 5.41 (s, 1H), 5.37 (s, 1H). $^{13}$C NMR (100 MHz, $CDCl_3$ and TFA) $\delta$ 155.2, 155.1, 154.7, 154.6, 140.6, 140.5, 138.2, 137.7, 136.0, 135.8, 131.4, 130.7, 130.5, 130.3, 130.1, 129.8, 129.7, 129.4, 129.1, 129.0, 128.9, 128.7, 128.3, 128.2, 128.1, 128.0, 127.9, 127.0, 126.6, 126.4, 126.0, 111.8, 52.2. Elemental analysis calcd. (%) for $C_{50}H_{32}N_2$: C, 90.88; H, 4.88; N, 4.24, found C, 90.73; H, 4.92; N, 4.47. HRMS (ESI) calcd. for $C_{50}H_{32}N_2^+$ $[M+H]^+$ = 661.2638, found 661.2634.

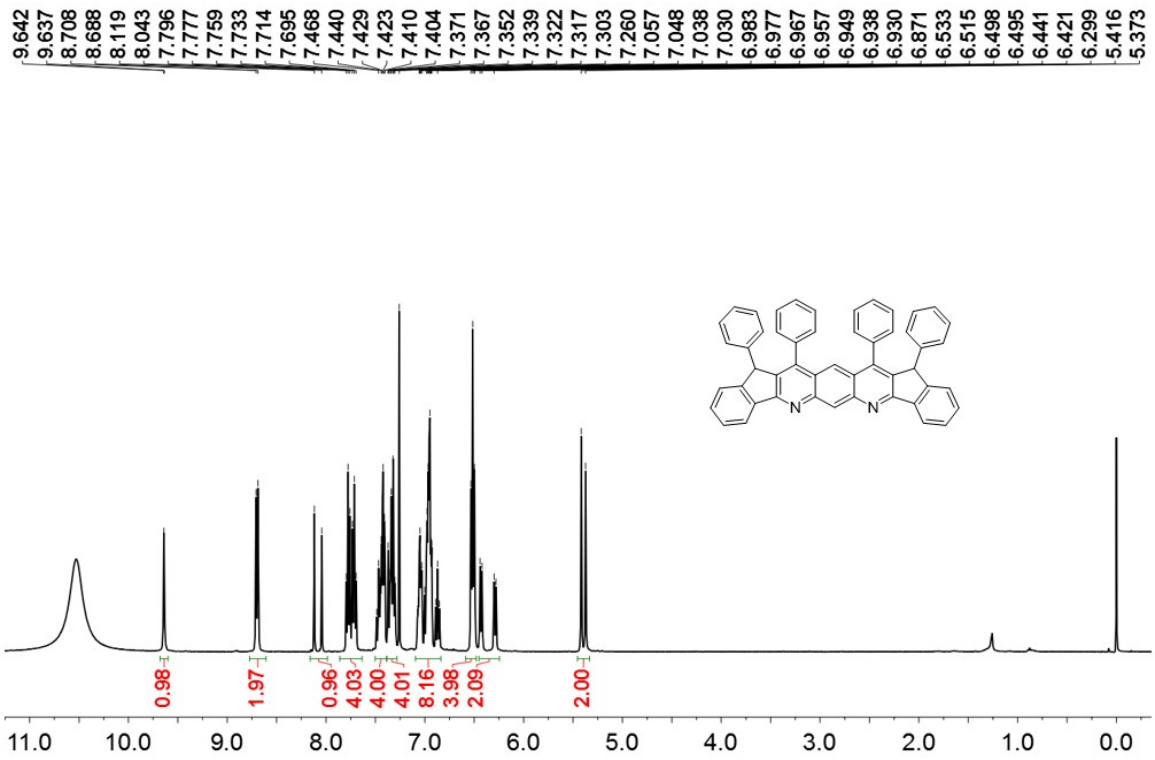


**Fig. S4** $^{1}$H NMR of photocatalyst **1b**

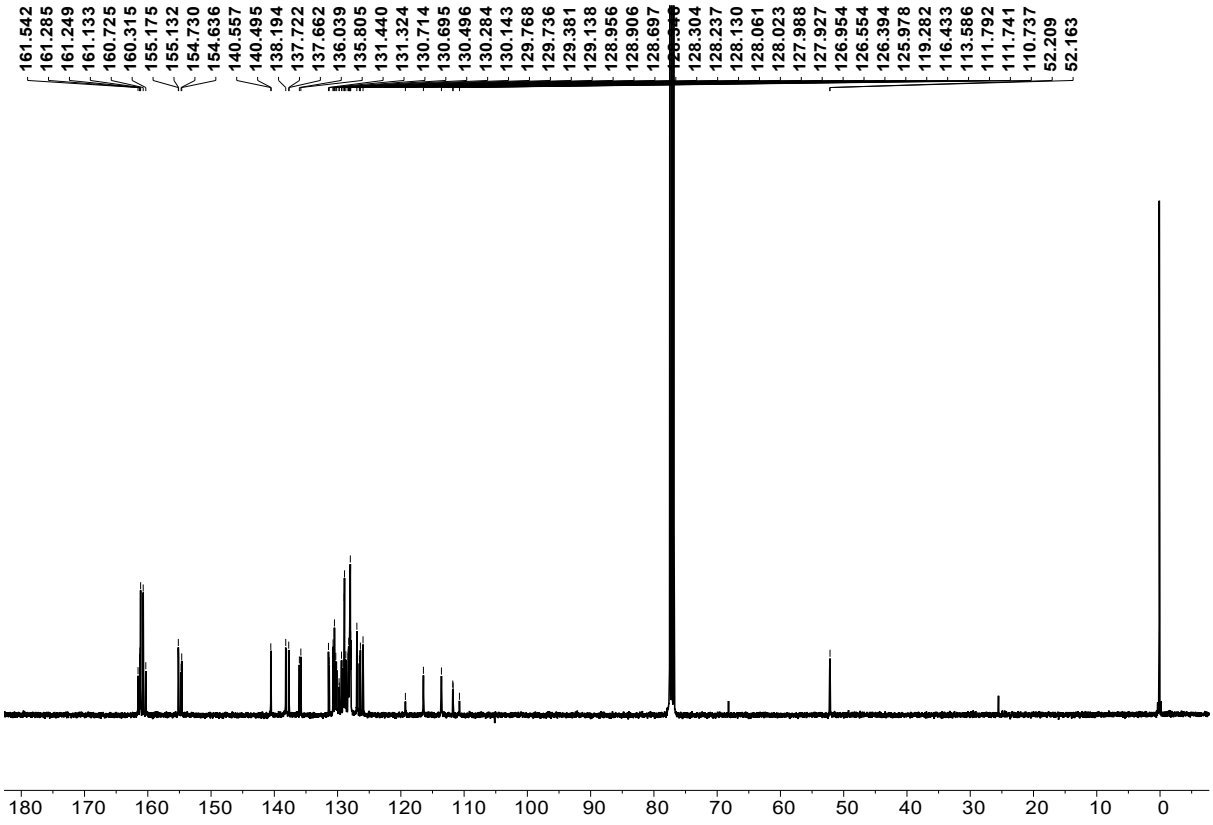


**Fig. S5** $^{13}C$ NMR of photocatalyst **1b**

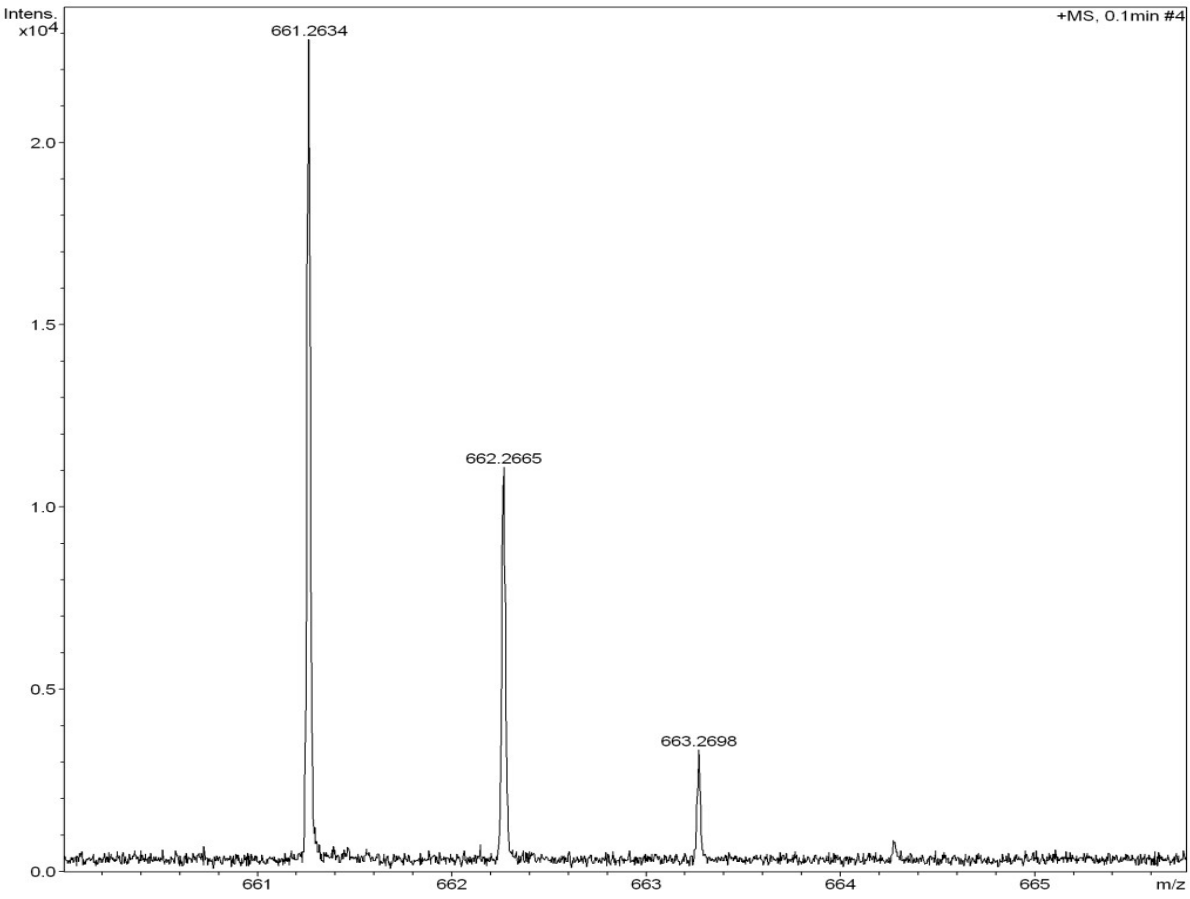

**Fig. S6** HRMS of photocatalyst **1b**

**DPBF** (**13,15-diphenylbenzo[4,5]furo[3,2-b]benzofuro[2',3':5,6] pyrido[3,2-g] quinoline**) **(1c)**.

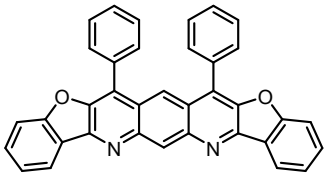

Orange solid 205 mg, yield: 80%. $^{1}$H NMR (500 MHz, $CDCl_3$) $\delta$ 9.48 (s, 1H), 8.81 (s, 1H), 8.54 (d, $J$ = 7.5 Hz, 2H), 7.75 (d, $J$ = 7.5 Hz, 4H), 7.69 (t, $J$ = 7.5 Hz, 2H), 7.62-7.51 (m, 10H). $^{13}$C NMR (100 MHz, $CDCl_3$ and TFA) δ 162.9, 146.3, 145.9, 139.2, 139.1, 136.1, 132.1, 130.8, 130.3, 129.7, 128.2, 126.8, 126.2, 125.0, 124.4, 113.5. Elemental analysis calcd. (%) for $C_{36}H_{20}N_2O_2$: C, 84.36; H, 3.93; N, 5.47, found C, 84.13; H, 4.12; N, 5.67. HRMS (ESI) calcd. for $C_{36}H_{20}N_2O_2^+$ $[M+H]^+$ = 513.1598, found 513.1600.

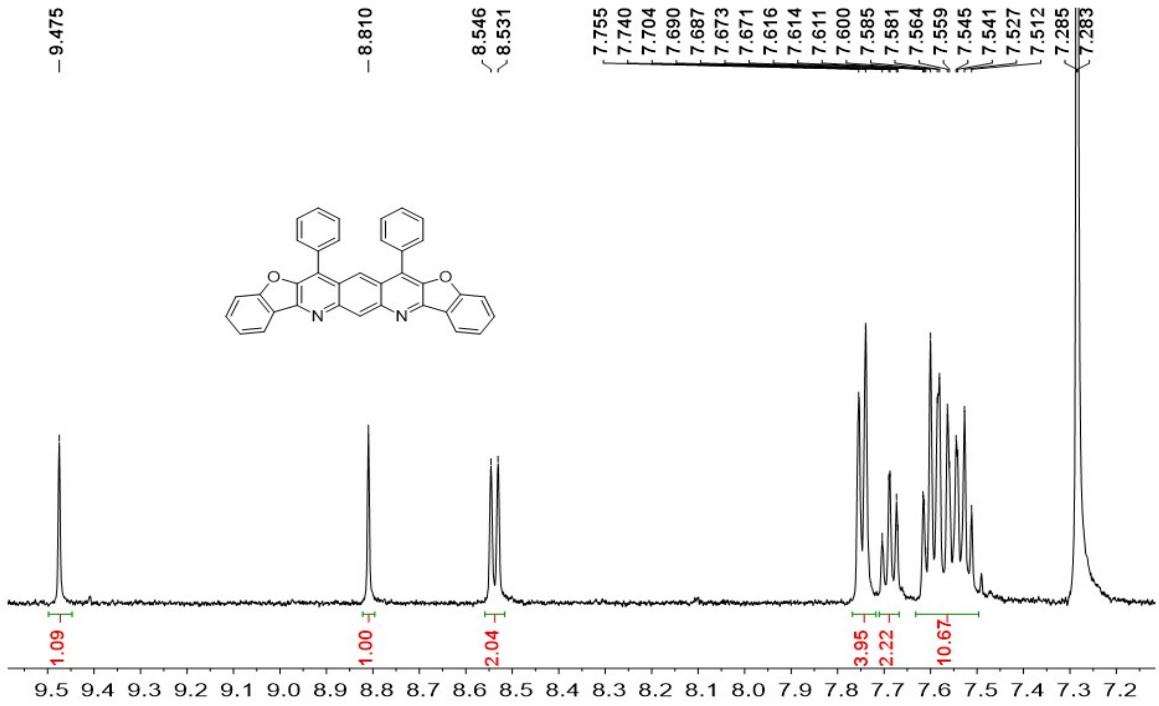


**Fig. S7** $^{1}$H NMR of photocatalyst **1c**

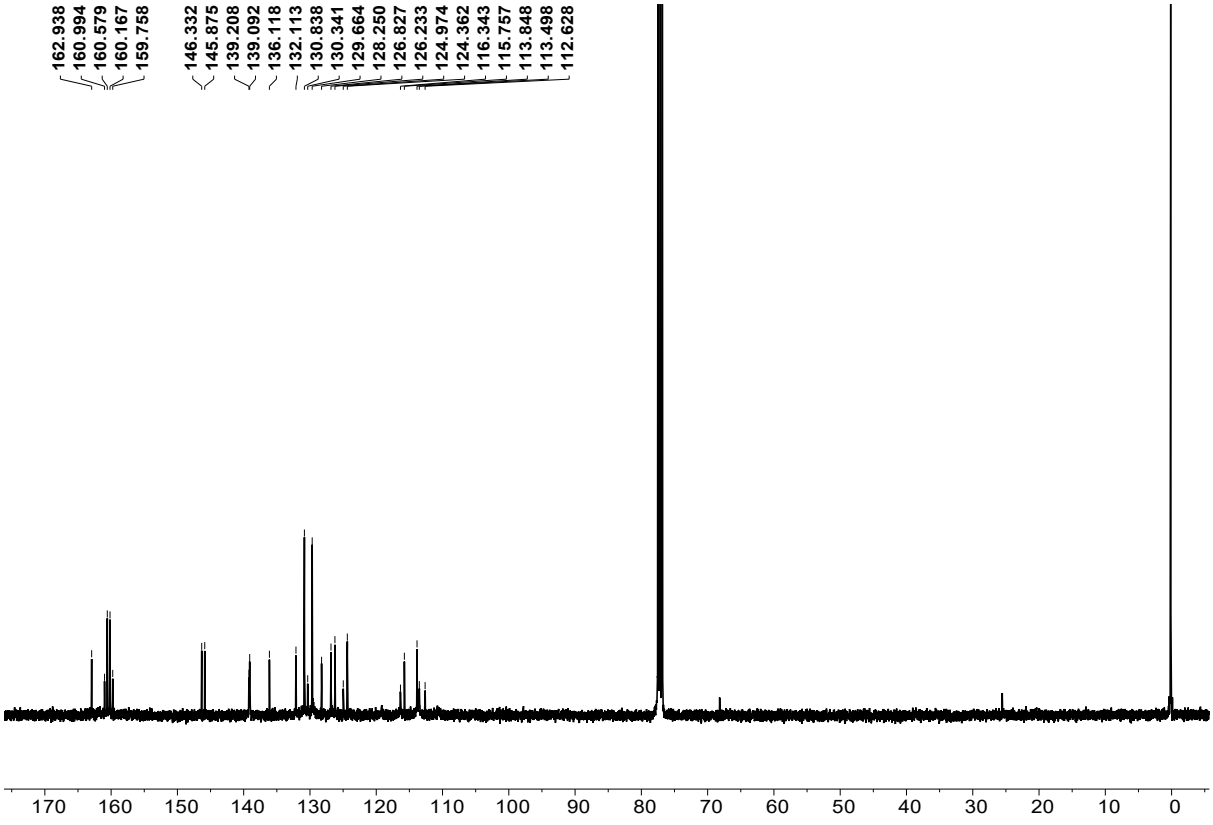


**Fig. S8** $^{13}$C NMR of photocatalyst **1c**

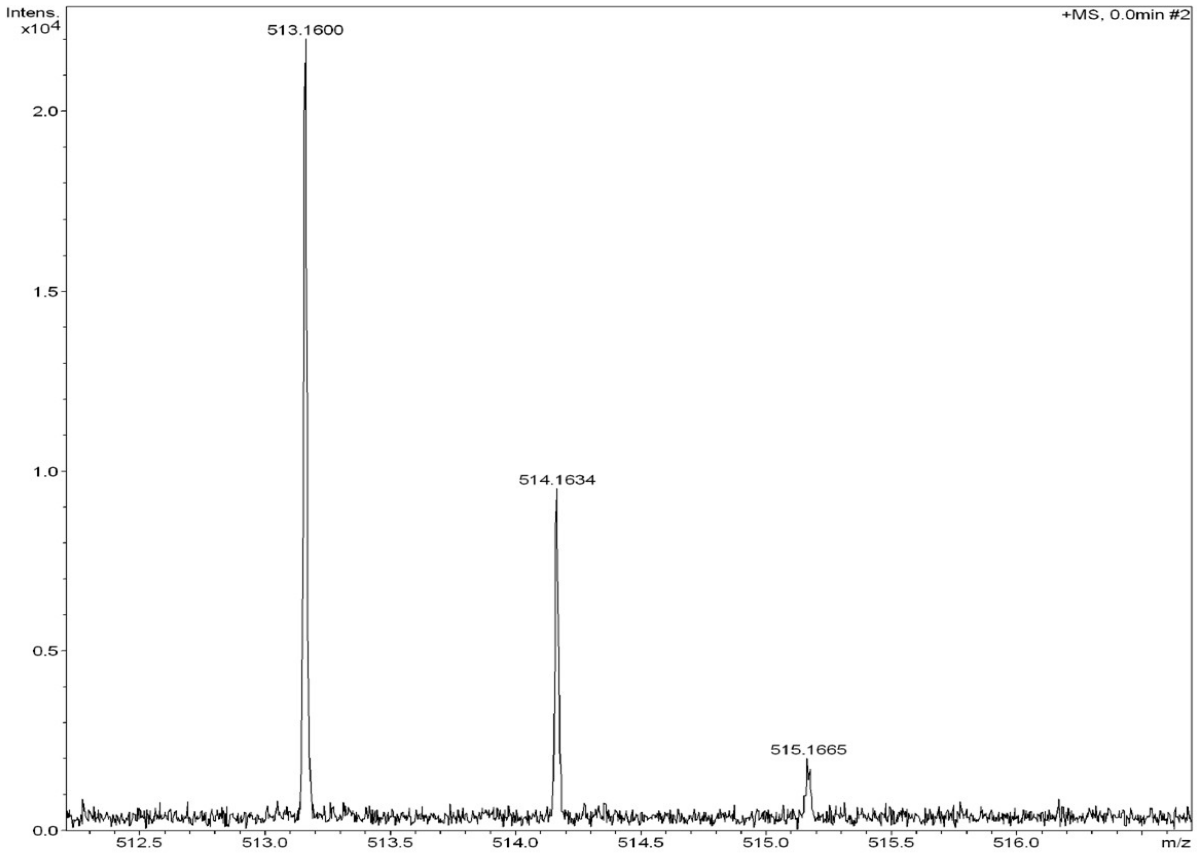


**Fig. S9** HRMS of **1c**

**3,9,13,15-Tetraphenyl-12,16-dihydroindeno[1,2-b]indeno[2',1':5,6]pyrido[3,2-g]quinoline (1d).**

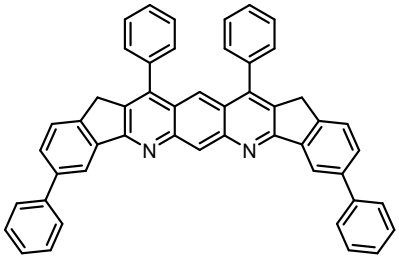

267 mg yellow solid was obtained, yield 81%. $^{1}$H NMR (400 MHz, $CDCl_3$) $\delta$ 9.55 (s, 1H), 8.80 (s, 2H), 8.58 (s, 1H), 8.12 (d, *J* = 8.0 Hz, 2H), 7.82 (d, *J* = 8.0 Hz, 2H), 7.68 -7.58 (m, 10H), 7.55-7.46 (m, 10H), 4.23 (s, 4H). $^{13}$C NMR (100 MHz, $CDCl_3$ and TFA) δ 153.7, 148.8, 143.4, 138.3, 137.5, 136.4, 136.0, 132.2, 131.9, 131.0, 130.0, 129.4, 129.2, 129.0, 128.8, 127.0, 127.0, 126.7, 125.5, 123.6, 111.5, 34.4. Elemental analysis calcd. (%) for $C_{50}H_{32}N_2$: C, 90.88; H, 4.88; N, 4.24, found C, 90.66; H, 5.02; N, 4.49. HRMS (ESI) calcd. for $C_{50}H_{32}N_2^+$ $[M+H]^+$ = 661.2638, found 661.2643.

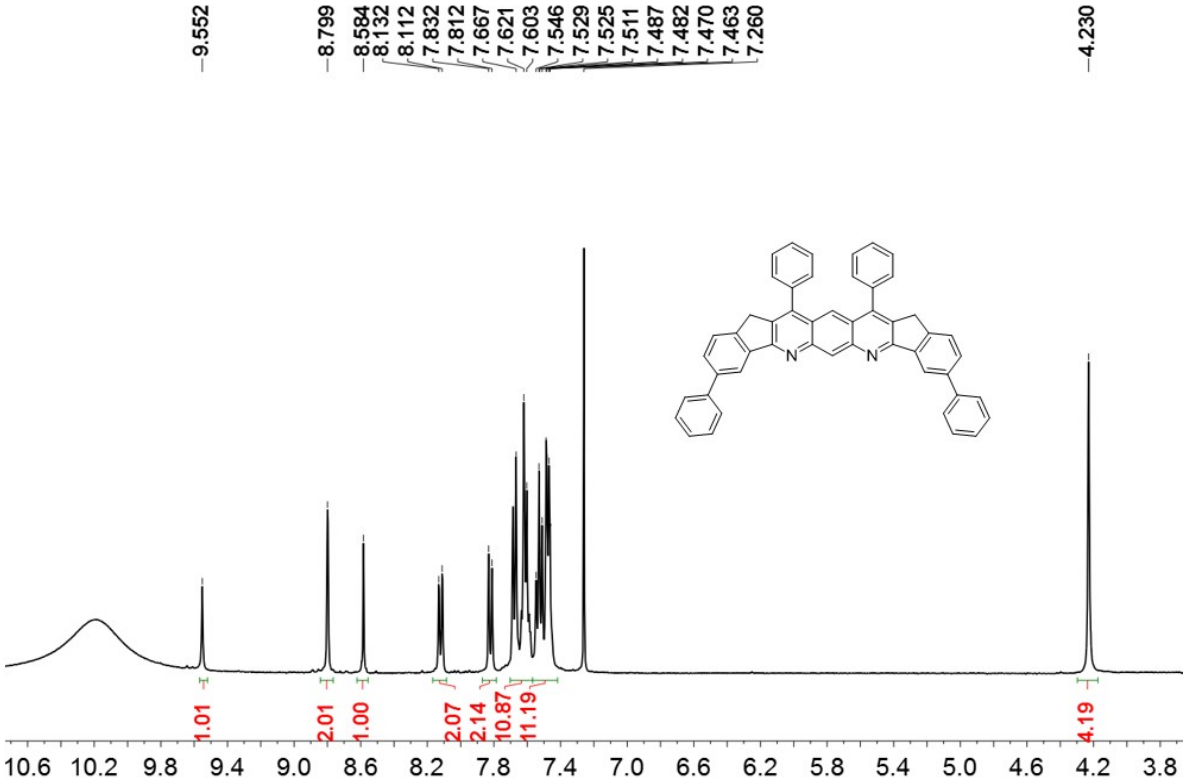


**Fig. S10** $^{1}$H NMR of photocatalyst **1d**

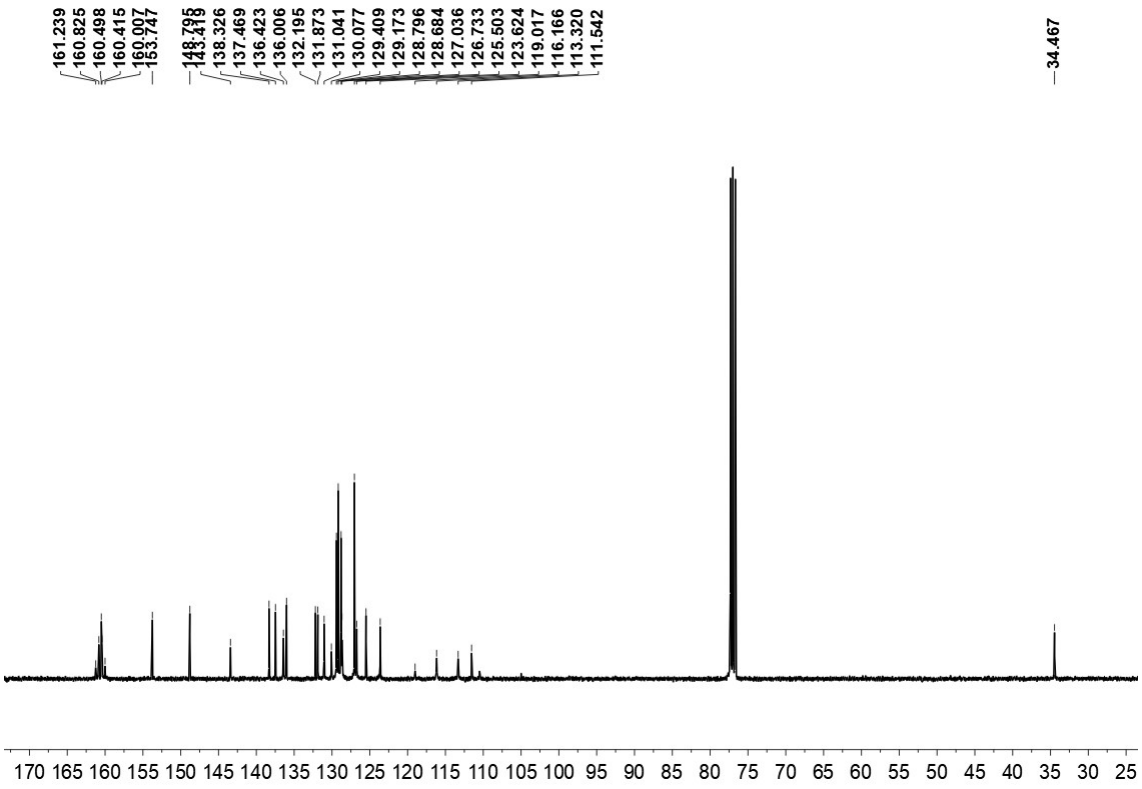


**Fig. S11** $^{13}$C NMR of photocatalyst **1d**

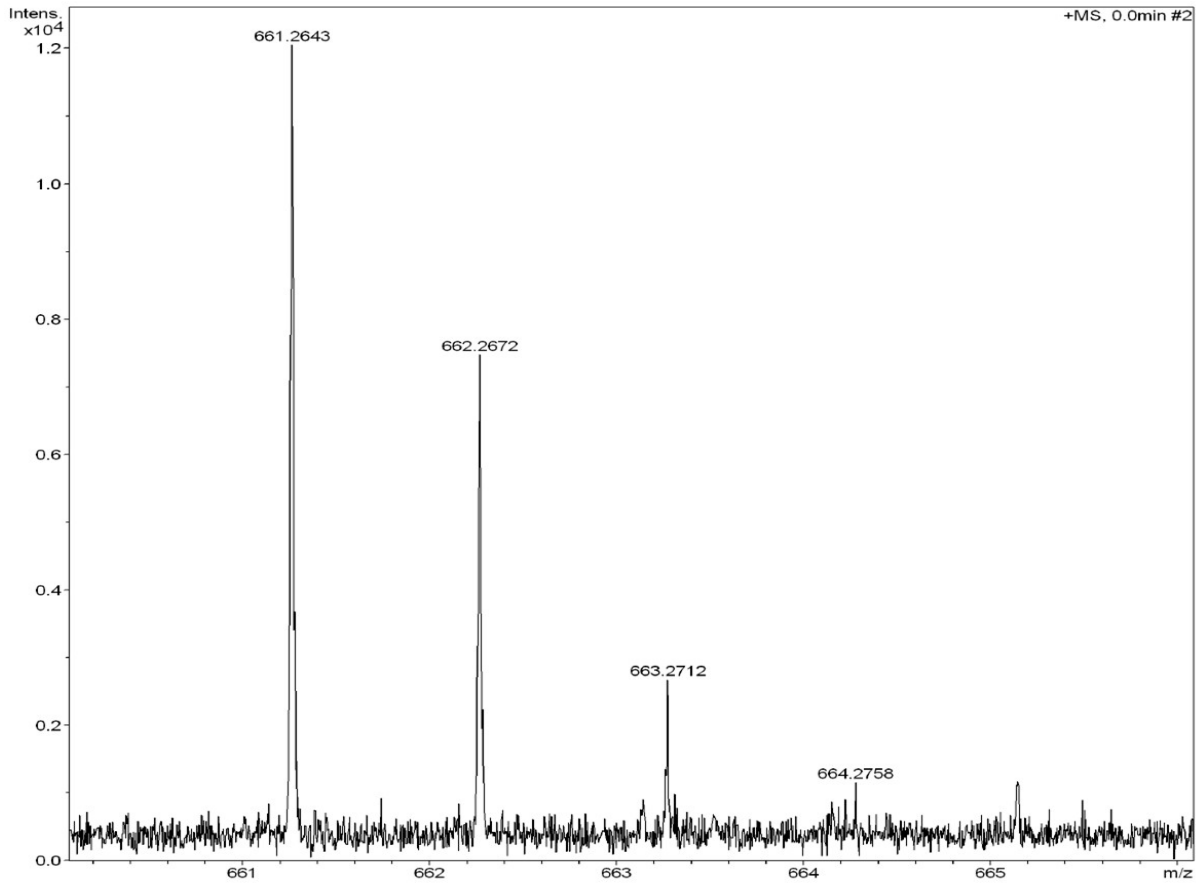


**Fig. S12** HRMS of **1d**

## X-ray Crystallographic Data

Crystals of compound **1b** suitable for X-ray crystallography was obtained, further confirmed the configuration of desired molecular (Figure S13). The phenyl rings B and C are in parallel, in contrast, the phenyl rings A and D that attached to five-membered rings are highly twisted at each side of the anthrazoline plane, respectively. Such conformation allows free rotation of the two distal phenyl rings which is important to its optical properties as the excitation energy can therefore be dissipated in a non-radiative pathway, allowing the effective population of triplet state which is essential to engage in photochemical events.[1]

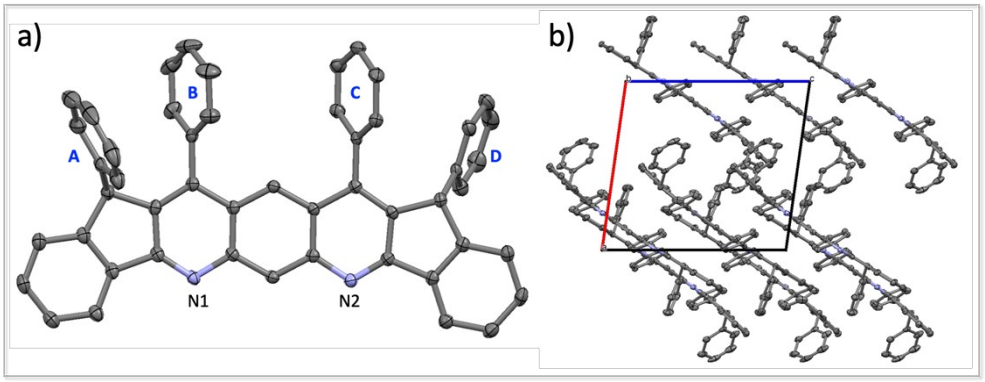


**Fig. S13** a) Front view of the molecular structure of **1b** derived from X-ray single crystal diffraction (CCDC 2102566); 2) Molecular packing of **1b** in a crystal unit. Thermal ellipsoids are drawn at 50% probability level.

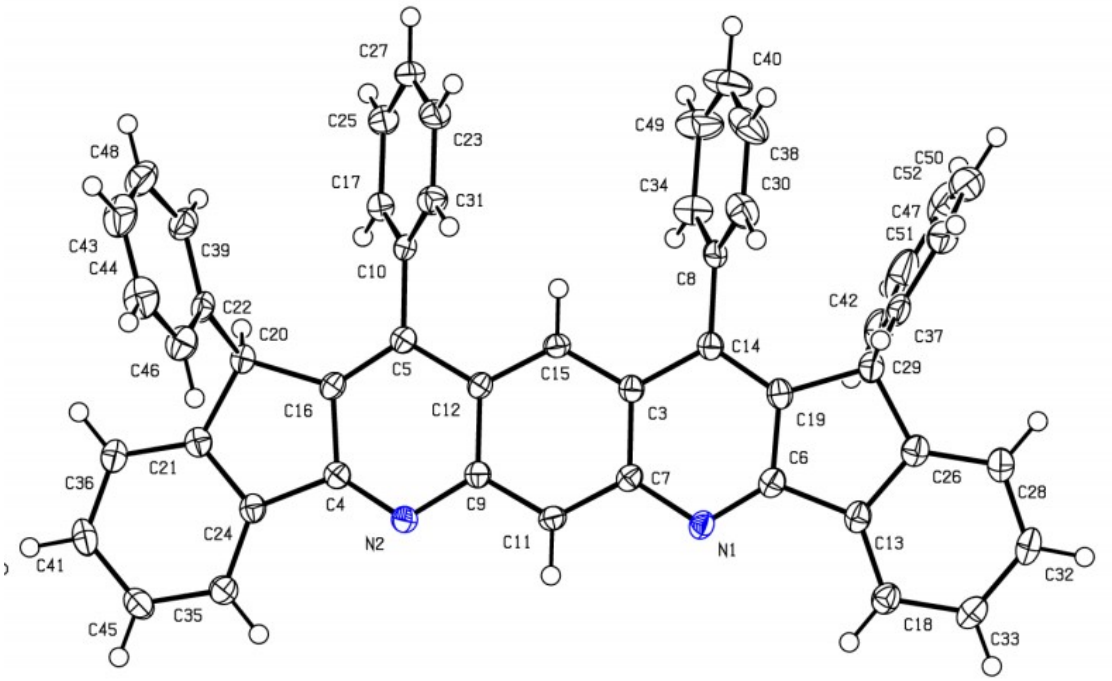


**Fig. S14** ORTEP[2] depiction of the molecular structure of photocatalyst **1b**.

**Table S1** Crystallographic data for compounds **1b**

| Complex | **1b** |
|---|---|
| CCDC number | 2102566 |
| Empirical formula | $C_{50}H_{32}N_2$ |
| Formula weight | 660.77 |
| Temperature/K | 273 |
| Crystal system | monoclinic |
| Space group | $P2_1/c$ |
| a/Å | 12.501(6) |
| b/Å | 21.209(9) |
| c/Å | 13.563(6) |
| α/° | 90 |
| β/° | 98.118(14) |
| γ/° | 90 |
| Volume/Å$^3$ | 3560(3) |
| Z | 4 |
| $\rho_{calc}$g/cm$^3$ | 1.233 |
| μ/mm$^{-1}$ | 0.07 |
| F(000) | 1384 |
| Radiation | MoKα (λ = 0.71073) |
| 2Θ range for data collection/° | 4.6 to 62.6 |
| Index ranges | -15 ≤ h ≤ 15, -26 ≤ k ≤ 26, -17 ≤ l ≤ 17 |
| Reflections collected | 93709 |
| Independent reflections | 7437 [$R_{int}$ = 0.033] |
| Goodness-of-fit on $F^2$ | 1.03 |
| Final R indexes [I>=2σ (I)] | $R_1$ = 0.045, $wR_2$ = 0.125 |

## Photophysical Characterization of the Photocatalysts

### The absorption and emission spectra

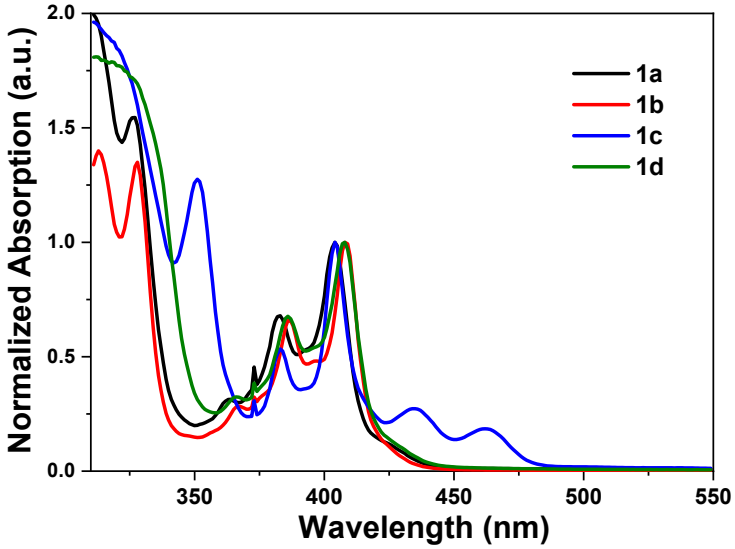


**Fig. S15** Normalized UV-vis spectra of photocatalysts **1a-1d** in DMF ($1x10^{-5}$ M) solution.

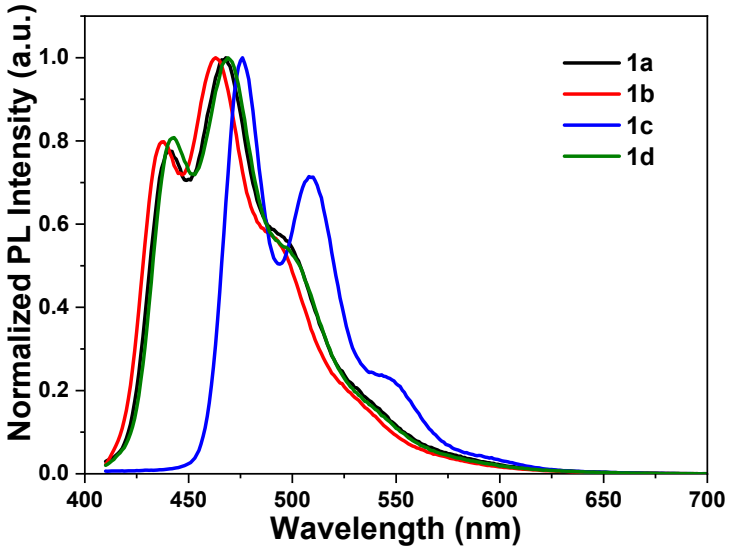


**Fig. S16** Normalized emission spectra of **1a-1d** in DMF ($1x10^{-5}$ M) solution.

## Fluorescent lifetime measurements

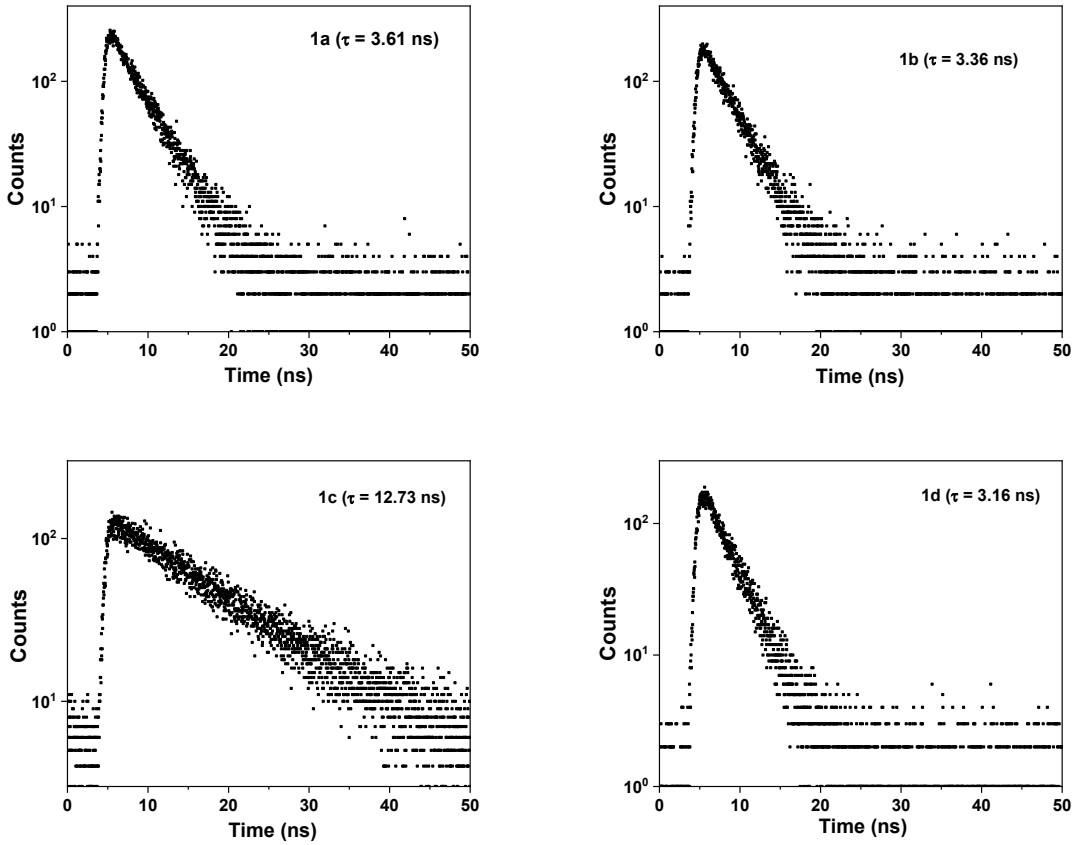


**Fig. S17** The emission decay profiles of **1a**-**1d** in diluted DMF.

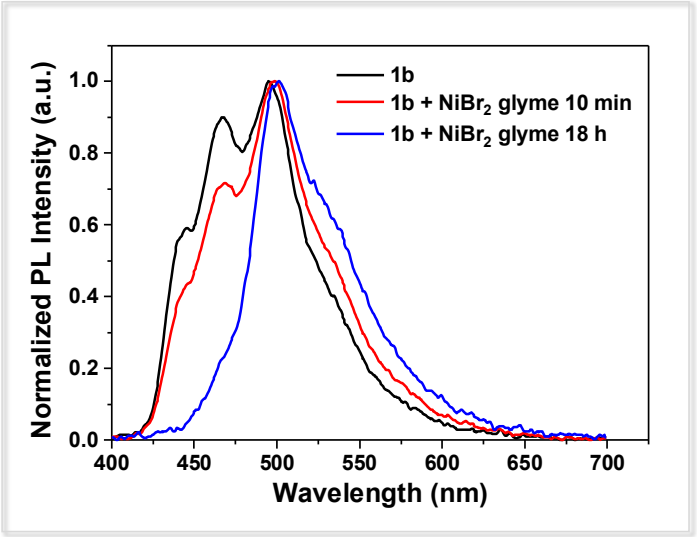


**Fig. S18** UV-vis spectra of **1b** (black), 1:1 mixture of 1b and $NiBr_2$•glyme under blue light irradiation for 10 minutes (red) and 1:1 mixture of 1b and $NiBr_2$•glyme under blue light irradiation for 24 hours.

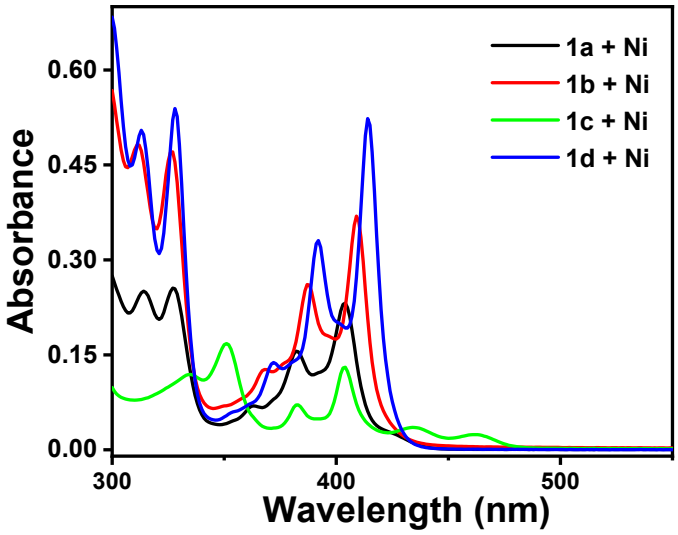


**Fig. S19** UV-vis spectra of **1a-1d** in DMF ($1x10^{-5}$ M) solution with the adding of exceeding amount $NiCl_2$•glyme.

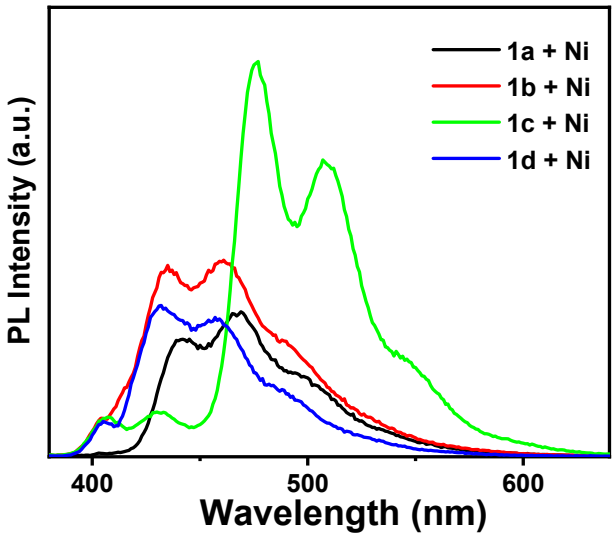


**Fig. S20** Emission spectra of **1a-1d** in DMF ($1x10^{-5}$ M) solution with the adding of exceeding amount $NiCl_2$•glyme.

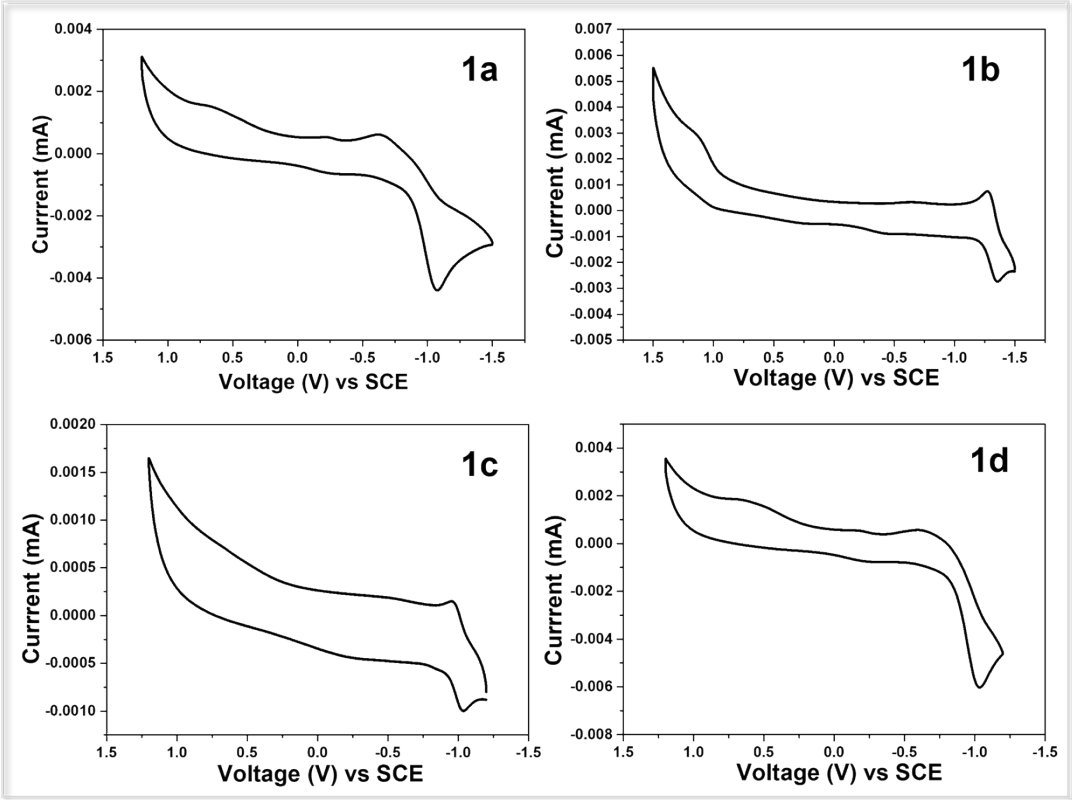


**Fig. S21** Cyclic voltammetry of compound **5a**-**5d**, measured in a 0.1 M solution of *n*-$Bu_4NBF_4$ in DMF (*vs*. SCE).

**Table S2.** Photophysical and electrochemical data of the catalysts **1a**-**1d**.

| PC | $\lambda_{abs}$(nm)[a] | $\lambda_{em}$(nm)[a] | $E_{S1}$ (eV)[b] | $E_{1/2}$ (eV)[c] | E1/2* S1 (eV)[d] | Eopt g (eV) | Ecal g (eV) | $\Phi_f$[e] (%) | $\tau_s$ (ns) |
|---|---|---|---|---|---|---|---|---|---|
| **1a** | 363, 382, 404 (major) | 444, 473, 499 (major) | 2.48 | -1.08 | 1.40 | 3.07 | 3.38 | 0.32 | 3.61 |
| **1b** | 367, 386, 408 (major) | 442, 467, 496 (major) | 2.50 | -1.30 | 1.20 | 3.04 | 3.39 | 38.7 | 3.36 |
| **1c** | 383, 404 (major), 434, 463 | 481, 511 (major), 548 | 2.43 | -1.03 | 1.40 | 3.07 | 3.01 | 95.3 | 12.73 |
| **1d** | 366, 386, 407 (major) | 446, 477, 500 (major) | 2.48 | -1.04 | 1.44 | 3.05 | 3.36 | 31.26 | 3.16 |

[a]UV–*vis* absorption spectra and emission spectra were acquired in DMF. [b]Singlet energies were calculated using the maximum wavelength of emission. [c]Cyclic voltammetry measurements were taken in a degassed DMF solution ([*n*-$Bu_4NBF_4$] = 0.1 M, [substrate] = 1 mM, [d]Singlet excited state reduction potentials were calculated using the singlet energies (estimated from the maximum wavelength of emission) and the $E_{1/2}$. [e] Fluorescent quantum yield obtained in DMF.

## Data of DFT Calculations for the Photocatalysts

DFT calculations were employed to interpret the orbitals of the related photoexcitation, to better gain insight of the photochemical events. Optimized geometries and the molecular orbital surfaces of the HOMOs and LUMOs of molecule **1a**–**1d** obtained at the B3LYP/6-31G* level in gas phase The results are summarized in Table 1. The LUMOs are mostly localized at the anthrazoline framework, only very few distributed at the attached phenyl rings, same as HOMOs. The energy gaps are relatively small for all compound, and the calculated energy gaps of **1a**-**1d** are in good accordance with the experimental Eopt g.

**Table S3** Contour plots of the occupied molecular orbital HOMO, HOMO-1, HOMO-2, HOMO-3 and unoccupied molecular orbital LUMO, LUMO+1, LUMO+2, LUMO+3 for complexes **1a**-**1d**.

| | **1a** | **1b** | **1c** | **1d** |
|---|---|---|---|---|
| Optimized geometry | 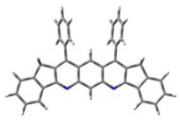 | 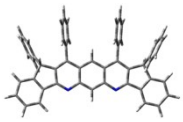 | 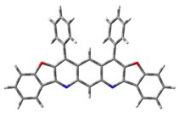 | 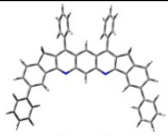 |
| **LUMO+3** | 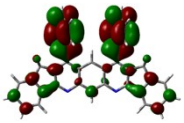 | 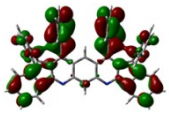 | 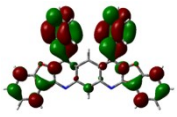 | 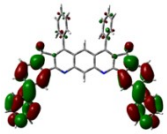 |
| **LUMO+2** | 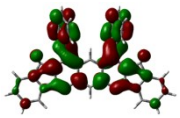 | 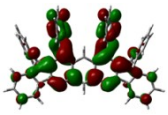 | 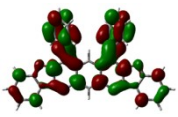 | 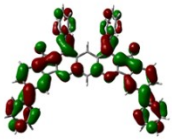 |
| **LUMO+1** | 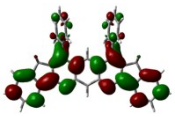 | 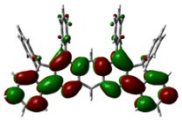 | 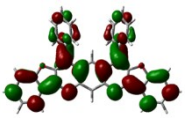 | 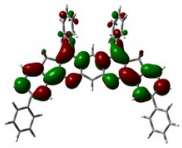 |
| **LUMO** | 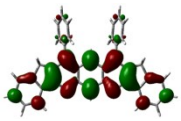 | 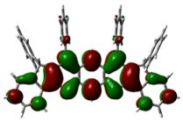 | 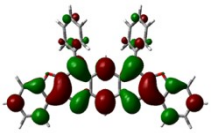 | 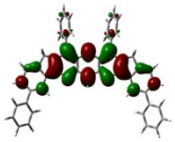 |
| **HOMO** | 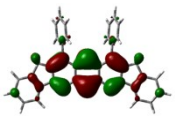 | 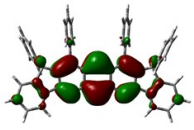 | 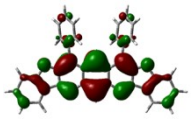 | 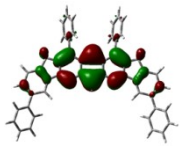 |
| **HOMO-1** | 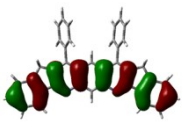 | 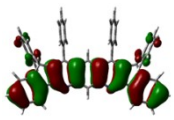 | 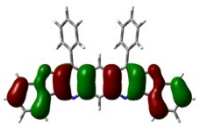 | 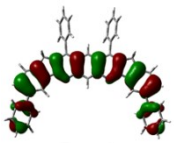 |
| **HOMO-2** | 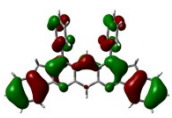 | 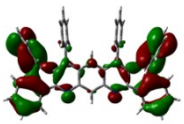 | 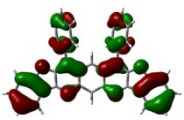 | 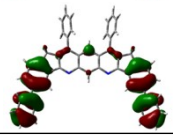 |

| | | | | |
|---|---|---|---|---|
| **HOMO-3** | 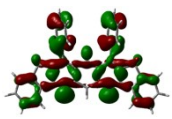 | 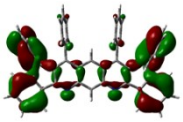 | 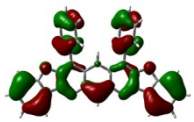 | 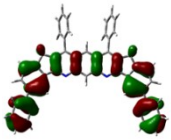 |

**Table S4 DFT-derived molecular orbital energies (eV) of 1a-1d.**

| | 1a | 1b | 1c | 1d |
|---|---|---|---|---|
| **LUMO+3** | -0.33851 | -0.32899 | -0.36926 | -0.70015 |
| **LUMO+2** | -0.64355 | -0.65662 | -0.55947 | -0.79022 |
| **LUMO+1** | -1.0335 | -1.03839 | -1.32412 | -1.06996 |
| **LUMO** | -2.02373 | -2.03679 | -2.28142 | -2.04985 |
| **HOMO** | -5.39933 | -5.43089 | -5.28721 | -5.41375 |
| **HOMO-1** | -5.82328 | -5.78573 | -6.06683 | -5.77294 |
| **HOMO-2** | -6.5482 | -6.30738 | -6.34221 | -6.01104 |
| **HOMO-3** | -6.60208 | -6.4086 | -6.70113 | -6.11472 |

## Optimization of the Reaction Conditions

Initially, 1-bromo-4-(trifluoromethyl)benzene and octan-1-amine were utilized as substrates for model reaction, in the presence of photocatalyst of anthrazoline derivatives and metal catalyst of $NiBr_2$•glyme, with 1,4-Diazabicyclo[2.2.2]octane (DABCO) as base and dimethylacetamide (DMA) as solvent under blue LED irradiation for 24 hours. The reaction proceeded when using photocatalyst **1a** in less than 5% conversion, whereas **1b** rendered the reaction excellent conversion of 95% (Table S5, entry 1 and 2). Catalytic competencies of **1c** and **1d** were both inferior to **1b**, with **1c** twice better than **1d** in respect of product conversion (entry 3 and 4). Variations of solvents (entry 5-7) implied that DMA works most effective for this catalytic system. Other bases such as $Cs_2CO_3$, triethylamine and DIPEA were tested, indicating DABCO was the favoured base for the reaction (entry 8-10). The reason behind was demonstrated by the Wu group that the role of DABCO is not only a neutralizer, but more importantly, it renders enhancement in singlet electron transfer by suppressing charge recombination.[3] The use of alternative Ni source such as $NiCl_2$•dtbbpy led to significant decrease in product conversion, suggesting $NiBr_2$ cannot be substituted as negative outcome was observed. Next, examination of various photocatalysts revealed that photocatalyst **1b** developed in this work was as efficient as the widely used metallaphotocatalyst $Ir(ppy)_3$ (entry

12), with conversion of 95% *vs.* 96%, and much more efficient than the known $Ru(bpy)_3Cl_2$ (54% conversion). In comparison with other organic dyes that resulted in either no reaction or less than 5% conversion (entry 14-16), except for **1a**, the other photocatalyst **1b-1d** all showcased the efficacy in promote C-N bond formation, with **1b** being the most efficient photocatalyst. Finally, control experiments (entry 17-20) revealed that deviations from the standard conditions, such as the absence of the either photocatalyst or metal catalyst, as well as base or light, resulting the failure of the reaction, with <5% conversion or even no reaction.

**Table S5 Optimization of the reaction conditions**[a]

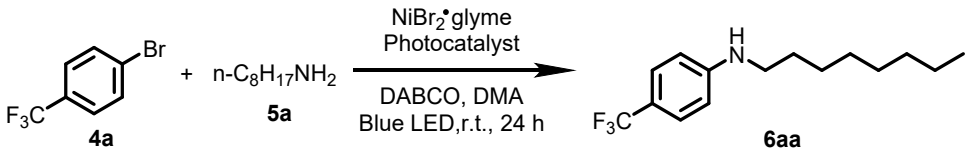


| Entry | Photocatalyst | Solvent | Base | Ni(II) catalyst | Conversion (%)[b] |
|---|---|---|---|---|---|
| 1 | **1a** | DMA | DABCO | $NiBr_2$•glyme | <5 |
| 2 | **1b** | DMA | DABCO | $NiBr_2$•glyme | 95 |
| 3 | **1c** | DMA | DABCO | $NiBr_2$•glyme | 56 |
| 4 | **1d** | DMA | DABCO | $NiBr_2$•glyme | 26 |
| 5 | **1b** | DMF | DABCO | $NiBr_2$•glyme | 71 |
| 6 | **1b** | $CH_3CN$ | DABCO | $NiBr_2$•glyme | 34 |
| 7 | **1b** | Dioxane | DABCO | $NiBr_2$•glyme | 23 |
| 8 | **1b** | DMA | $Cs_2CO_3$ | $NiBr_2$•glyme | 17 |
| 9 | **1b** | DMA | TEA | $NiBr_2$•glyme | 37 |
| 10 | **1b** | DMA | DIPEA | $NiBr_2$•glyme | 45 |
| 11 | **1b** | DMA | DABCO | $NiCl_2$ dtbbpy | 63 |
| 12 | $Ir(ppy)_3$ | DMA | DABCO | $NiBr_2$•glyme | 96 |
| 13 | $Ru(bpy)_3Cl_2$ | DMA | DABCO | $NiBr_2$•glyme | 54 |
| 14 | fluorescein | DMA | DABCO | $NiBr_2$•glyme | N.R. |
| 15 | Eosin Y | DMA | DABCO | $NiBr_2$•glyme | <5 |
| 16 | Mes-Acr-$Me^+$ | DMA | DABCO | $NiBr_2$•glyme | <5 |
| 17[c] | **1b** | DMA | DABCO | $NiBr_2$•glyme | <5 |
| 18 | **1b** | DMA | None | $NiBr_2$•glyme | N.R. |
| 19 | None | DMA | DABCO | $NiBr_2$•glyme | N.R. |
| 20 | **1b** | DMA | DABCO | None | N.R. |

[a]Reaction conditions: To a 4 mL vial, amine (0.8 mmol, 2.0 equiv), aryl bromide (0.4 mmol, 1.0 equiv), Ni(II) catalyst (0.02 mmol, 0.05 equiv), DABCO (0.8 mmol, 2.0 equiv) and 2 mL DMA were added. The suspension was sonicated for 2 minutes, followed by the addition of

photocatalyst (0.5 mol%). The reaction mixture was bubbled with $N_2$ for 5 minutes and then sealed, which was stirred at room temperature under irradiation with two 12 W blue LED lights (distance ~ 5 cm) for 24 hours. [b]Conversions were calculated by $^1H$ NMR using 1,3,5-trimethyoxybenzene as internal standard. [c]Without irradiation. N.R. = no reaction.

**Table S6 Solvent screening**

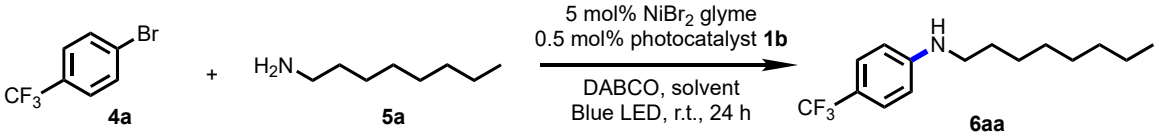


| Entry | Photocatalyst | Solvent | Base | Ni(II) catalyst | Conversion (%) |
|---|---|---|---|---|---|
| 1 | **1b** | DMF | DABCO | $NiBr_2$•glyme | 71 |
| 2 | **1b** | $CH_3CN$ | DABCO | $NiBr_2$•glyme | 34 |
| 3 | **1b** | Dioxane | DABCO | $NiBr_2$•glyme | 23 |
| 4 | **1b** | DMSO | DABCO | $NiBr_2$•glyme | 45 |
| 5 | **1b** | MeOH | DABCO | $NiBr_2$•glyme | 22 |

**Table S7 Base screening**

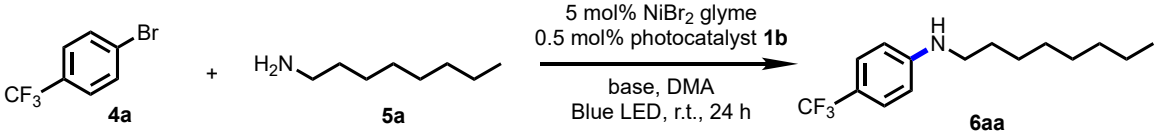


| Entry | Photocatalyst | Solvent | Base | Ni(II) catalyst | Conversion (%) |
|---|---|---|---|---|---|
| 1 | **1b** | DMA | $Cs_2CO_3$ | $NiBr_2$•glyme | 17 |
| 2 | **1b** | DMA | TEA | $NiBr_2$•glyme | 37 |
| 3 | **1b** | DMA | DIPEA | $NiBr_2$•glyme | 45 |

**Table S8 Ni(II) catalyst screening**

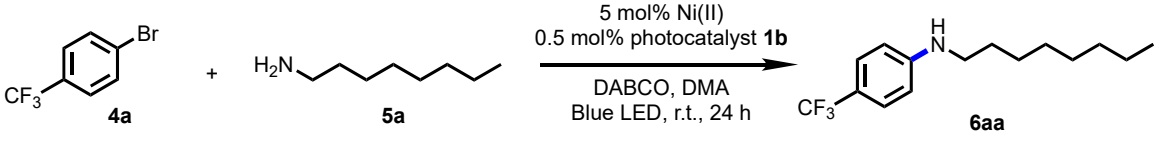


| Entry | Photocatalyst | Solvent | Base | Ni(II) catalyst | Conversion (%) |
|---|---|---|---|---|---|
| 1 | **1b** | DMA | DABCO | $NiBr_2$•glyme | 95 |

| | | | | | |
|---|---|---|---|---|---|
| 2 | **1b** | DMA | DABCO | $NiBr_2$ | 45 |
| 3 | **1b** | DMA | DABCO | $NiBr_2•3H_2O$ | 65 |
| 4 | **1b** | DMA | DABCO | $NiCl_2$•dtbbpy | 63 |

**Table S9 Comparisons of other commonly used photocatalysts**

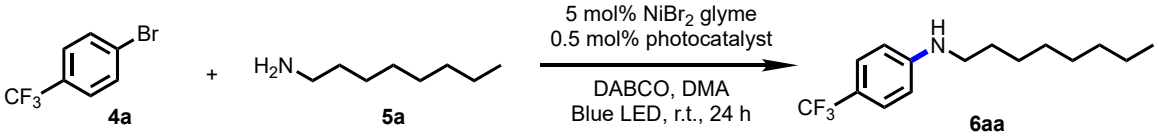


| Entry | Photocatalyst | Solvent | Base | Ni(II) catalyst | Conversion (%) |
|---|---|---|---|---|---|
| 1 | **1b** | DMA | DABCO | $NiBr_2$•glyme | 95 |
| 2 | $Ir(ppy)_3$ | DMA | DABCO | $NiBr_2$•glyme | 96 |
| 3 | $Ru(bpy)_3Cl_2$ | DMA | DABCO | $NiBr_2$•glyme | 54 |
| 4 | fluorescein | DMA | DABCO | $NiBr_2$•glyme | N.R. |
| 5 | Eosin Y | DMA | DABCO | $NiBr_2$•glyme | <5 |
| 6 | Mes-Acr-$Me^+$ | DMA | DABCO | $NiBr_2$•glyme | <5 |

**Table S10 Control experiments**

| Entry | Photocatalyst | light | Solvent | Base | Ni(II) catalyst | Conversion (%) |
|---|---|---|---|---|---|---|
| 1 | **1b** | Blue Led | DMA | DABCO | $NiBr_2$•glyme | <5 |
| 2 | **1b** | Blue Led | DMA | None | $NiBr_2$•glyme | N.R. |
| 3 | None | Blue Led | DMA | DABCO | $NiBr_2$•glyme | N.R. |
| 4 | **1b** | Blue Led | DMA | DABCO | None | N.R. |
| 5 | **1b** | None | DMA | DABCO | $NiBr_2$•glyme | N.R. |

## General Procedure of the Couplings of Aryl Bromides and Amines

To a 4 mL vial, amine (0.8 mmol, 2.0 equiv), aryl bromide (0.4 mmol, 1.0 equiv),·$NiBr_2$•glyme(8.0 mg, 0.02 mmol, 0.05 equiv), DABCO (0.8 mmol, 2.0 equiv) and 2 mL DMA were added. The suspension was sonicated for 2 min, followed by photocatalyst **1b** (1.0 mg, 0.5 mol%) were added, and then the mixture was stirred at room temperature under the

irradiation with two 12 W Blue LED lights, distance ~ 5 cm. After 24~48 hours, the mixture was poured into water, and extracted with EtOAc (3 × 10 mL). The combined organic layers were washed with water, dried over anhydrous $Na_2SO_4$ and concentrated under reduced pressure. Purifications of the crude products by column chromatography (silica gel) afforded the desired products which was further dried *under vacuo* for NMR analyses.

**Synthesis of secondary amines**

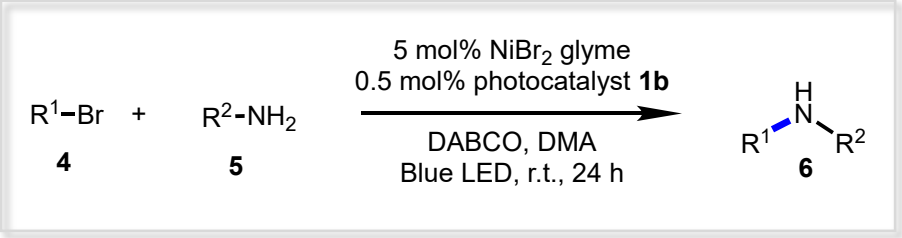


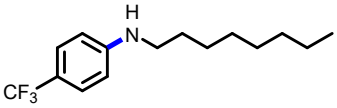


***N*-octyl-4-(trifluoromethyl)aniline (6aa)**.

The crude product was purified by column chromatography (silica gel, Hexane/EtOAc = 20:1) to afford 100.2 mg colorless oil, yield: 91 %). $^1$H NMR (500 MHz, $CDCl_3$) $\delta$ 7.41 (d, $J$ = 8.5 Hz, 2H), 6.60 (d, $J$ = 8.5 Hz, 2H), 3.15 (m, 2H), 1.65-1.62 (m, 2H), 1.42-1.28 (m, 11H), 0.91 (t, $J$ = 6.0 Hz, 3H). The data is in good accordance with that reported in the literature.[4]

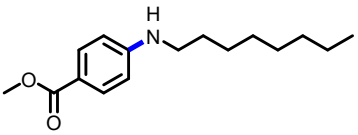


**Methyl 4-(octylamino)benzoate (6ba)**.

The crude product was purified by column chromatography (silica gel, Hexane/EtOAc = 20:1) to afford 87.4 mg white crystals, yield: 83%). $^1$H NMR (500 MHz, $CDCl_3$) $\delta$ 7.88 (d, $J$ = 9.0 Hz, 2H), 6.55 (d, $J$ = 8.5 Hz, 2H), 4.14 (s, 1H), 3.87 (s, 3H), 3.17 (t, $J$ = 7.5 Hz, 2H), 1.67-1.62 (m, 2H), 1.43-1.28 (m, 10H), 0.91 (t, $J$ = 6.5 Hz, 3H). The data is in good accordance with that reported in the literature.[5]

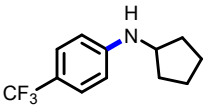


***N*-cyclopentyl-4-(trifluoromethyl)aniline (6ab).**

The crude product was purified by column chromatography (silica gel, Hexane/EtOAc = 20:1) to afford 79.8 mg colorless oil, yield: 87 %). $^1$H NMR (500 MHz, $CDCl_3$) $\delta$ 7.41 (d, $J$ = 8.5 Hz, 2H), 6.60 (d, $J$ = 8.5 Hz, 2H), 4.01 (bs, 1H), 3.83 (m, 1H), 2.09-2.03 (m, 2H), 1.80-1.73 (m, 2H), 1.71-1.64 (m, 2H), 1.53-1.46 (m, 2H). The data is in good accordance with that reported in the literature.[6]

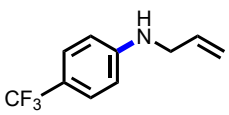


**4-(Trifluoromethyl)-*N*-vinylaniline (6ac).**

The crude product was purified by column chromatography (silica gel, Hexane/EtOAc = 50:1) to afford 59.1 mg colorless oil, yield: 79 %). $^1$H NMR (500 MHz, $CDCl_3$) $\delta$ 7.42 (d, $J$ = 8.0 Hz, 2H), 6.64 (d, $J$ = 8.0 Hz, 2H), 5.99-5.91 (m, 1H), 5.31 (dd,

$J_1$ = 17.5 Hz, $J_2$ = 2.0 Hz, 1H), 5.20 (dd, $J_1$ = 17.5, $J_2$ = 2.0 Hz, 1H), 4.16 (s, 1H), 3.84 (s, 2H). The data is in good accordance with that reported in the literature.[7]

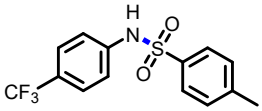

**4-Methyl-N-(4-(trifluoromethyl)phenyl)benzenesulfonamide (6ad).** The crude product was purified by column chromatography (silica gel, Hexane/EtOAc = 3:1) to afford 99.6 mg colorless oil, yield: 79%). $^1$H NMR (500 MHz, $CDCl_3$) $\delta$ 7.78 (d, $J$ = 8.0 Hz, 2H), 7.60-7.50 (m, 3H), 7.29 (d, $J$ = 8.0 Hz, 2H), 7.22 (d, $J$ = 8.5 Hz, 2H), 2.41 (s, 3H). The data is in good accordance with that reported in the literature.[7]

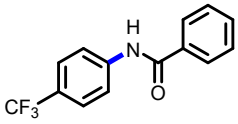

***N*-(4-(trifluoromethyl)phenyl)benzamide (6ae)**.
The crude product was purified by column chromatography (silica gel, Hexane/EtOAc = 8:1) to afford 80.6 mg white powder, yield: 76 %). $^1$H NMR (500 MHz, $CDCl_3$) $\delta$ 7.95 (s, 1H), 7.92 (d, $J$ = 7.5 Hz, 2H), 7.81 (d, $J$ = 8.5 Hz, 2H), 7.66 (d, $J$ = 8.5 Hz, 2H), 7.62 (t, $J$ = 7.5 Hz, 2H), 7.54 (t, $J$ = 7.5 Hz, 2H). The data is in good accordance with that reported in the literature.[6]

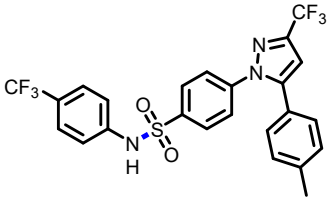

**4-(5-(p-Tolyl)-3-(trifluoromethyl)-1H-pyrazol-1-yl)-N-(4-(trifluoromethyl)phenyl)benzenesulfonamide (6af)**.
The crude product was purified by column chromatography (silica gel, Hexane/EtOAc = 5:1) to afford 136.6 mg white solid, yield: 65%). $^1$H NMR (500 MHz, $CDCl_3$) $\delta$ 7.81 (d, $J$ = 8.5 Hz, 2H), 7.53 (d, $J$ = 8.5 Hz, 2H), 7.81 (d, $J$ = 9.0 Hz, 2H), 7.21-7.15 (m, 5H), 7.06 (d, $J$ = 8.0 Hz, 2H), 6.74 (s, 1H), 2.39 (s, 3H). $^{13}$C NMR (101 MHz, $CDCl_3$) $\delta$ 145.5, 144.4, 143.2, 140.1, 139.4, 138.0, 129.9, 128.8, 128.4, 127.7, 126.9, 125.8, 125.7, 125.3, 125.1, 122.6, 122.4, 120.6, 120.6, 119.8, 117.1, 106.7, 106.6, 21.4, 21.3. $^{19}$F NMR (470 MHz, $CDCl_3$) δ -62.3, -62.5.

**Synthesis of tertiary amines**

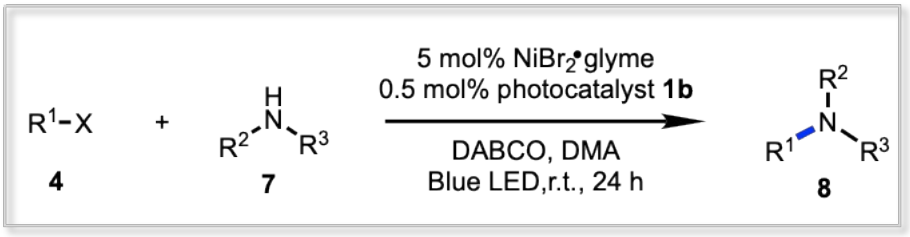


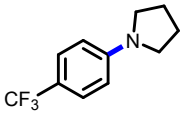

**1-(4-(Trifluoromethyl)phenyl)pyrrolidine (8aa).**
The crude product was purified by column chromatography (silica gel, Hexane/EtOAc = 50:1) to afford white solid, the aryl bromide **4a** resulted 82.8 mg of the product, yield: 96 %; the aryl chloride **4a'** resulted 78.5 of the product, yield: 91%). $^1$H NMR (400 MHz, $CDCl_3$) $\delta$ 7.43 (d, $J$ = 8.4 Hz, 2H), 6.54 (d, $J$ = 8.4 Hz, 2H), 3.31 (d, $J$ = 6.2 Hz,

4H), 2.03 (q, *J* = 6.2, 4.5 Hz, 4H). The data is in good accordance with that reported in the literature. [7,8]

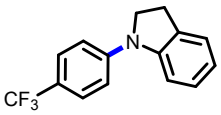

**1-(4-(Trifluoromethyl)phenyl)indoline (8ab).**

The crude product was purified by column chromatography (silica gel, Hexane/EtOAc = 10:1) to afford 52 mg colorless oil, yield: 63 %). $^1$H NMR (500 MHz, $CDCl_3$) *δ* 7.61 (d, *J* = 8.5 Hz, 2H), 7.31-7.25 (m, 4H), 7.17 (t, *J* = 7.5 Hz, 1H), 6.88 (t, *J* = 7.0 Hz, 1H), 4.02 (t, *J* = 8.5 Hz, 2H), 3.20 (t, *J* = 8.5 Hz, 2H). The data is in good accordance with that reported in the literature.[7]

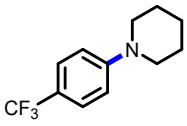

**1-(4-(Trifluoromethyl)phenyl)piperidine (8ac).**

The crude product was purified by column chromatography (silica gel, Hexane/EtOAc = 50:1) to afford 78.8 mg white crystals, yield: 86 %). $^1$H NMR (400 MHz, $CDCl_3$) δ 7.45 (d, *J* = 8.4 Hz, 2H), 6.91 (d, *J* = 8.4 Hz, 2H), 3.27 (t, *J* = 5.2 Hz, 4H), 1.68 (m, 6H). The data is in good accordance with that reported in the literature.[9]

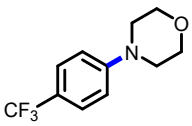

**4-(4-(Trifluoromethyl)phenyl)morpholine (8ad).**

The crude product was purified by column chromatography (silica gel, Hexane/EtOAc = 20:1) to afford 86.9 mg white crystals, yield: 94%). $^1$H NMR (500 MHz, $CDCl_3$) *δ* 7.53 (t, *J* = 8.5 Hz, 2H), 6.94 (d, *J* = 8.5 Hz, 2H), 3.89 (t, *J* = 4.5 Hz, 4H), 3.26 (t, *J* = 5.0 Hz, 4H). The data is in good accordance with that reported in the literature.[7, 9]

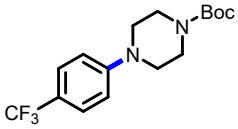

***tert*-Butyl 4-(4-(trifluoromethyl)phenyl)piperazine-1-carboxylate (8ae).**

The crude product was purified by column chromatography (silica gel, Hexane/EtOAc = 5:1) to afford 113.6 mg white crystals, yield: 86%). $^1$H NMR (500 MHz, $CDCl_3$) *δ* 7.52 (t, *J* = 8.5 Hz, 2H), 6.95 (d, *J* = 8.5 Hz, 2H), 3.61 (t, *J* = 5.0 Hz, 4H), 3.26 (t, *J* = 5.0 Hz, 4H), 1.51 (s, 9H). The data is in good accordance with that reported in the literature.[8, 9]

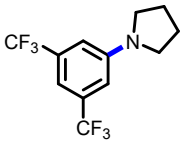

**1-(3,5-bis(trifluoromethyl)phenyl)pyrrolidine (8ba).**

The crude product was purified by column chromatography (silica gel, Hexane/EtOAc = 50:1) to afford 105.0 mg colorless oil, yield: 92 %). $^1$H NMR (500 MHz, $CDCl_3$) *δ* 7.28 (s, 1H), 6.88 (s, 2H), 3.37 (t, *J* = 6.5 Hz, 4H), 2.11-2.07 (m, 4H). The data is in good accordance with that reported in the literature.[10]

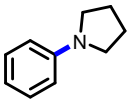

**1-Phenylpyrrolidine (8ca).**

The crude product was purified by column chromatography (silica gel, Hexane/EtOAc = 50:1) to afford 54.8 mg colorless oil, yield: 93%). $^1$H NMR (500 MHz, $CDCl_3$) *δ* 7.30 (t, *J* = 7.5 Hz, 2H), 6.73 (t, *J* = 7.0 Hz, 1H), 6.64 (d, *J* = 8.0 Hz, 2H), 3.35 (t, *J* = 6.5 Hz, 4H), 2.08-2.05 (m, 4H). The data is in good accordance with that reported in the literature.[11]

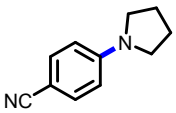

**4-(Pyrrolidin-1-yl)benzonitrile (8da).**

The crude product was purified by column chromatography (silica gel, Hexane/EtOAc = 20:1) to afford 61.1 mg white solid, yield: 89 %). $^1$H NMR (500 MHz, $CDCl_3$) $\delta$ 7.46 (d, $J$ = 9.0 Hz, 2H), 6.51 (d, $J$ = 9.0 Hz, 2H), 3.34 (t, $J$ = 7.0 Hz, 4H), 2.07-2.05 (m, 4H). The data is in good accordance with that reported in the literature.[11]

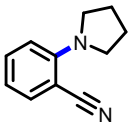

**2-(pyrrolidin-1-yl)benzonitrile (8ea).**

The crude product was purified by column chromatography (silica gel, Hexane/EtOAc = 20:1) to afford 42.7 mg white powder, yield: 62 %). $^1$H NMR (500 MHz, $CDCl_3$) $\delta$ 7.46 (dd, $J_1$ = 8.5 Hz, $J_2$ = 2.0 Hz, 1H), 7.34 (td, $J_1$ = 8.5 Hz, $J_2$ = 2.0 Hz, 1H), 6.66 (t, $J$ = 8.0 Hz, 2H), 3.62 (t, $J$ = 7.0 Hz, 4H), 2.04-2.01 (m, 4H). $^{13}$C NMR (125 MHz, $CDCl_3$) $\delta$ 150.1, 135.8, 133.4, 127.7, 121.5, 115.9, 114.2, 94.4, 49.8, 25.8. The data is in good accordance with that reported in the literature.[12]

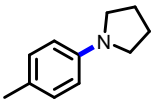

**1-(*p*-Tolyl)pyrrolidine (8fa).**

The crude product was purified by column chromatography (silica gel, Hexane/EtOAc = 50:1) to afford 45.7 mg white solid, yield: 71 %). $^1$H NMR (500 MHz, $CDCl_3$) $\delta$ 7.06 (d, $J$ = 8.0 Hz, 2H), 6.53 (d, $J$ = 8.0 Hz, 2H), 3.28 (t, $J$ = 6.5 Hz, 4H), 2.28 (s, 3H), 2.23-2.00 (m, 4H). The data is in good accordance with that reported in the literature.[8]

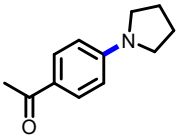

**1-(4-(Pyrrolidin-1-yl)phenyl)ethan-1-one (8ga).**

The crude product was purified by column chromatography (silica gel, Hexane/EtOAc = 50:1) to afford white crystals, the aryl bromide **4a** resulted 53.9 mg of the product, yield: 83%; the aryl chloride **4a'** resulted 59.1 mg of the product, yield: 91%). $^1$H NMR (500 MHz, $CDCl_3$) $\delta$ 7.89 (d, $J$ = 9.0 Hz, 2H), 6.53 (d, $J$ = 8.5 Hz, 2H), 3.39 (t, $J$ = 6.5 Hz, 4H), 2.53 (s, 3H), 2.27-2.05 (m, 4H). The data is in good accordance with that reported in the literature.[13]

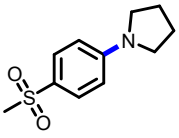

**1-(4-(Methylsulfonyl)phenyl)pyrrolidine (8ha).**

The crude product was purified by column chromatography (silica gel, Hexane/EtOAc = 3:1) to afford 82.0 mg white crystals, yield: 91%). $^1$H NMR (500 MHz, $CDCl_3$) $\delta$ 7.72 (t, $J$ = 8.5 Hz, 2H), 6.56 (d, $J$ = 9.0 Hz, 2H), 3.35 (t, $J$ = 6.5 Hz, 4H), 3.00 (s, 3H), 2.07-2.04 (m, 4H). $^{13}$C NMR (125 MHz, $CDCl_3$) $\delta$ 151.0, 129.1, 125.1, 111.0, 47.7, 45.2, 25.5. The data is in good accordance with that reported in the literature.[14]

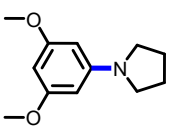

**1-(3,5-dimethoxyphenyl)pyrrolidine (8ia).**

The crude product was purified by column chromatography (silica gel, Hexane/EtOAc = 50:1) to afford 52 mg colorless oil, yield: 63 %). $^1$H NMR (500 MHz, $CDCl_3$) $\delta$ 5.89 (t, $J$ = 2.0 Hz, 1H), 5.79 (t, $J$ = 2.0 Hz, 2H), 3.81 (s, 6H), 3.29 (t, $J$ = 7.0 Hz, 4H), 2.02-1.99 (m, 4H). The data is in good accordance with that reported in the literature.[15]

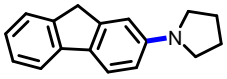

**1-(9*H*-fluoren-2-yl)pyrrolidine (8ja).**

The crude product was purified by column chromatography (silica gel, Hexane/EtOAc = 50:1) to afford 71.5 mg white solid, yield: 76%). $^1$H NMR (500 MHz, $CDCl_3$) $\delta$ 7.65-7.63 (m, 2H), 7.47 (d, $J$ = 7.5 Hz, 1H), 7.32 (t, $J$ = 8.0 Hz, 1H), 7.17 (t, $J$ = 7.5 Hz, 1H), 6.80 (s, 1H), 6.62 (dd, $J_1$ = 8.0 Hz, $J_2$ = 2.5 Hz, 1H), 3.87 (s, 2H), 3.38 (t, $J$ = 6.5 Hz, 4H), 2.07-2.05 (m, 4H). $^{13}$C NMR (125 MHz, $CDCl_3$) $\delta$ 145.2, 142.1, 126.6, 124.6, 124.4, 120.6, 119.6, 118.2, 110.6, 110.3, 108.1, 106.3, 47.9, 37.1, 25.5.

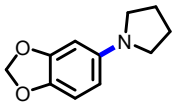

**1-(benzo[d][1,3]dioxol-5-yl)pyrrolidine (8ka).**

The crude product was purified by column chromatography (silica gel, Hexane/EtOAc = 50:1) to afford 62.7 mg white solid, yield: 82%). $^1$H NMR (500 MHz, $CDCl_3$) $\delta$ 6.75 (d, $J$ = 8.5 Hz, 1H), 6.26 (d, $J$ = 2.0 Hz, 1H), 6.00 (dd, $J_1$ = 8.5 Hz, $J_2$= 2.5 Hz, 1H), 5.88 (s, 2H), 3.25 (t, $J$ = 6.5 Hz, 4H), 2.03-2.00 (m, 4H). $^{13}$C NMR (125 MHz, $CDCl_3$) $\delta$ 148.3, 144.6, 138.1, 108.7, 103.0, 100.4, 94.5, 48.4, 25.4. The data is in good accordance with that reported in the literature.[16]

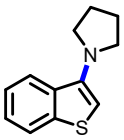

**1-(Benzo[b]thiophen-3-yl)pyrrolidine (8la).**

The crude product was purified by column chromatography (silica gel, Hexane/EtOAc = 5:1) to afford 73.2 mg yellow oil, yield: 90%). $^1$H NMR (500 MHz, $CDCl_3$) $\delta$ 8.01 (d, $J$ = 7.5 Hz, 1H), 7.82 (d, $J$ = 7.5 Hz, 1H), 7.38-7.33 (m, 2H), 6.23 (s, 1H), 3.47 (t, $J$ = 3.5 Hz, 4H), 2.08-2.03 (m, 4H). $^{13}$C NMR (125 MHz, $CDCl_3$) $\delta$ 145.1, 139.8, 134.5, 124.13, 123.3, 123.2, 123.00, 98.9, 51.7, 25.0.

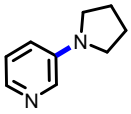

**3-(Pyrrolidin-1-yl)pyridine (8ma).**

The crude product was purified by column chromatography (silica gel, Hexane/EtOAc = 2:1) to afford 43.2 mg white solid, yield: 73 %). $^1$H NMR (500 MHz, $CDCl_3$) $\delta$ 8.00 (d, $J$ = 3.0 Hz, 1H), 7.94 (d, $J$ = 5.0 Hz, 1H), 7.11 (d, $J_1$ = 8.5 Hz, $J_2$ = 4.5 Hz, 1H), 6.81 (d, $J_1$ = 8.0 Hz, $J_2$ = 2.5 Hz, 1H), 3.31 (t, $J$ = 7.0 Hz, 4H), 2.05-2.02 (m, 4H). The data is in good accordance with that reported in the literature.[8,13,14]

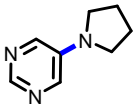

**5-(Pyrrolidin-1-yl)pyrimidine (8na).**

The crude product was purified by column chromatography (silica gel, Hexane/EtOAc = 2:1) to afford 51.9 mg white solid, yield: 87 %). $^1$H NMR (500 MHz, $CDCl_3$) $\delta$ 8.55 (s, 1H), 8.05 (s, 2H), 3.31 (t, $J$ = 6.5 Hz, 4H), 2.07-2.04 (m, 4H). The data is in good accordance with that reported in the literature.[14]

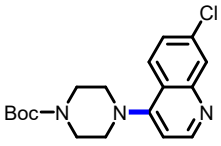

***tert*-Butyl 4-(7-chloroquinolin-4-yl)piperazine-1-carboxylate (8of).**

The crude product was purified by column chromatography (silica gel, Hexane/EtOAc = 3:1) to afford 119.4 mg white solid, yield: 86%. $^1$H NMR (500 MHz, $CDCl_3$) $\delta$ 8.76 (s, 1H), 8.07 (s, 1H), 7.97 (d, $J$ = 9.0 Hz, 1H), 7.46

(d, *J* = 9.0 Hz, 1H), 6.86 (d, *J* = 5.0 Hz, 1H), 3.73 (t, *J* = 5.0 Hz, 4H), 3.18 (t, *J* = 5.0 Hz, 4H), 1.52 (s, 9H). $^{13}$C NMR (125 MHz, $CDCl_3$) *δ* 156.8, 154.7, 151.9, 150.1, 135.1, 129.0, 126.5, 124.9, 121.9, 109.2, 80.3, 52.1, 28.4.

## General Procedure of the Couplings of Aryl Aldehydes and Amines

To a 100 mL round-bottomed flask, amine (0.8 mmol, 2.0 equiv), aryl aldehyde (0.4 mmol, 1.0 equiv), **5b** (1.0 mg, 0.5 mol%) and DMF (2 mL) were added. The sample preparation was performed in atmospheric conditions. The flask was sealed with a septum with an air balloon attached. Then the mixture was stirred at room temperature under the irradiation with two 12 W Blue LED lights, distance ~ 5 cm. After 16 hours, the mixture was poured into water, and extracted with EtOAc (3 × 10 mL). The combined organic layers were washed with water, dried over anhydrous $Na_2SO_4$ and concentrated under reduced pressure. Purifications of the crude products by column chromatography (silica gel) using hexane/EtOAc as eluent to afforded the desired products which was further dried *under vacuo* for NMR analyses.

### Synthesis of amides

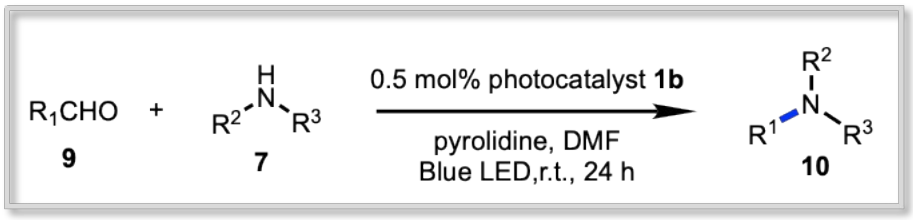


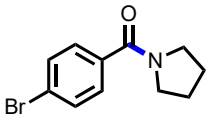


**(4-Bromophenyl)(pyrrolidin-1-yl)methanone (10aa)**.
The crude product was purified by column chromatography (silica gel, Hexane/EtOAc = 2:1) to afford 91.1 mg white crystals, yield: 90%). $^1$H NMR (500 MHz, $CDCl_3$) *δ* 7.56 (d, *J* = 8.0 Hz, 2H), 7.43 (d, *J* = 8.0 Hz, 2H), 3.66 (t, *J* = 7.0 Hz, 2H), 3.43 (t, *J* = 6.5 Hz, 2H), 2.00-1.90 (m, 4H). The data is in good accordance with that reported in the literature.[17]

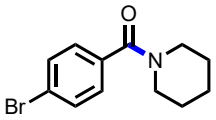


**(4-Bromophenyl)(piperidin-1-yl)methanone (10ab)**.
The crude product was purified by column chromatography (silica gel, Hexane/EtOAc = 2:1) to afford 94.0 mg white crystals, yield: 88%). $^1$H NMR (500 MHz, $CDCl_3$) *δ* 7.55 (d, *J* = 8.0 Hz, 2H), 7.29 (d, *J* = 8.0 Hz, 2H), 3.71 (s, 2H), 3.34 (s, 2H), 1.71-1.53 (m, 6H). The data is in good accordance with that reported in the literature.[18]

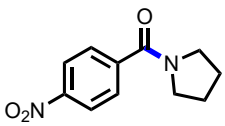


**(4-Nitrophenyl)(pyrrolidin-1-yl)methanone (10ba)**.
The crude product was purified by column chromatography (silica gel, Hexane/EtOAc = 1:1) to afford 81.0 mg yellow crystals, yield: 92%). $^1$H NMR (500 MHz, $CDCl_3$) *δ* 8.29 (d, *J* = 8.0 Hz, 2H), 7.70 (d, *J* = 8.0 Hz, 2H), 3.69 (t, *J* = 7.0 Hz, 2H),

3.40 (t, *J* = 6.5 Hz, 2H), 2.03-1.93 (m, 4H). The data is in good accordance with that reported in the literature.[17]

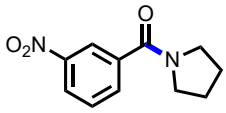

**(3-Nitrophenyl)(pyrrolidin-1-yl)methanone (10ca)**.

The crude product was purified by column chromatography (silica gel, Hexane/EtOAc = 1:1) to afford 66.0 mg yellow crystals, yield: 75%). $^1$H NMR (400 MHz, $CDCl_3$) $\delta$ 8.37 (s, 1H), 8.27 (ddd, *J* = 8.2, 2.3, 1.1 Hz, 1H), 7.90 – 7.84 (m, 1H), 7.60 (dd, *J* = 8.2, 7.6 Hz, 1H), 3.66 (t, *J* = 6.9 Hz, 2H), 3.43 (t, *J* = 6.5 Hz, 2H), 2.05 – 1.88 (m, 4H).

$^{13}$C NMR (100 MHz, $CDCl_3$) $\delta$ 167.1, 148.1, 138.8, 133.4, 129.8, 124.7, 122.4, 49.7, 46.6, 26.6, 24.5.

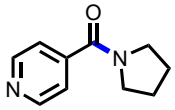

**Pyridin-4-yl(pyrrolidin-1-yl)methanone (10da)**.

The crude product was purified by column chromatography (silica gel, Hexane/EtOAc = 1:1) to afford 58.5 mg white crystals, yield: 83%). $^1$H NMR (500 MHz, $CDCl_3$) $\delta$ 8.71 (d, *J* = 3.5 Hz, 2H), 7.39 (dd, $J_1$ = 4.5 Hz, $J_2$ = 1.5 Hz, 2H), 3.67 (t, *J* = 7.0 Hz, 2H), 3.40 (t, *J* = 7.0 Hz, 2H), 2.02-1.91 (m, 4H). The data is in good accordance with that reported in the literature.[17]

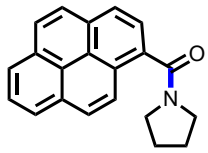

**Pyren-2-yl(pyrrolidin-1-yl)methanone (10ea)**.

The crude product was purified by column chromatography (silica gel, Hexane/EtOAc = 2:1) to afford 93.3 mg white crystals, yield: 78%). $^1$H NMR (500 MHz, $CDCl_3$) $\delta$ 8.25-8.21 (m, 3H), 8.15-8.00 (m, 6H), 3.92 (t, *J* = 7.0 Hz, 2H), 3.43 (t, *J* = 7.0 Hz, 2H), 2.10-2.05 (m, 2H), 1.90-1.84 (m, 2H). $^{13}$C NMR (125 MHz, $CDCl_3$) $\delta$ 169.8, 132.3, 131.7, 131.2, 130.9, 128.7, 128.1, 127.2, 127.0, 126.3, 125.7, 125.5, 124.8, 124.7, 124.6, 124.1, 123.8, 48.7, 45.9, 26.1, 24.7. The data is in good accordance with that reported in the literature.[17]

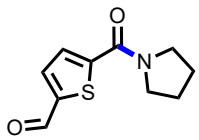

**5-(Pyrrolidine-1-carbonyl)thiophene-2-carbaldehyde (10fa)**.

The crude product was purified by column chromatography (silica gel, Hexane/EtOAc = 2:1) to afford 41.8 mg white crystals, yield: 50%). $^1$H NMR (500 MHz, $CDCl_3$) $\delta$ 9.98 (s, 1H), 7.75 (d, *J* = 3.5 Hz, 1H), 7.62 (d, *J* = 3.5 Hz, 1H), 3.77 (t, *J* = 6.5 Hz, 2H), 3.71 (t, *J* = 6.5 Hz, 2H), 2.07-1.98 (m, 4H). $^{13}$C NMR (125 MHz, $CDCl_3$) $\delta$ 183.3, 160.8, 146.9, 145.3, 135.0, 130.2, 49.1, 47.5, 26.7, 24.1.

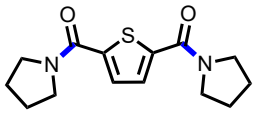

**Thiophene-2,5-diylbis(pyrrolidin-1-ylmethanone) (10faa)**.

The crude product was purified by column chromatography (silica gel, Hexane/EtOAc = 2:1) to afford 24.5 mg white crystals, yield: 22%). $^1$H NMR (500 MHz, $CDCl_3$) $\delta$ 7.50 (s, 2H), 3.78 (t, *J* = 7.0 Hz, 4H), 3.71 (t, *J* = 6.5 Hz, 4H), 2.05-1.94 (m, 8H). $^{13}$C NMR (125 MHz, $CDCl_3$) $\delta$ 161.3, 141.9, 129.5, 49.0, 47.4, 26.7, 24.1.

## Mechanistic Studies

### Mechanism of amination

In light of the fact that the photocatalyst **1b** only displayed reversible reductive activities, the mostly likely reaction model for the photocatalyst is through a reductive quenching cycle, that interacts with DABCO to abstract a singlet electron, and with a Ni catalytic cycle to transfer a singlet electron. However, it is questionable for the valence of Ni complex involved in the reductive elimination step, i.e. the possible actual complex, whether through Ni(II) or Ni(III) reductive elimination, which is of great challenge to achieved. The earlier work from the Macmillan group proposed a Ni(II)-reductive elimination,[7] but the pioneer work from the Hillhouse group[19] and the recent work from the Zargarian group[20] demonstrated that Ni(III) amido complex could undergo more rapid C-N bond formation than their Ni(II) congeners. More importantly, the very recent work of Macmillan and co-workers revealed a more rational reaction mechanism of Ni(III)-reductive elimination by take advantage of transient absorption technology along with electrochemistry, once again highlighted the more likely reaction pathway of Ni(III) complex engaging in organometallic elementary step for the amination approach.[21] Therefore, we believed that in the presence of our organic photocatalyst, for the Ni catalytic cycle, the Ni(I)-Ni(III) cycle is likely to be the most reasonable reaction pathway (Scheme S2 ). Firstly, the photoredox cycle is initiated by visible light, the formed $PC^{\bullet-}$ activates the Ni catalytic cycle by reducing $NiBr_2$•glyme to Ni(I), followed by accepting an electron from $PC^{\bullet-}$ to facilitate the accomplishment of reductive quenching photoredox cycle as well as generating the active Ni(0) catalyst. Through oxidative addition with the participation of Ar-Br **4**, Ni(II) complex is therefore formed. The $DABCO^{\bullet+}$ obtained from photocatalytic cycle is a competent oxidant which can readily oxidize Ni(II) to Ni(III), while the aniline substrate **5** or **7** simultaneously take place in the ligation to form Ni(III) complex. As stated above, the Ni(III) complex undergoes rapid elimination to forge the C-N bond, delivering the desired aminated products.

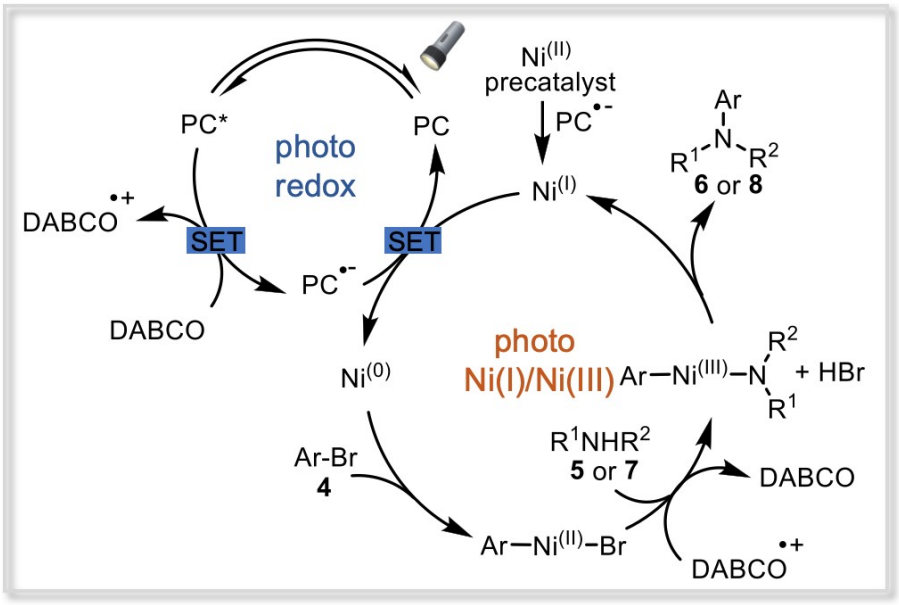

**Scheme S2** Proposed mechanism for the organophotocatalyst promoted the dual catalytic amination reaction. SET, single electron transfer.

To further confirm that the reaction undertake electron transfer (ET) process rather than energy transfer (EnT) process, a set of experiments were conducted. First of all, as known radical scavenger, TEMPO was utilised to confirm the involvement of radical species in the dual catalysis under the standard reaction conditions (eq. 1). The reaction only delivered only 10% of the **4aa** product, suggesting that the significant role of radical species in the reaction, which is a convincible proof for the ET reaction pathway.


(eq. 1)

Moreover, steady state UV-vis experiments that assessing the interaction of photocatalyst **1b** and metal catalyst $NiBr_2$•glyme were performed. The absorption spectrum of photocatalyst **1b** is similar to the spectrum of **1b** + $NiBr_2$•glyme irradiated for 10 minutes, but the later exhibits a remarkable decrease at the first two peaks (Figure S17), whereas the spectrum of the one irradiated for 18 hours showed complete disappearance of those two peaks which are likely resulted from the pyridine ring and the cyclic hexane ring from the parent anthrazoline. To demonstrate the interaction between photocatalyst and Ni catalyst, a set of absorption and emission experiments upon the solution of excessive Ni catalyst + photocatalyst **1a**-**1d** were performed, which suggests there are effective interactions between photocatalyst and $NiBr_2$•glyme by comparing both absorption and emission spectra (Figure S14-15, and S18-19), likely due to the ET process.

**Mechanism of amidation**

Radical scavenger TEMPO and oxygen scavenger DABCO were employed to determine whether the reaction undergoes energy transfer or electron transfer pathways [17,19], respectively. Amide **10aa** was obtained in 90% yield in the absence of radical scavenger or singlet oxygen scavenger (Scheme S3). Significant decrease in yields of amide **10aa** were observed when radical scavenger TEMPO was added. While sightly decrease of yield was found for the adding of singlet oxygen scavenger DABCO. Moreover, the room temperature phosphorescence measurement was carried out for **1b**. However, almost no signal can be obtained at room temperature. Overall, our observation may rule out the potential Energy transfer mechanism using a triplet excited photosensitizer[17]. Thus, the plausible SET mechanism was proposed in Scheme S4 in this system.

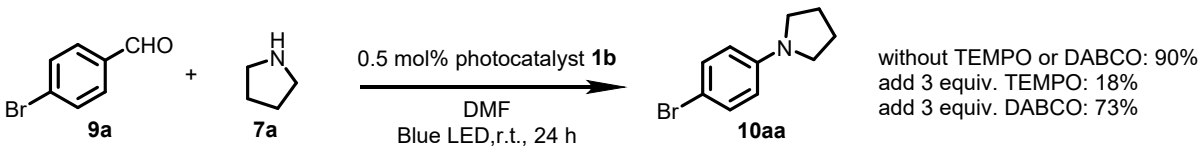

**Scheme S3** Control experiments of adding radical scavenger TEMPO and oxygen scavenger DABCO.

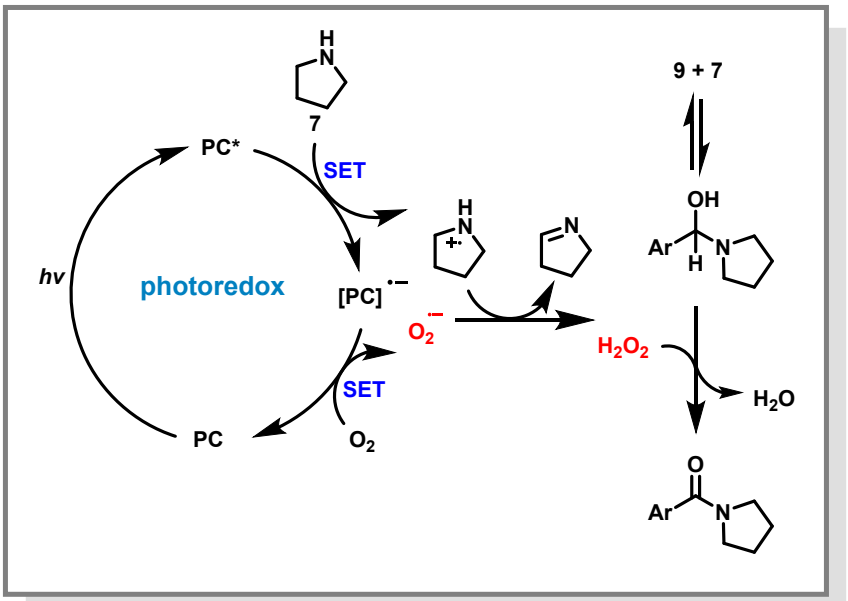


**Scheme S4** Proposed mechanism of photoinduced amidation.

**References:**


1. K.-H. Ong and B. Liu, *Molecules*, 2017, **22**, 897.
2. L. J. Farrugia, *J. Appl. Crystallogr*, 2012, **45**, 849-854.
3. C. Zhou, T. Lei, X.-Z. Wei, C. Ye, Z. Liu, B. Chen, C.-H. Tung and L.-Z. Wu, *J. Am. Chem. Soc.*, 2020, **142**, 16805-16813.
4. S. Ge, R. A. Green and J. F. Hartwig, *J. Am. Chem. Soc.*, 2014, **136**, 1617-1627.
5. S. Sharif, R. P. Rucker, N. Chandrasoma, D. Mitchell, M. J. Rodriguez, R. D. J. Froese and M. G. Organ, *Angew. Chem. Int. Ed.*, 2015, **54**, 9507-9511.
6. R. A. Escobar and J. W. Johannes, *Chem. Eur. J*, 2020, **26**, 5168-5173.
7. E. B. Corcoran, M. T. Pirnot, S. Lin, S. D. Dreher, D. A. DiRocco, I. W. Davies, S. L. Buchwald and D. W. MacMillan, *Science*, 2016, **353**, 279-283.
8. G. Manolikakes, A. Gavryushin and P. Knochel, *J. Org. Chem.*, 2008, **73**, 1429-1434.
9. C.-H. Lim, M. Kudisch, B. Liu and G. M. Miyake, *J. Am. Chem. Soc.*, 2018, **140**, 7667-7673.
10. D. M. Volochnyuk, A. N. Kostyuk, D. A. Sibgatulin and A. N. Chernega, *Tetrahedron*, 2005, **61**, 2839-2847.
11. C. Desmarets, R. Schneider and Y. Fort, *J. Org. Chem.*, 2002, **67**, 3029-3036.
12. I. Ghosh, J. Khamrai, A. Savateev, N. Shlapakov, M. Antonietti and B. König, *Science*, 2019, **365**, 360-366.
13. H. Zhang, Q. Cai and D. Ma, *J. Org. Chem.*, 2005, **70**, 5164-5173.
14. Y.-Y. Liu, D. Liang, L.-Q. Lu and W.-J. Xiao, *Chem. Commun.*, 2019, **55**, 4853-4856.
15. Y. Zhang, B. S. Takale, F. Gallou, J. Reilly and B. H. Lipshutz, *Chem. Sci.*, 2019, **10**, 10556-10561.
16. D. Wei, C. Netkaew, J. Wu and C. Darcel, *ChemCatChem*, 2020, **12**, 5449-5455.
17. X.-F. Wang, S.-S. Yu, C. Wang, D. Xue and J. Xiao, *Org. Bio. Chem.*, 2016, **14**, 7028-7037.

18. G. Pandey, S. Koley, R. Talukdar and P. K. Sahani, *Org. Lett.*, 2018, **20**, 5861-5865.
19. D. Leow, *Org. Lett.*, 2014, **16**, 5812-5815.
20 K. Koo and G. L. Hillhouse, *Organometallics*, 1995, **14**, 4421-4423.
21. J.-P. Cloutier and D. Zargarian, *Organometallics*, 2018, **37**, 1446-1455.
22. N. A. Till, L. Tian, Z. Dong, G. D. Scholes and D. W. C. MacMillan, *J. Am. Chem. Soc.*, 2020, **142**, 15830-15841.

# Copies of NMR Spectra of the Cross Coupling Products

**$^1$H NMR of 6ba**

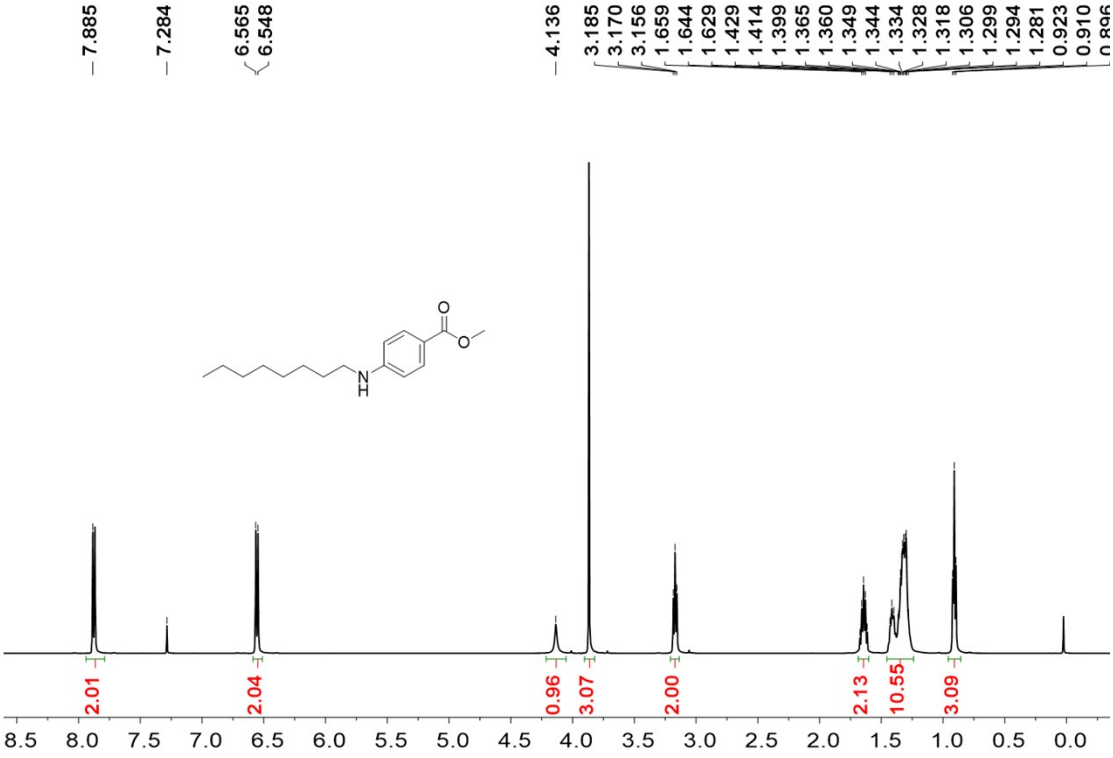


**$^1$H NMR of 6ab**

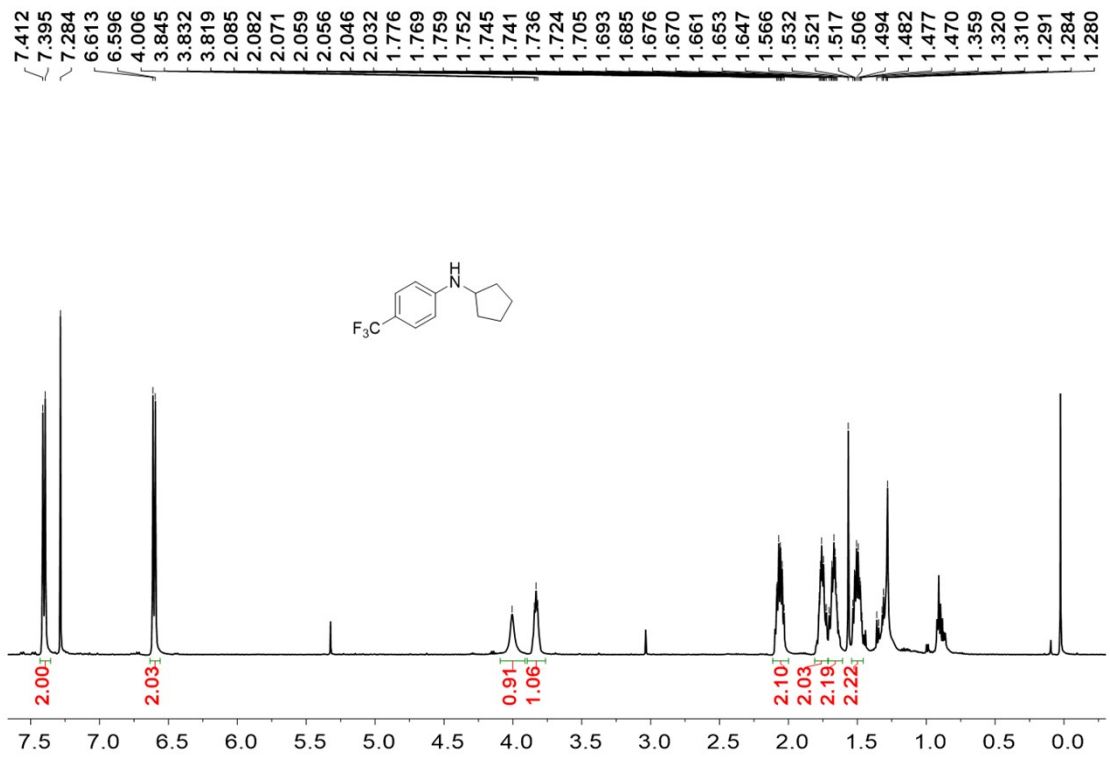

**$^1$H NMR of 6ac**

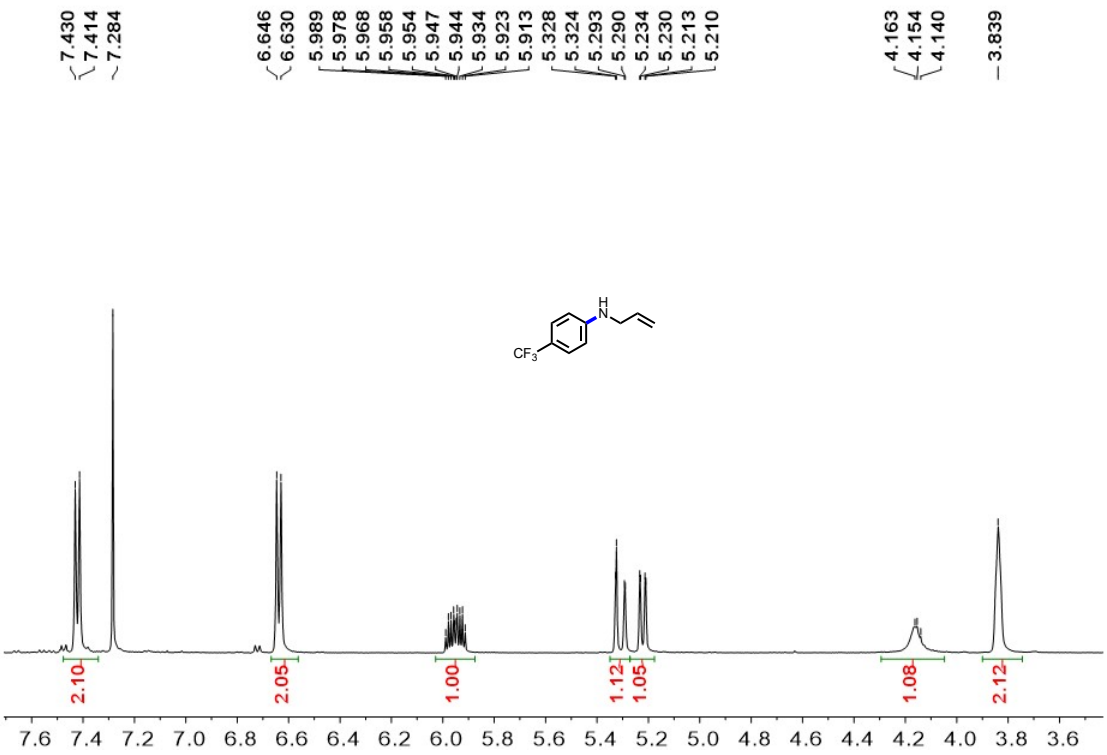


**$^1$H NMR of 6ad**

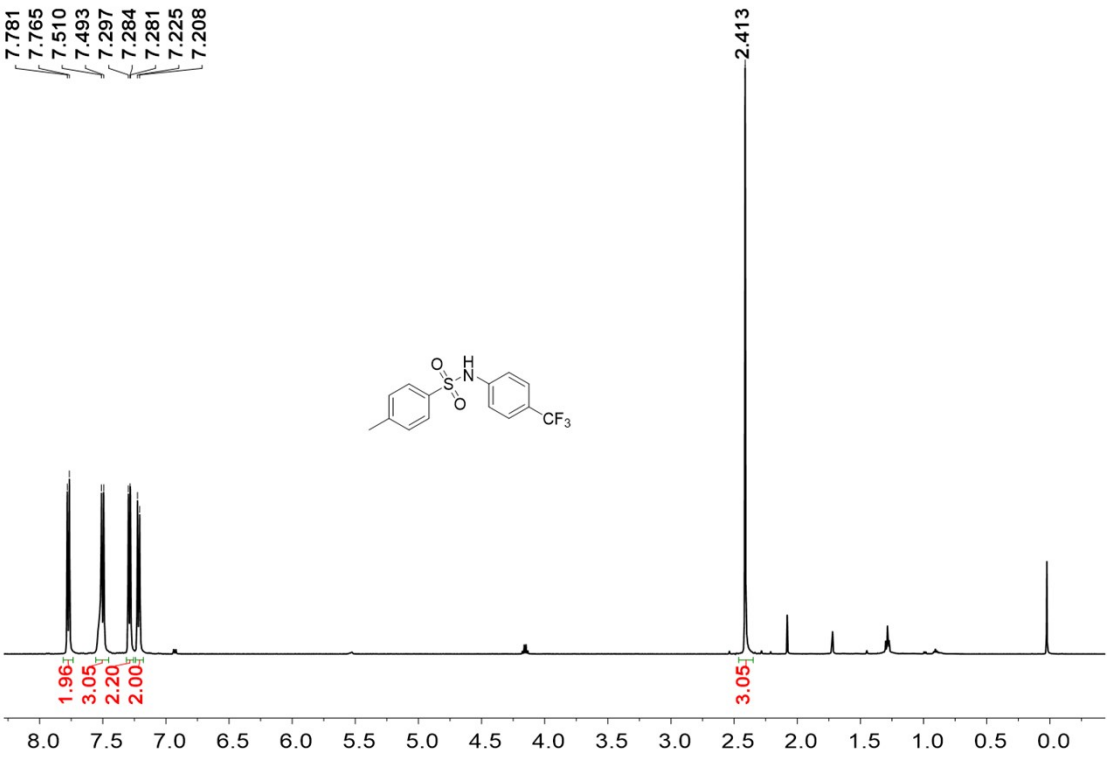

**$^1$H NMR of 6ae**

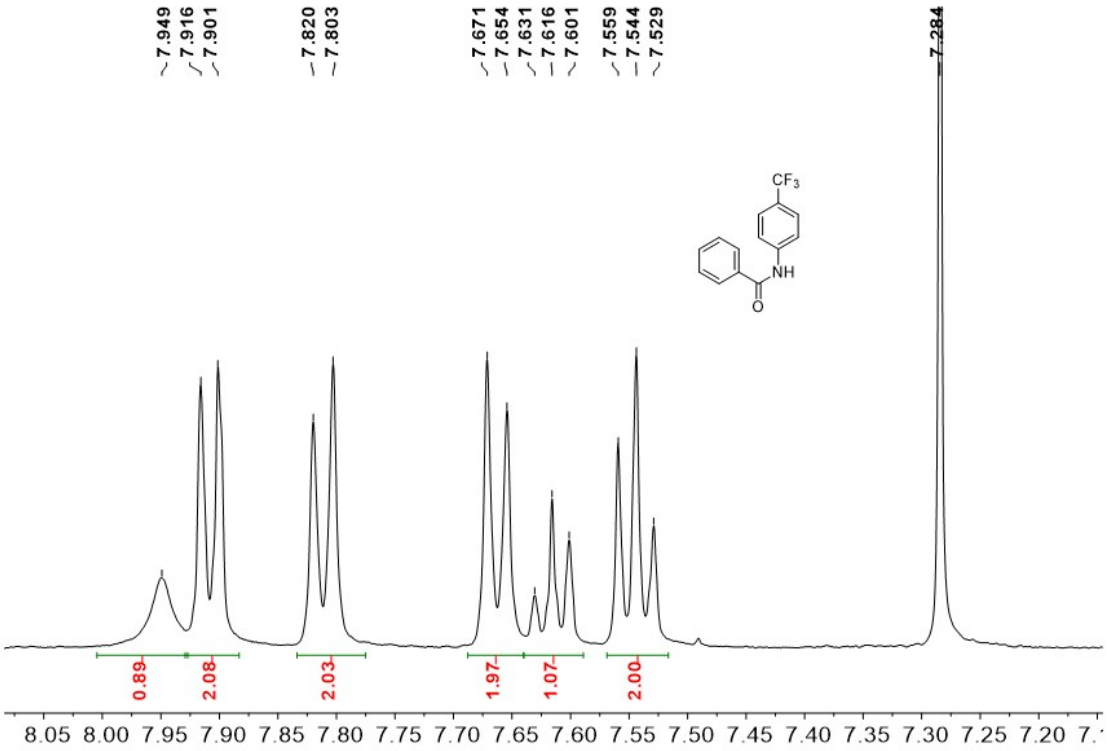


**$^1$H NMR of 6af**

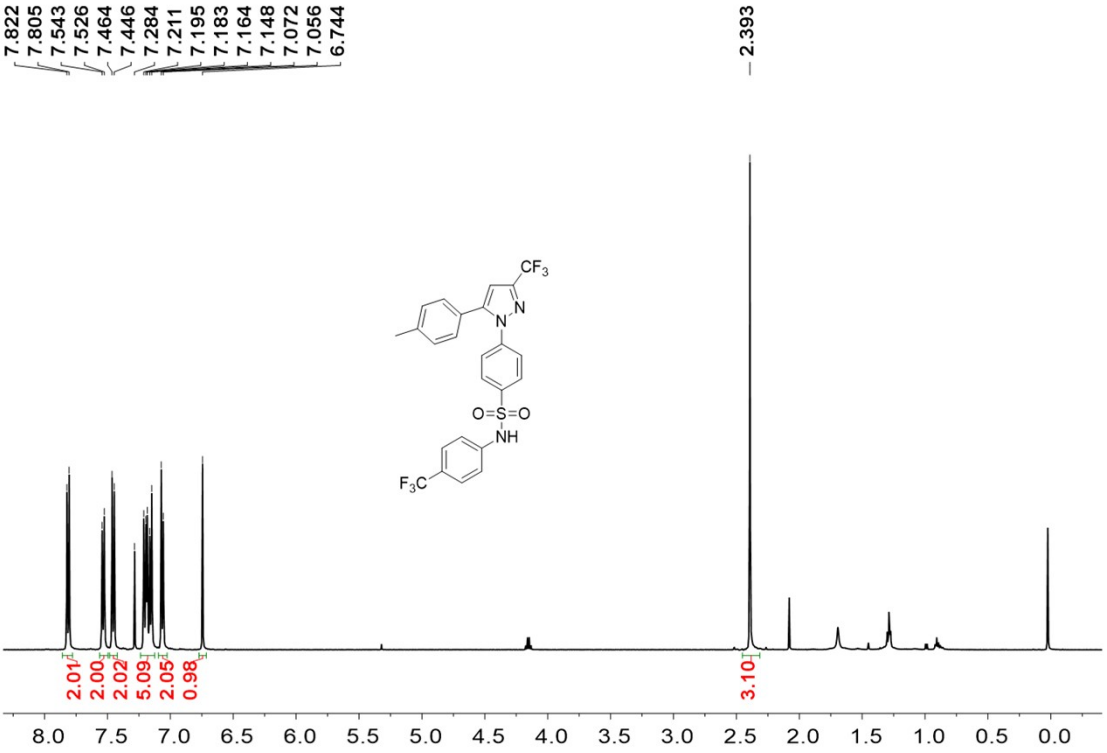

## $^{13}$C NMR of 6af

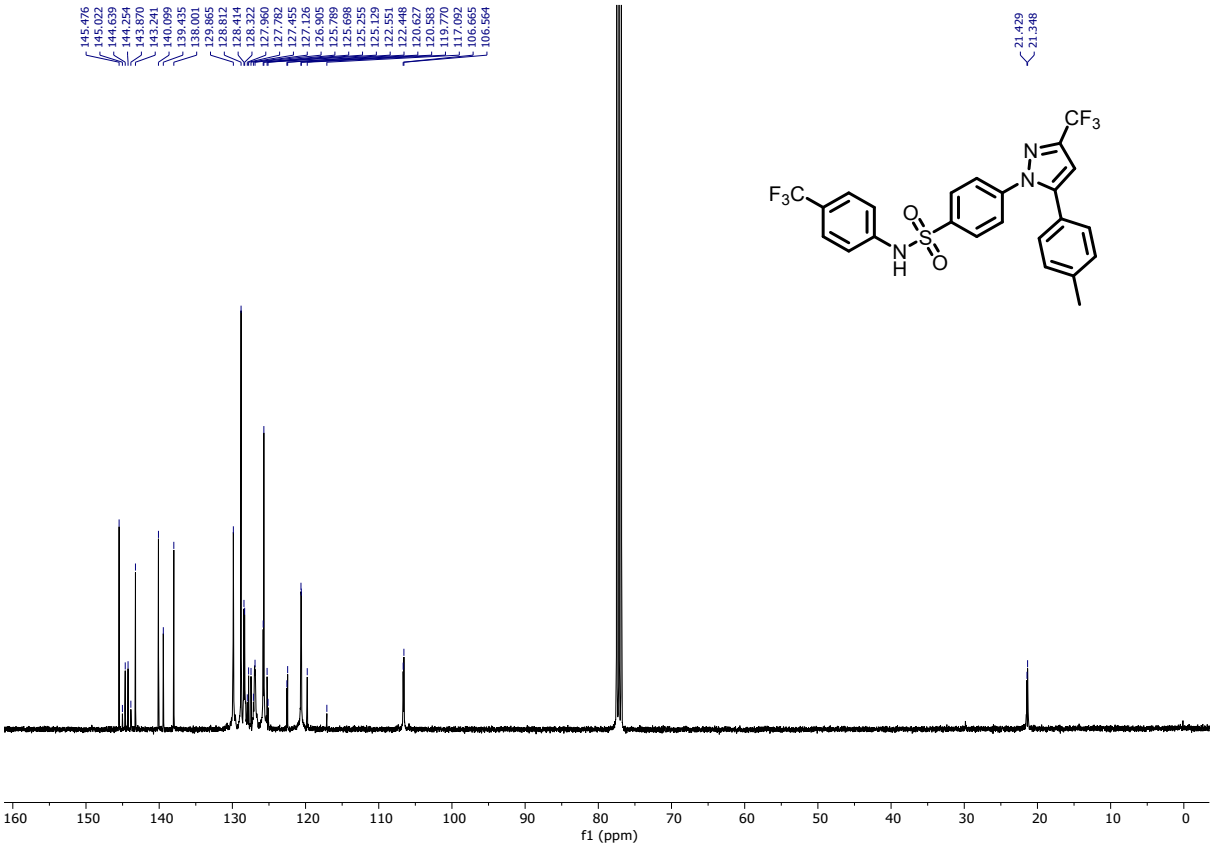


## $^{19}$F NMR of 6af

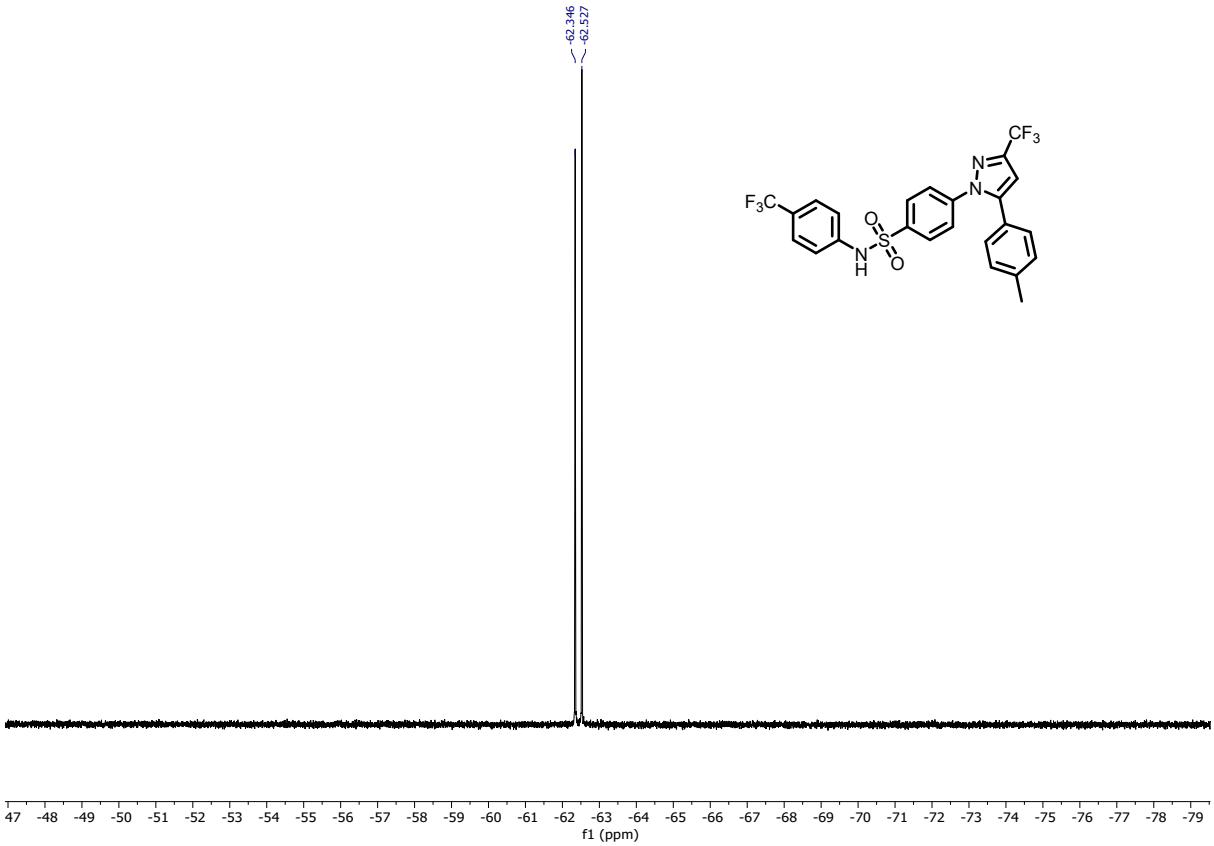
-62.346
-62.527
F3C
CF3
N
N
O
S
O
N
H
47 -48 -49 -50 -51 -52 -53 -54 -55 -56 -57 -58 -59 -60 -61 -62 -63 -64 -65 -66 -67 -68 -69 -70 -71 -72 -73 -74 -75 -76 -77 -78 -79
f1 (ppm)

## $^1$H NMR of 8aa

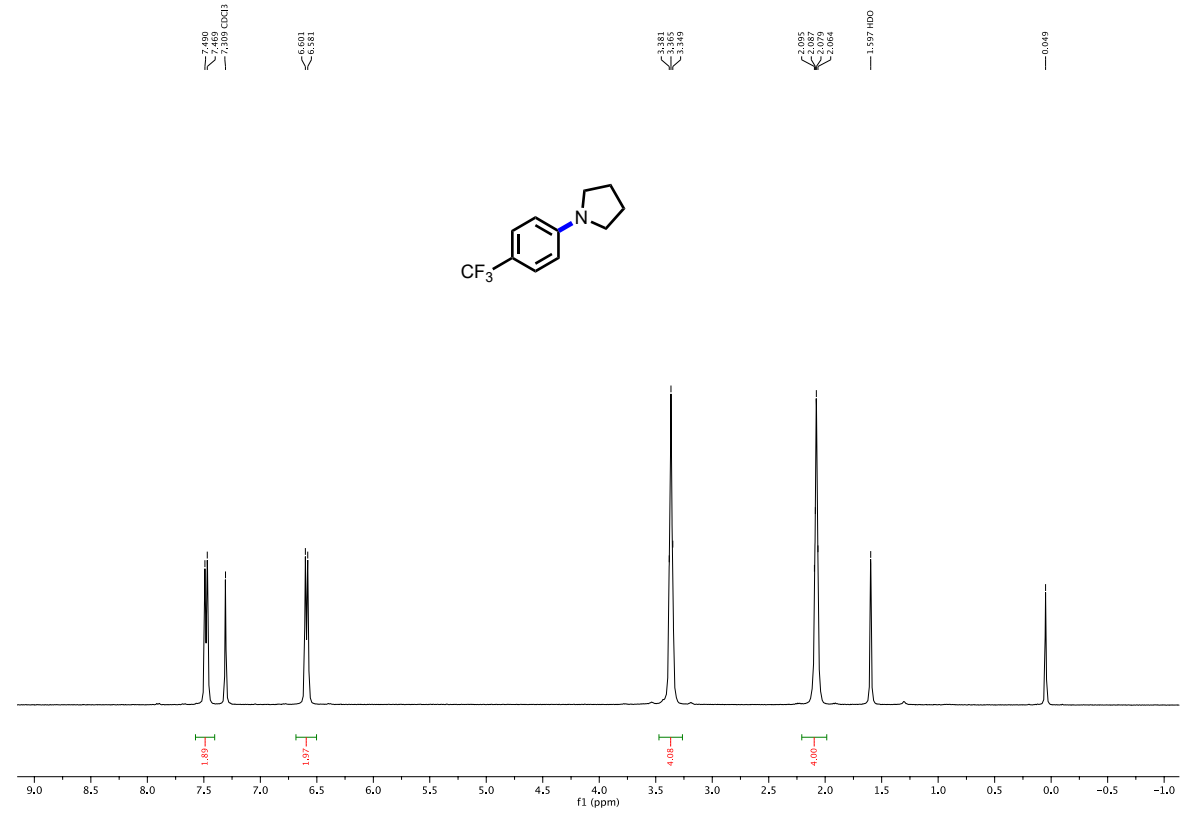


## $^1$H NMR of 8ab

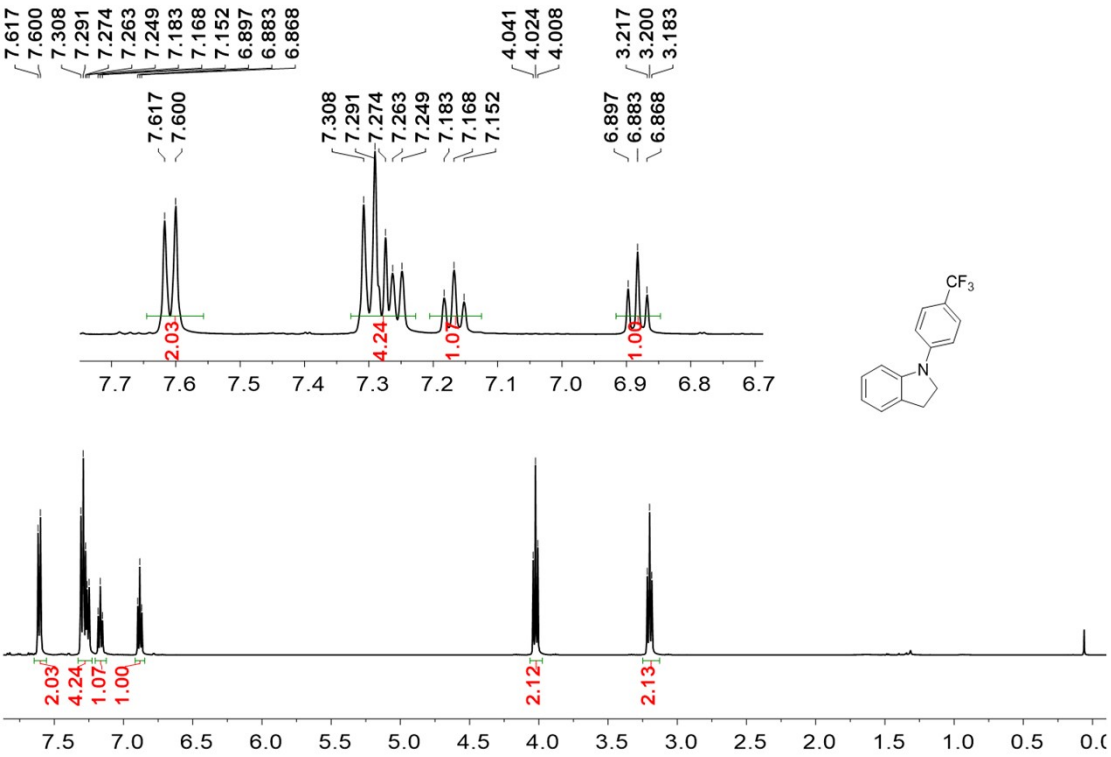

## $^1$H NMR of 8ac

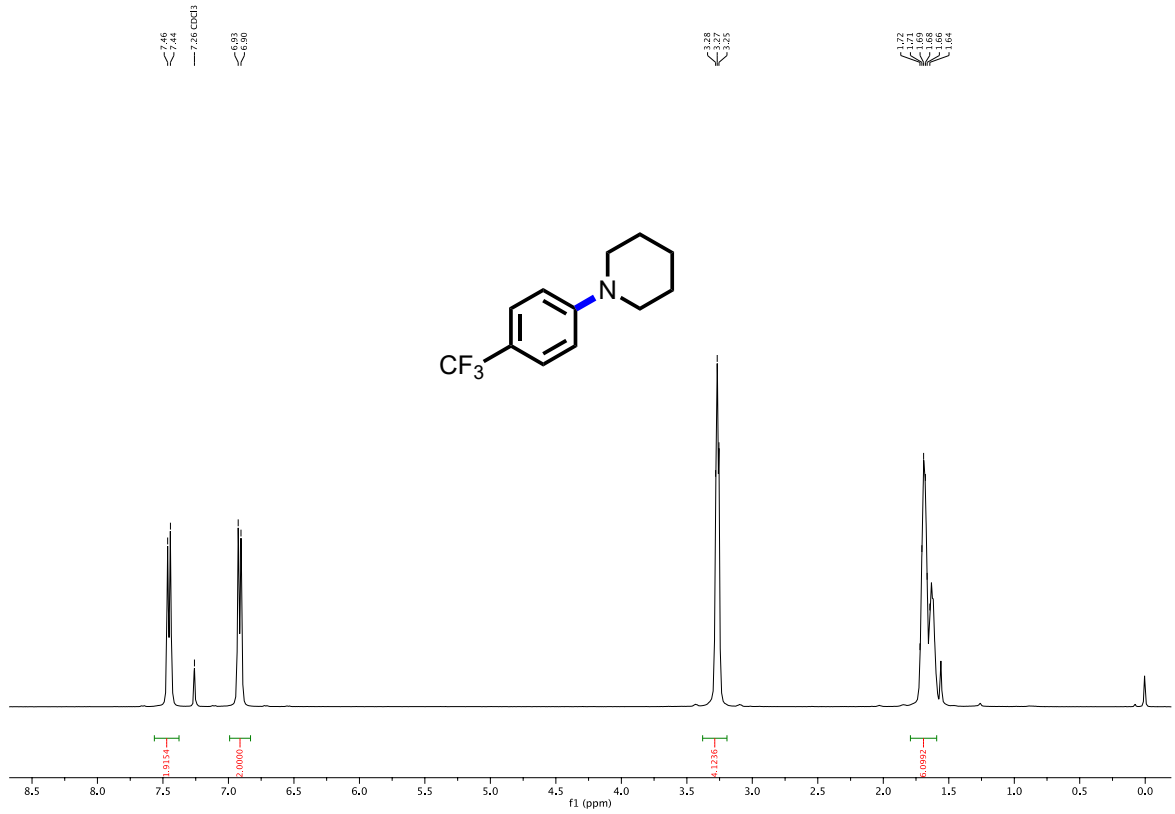


## $^1$H NMR of 8ad

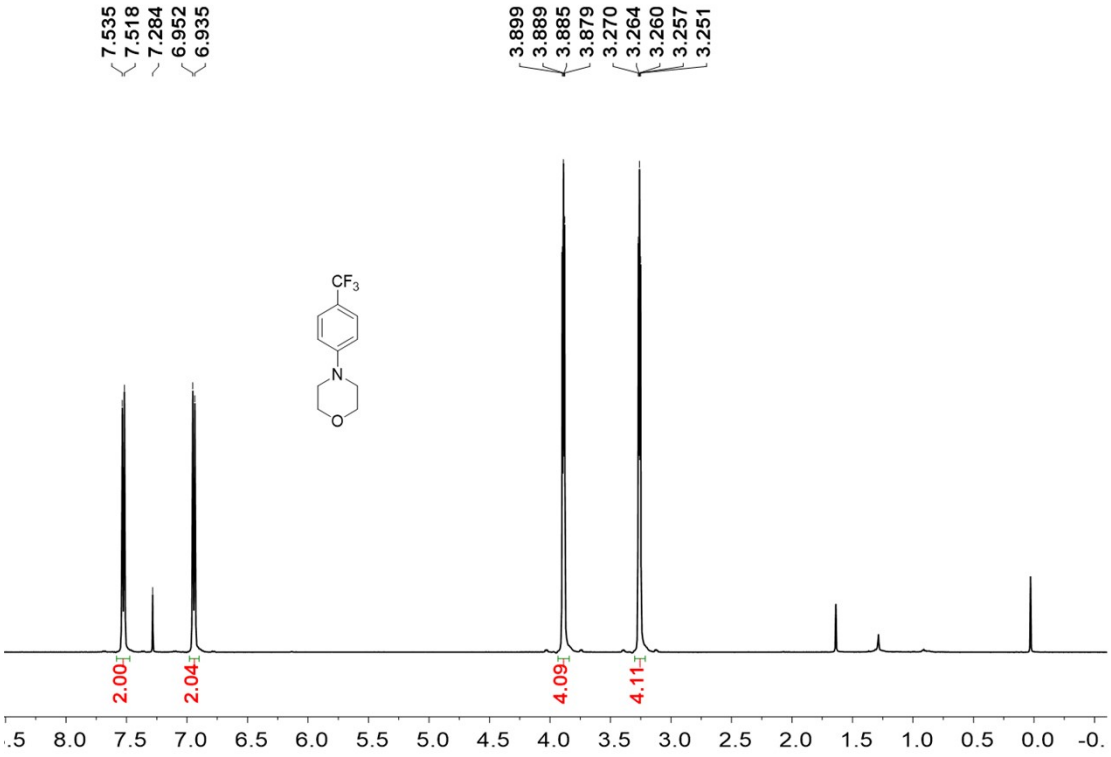

**$^1$H NMR of 8ae**

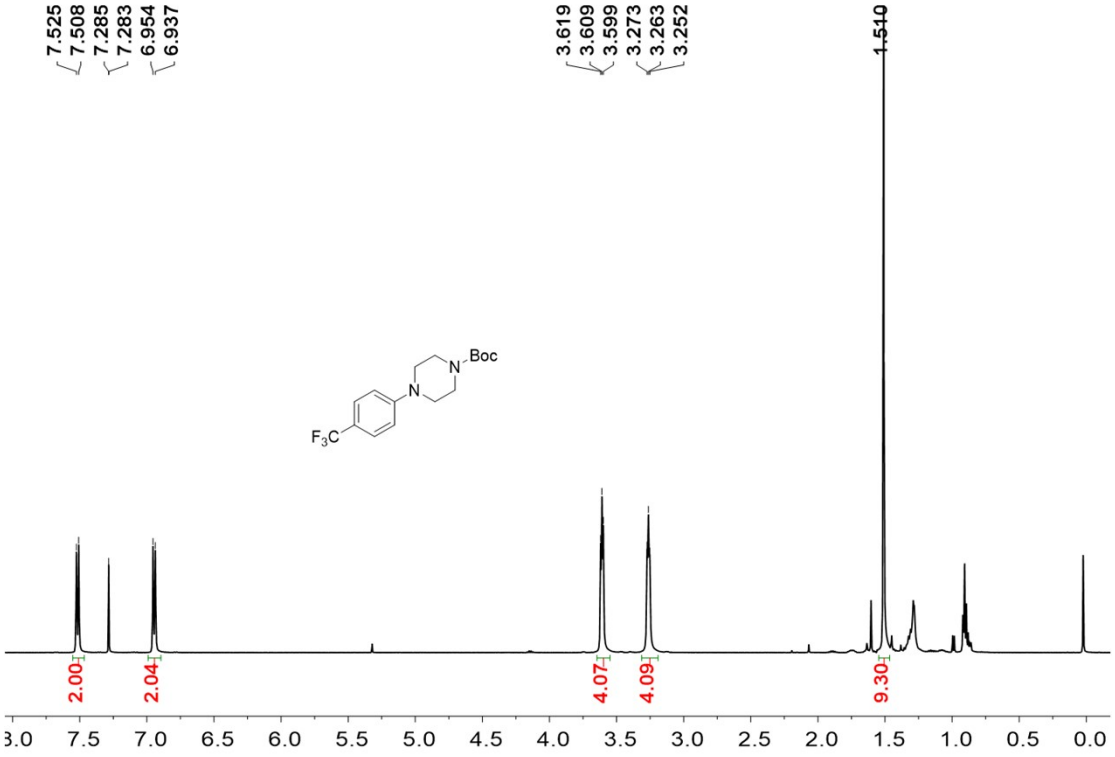


**$^1$H NMR of 8ba**

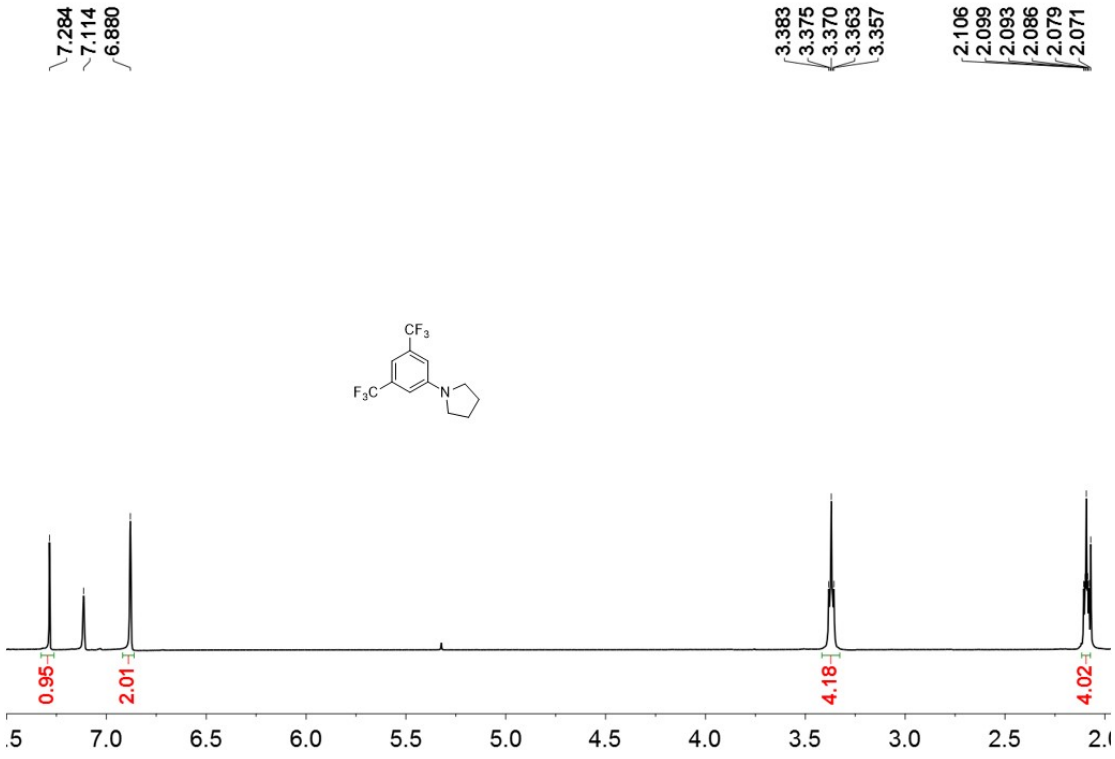

**$^1$H NMR of 8ca**

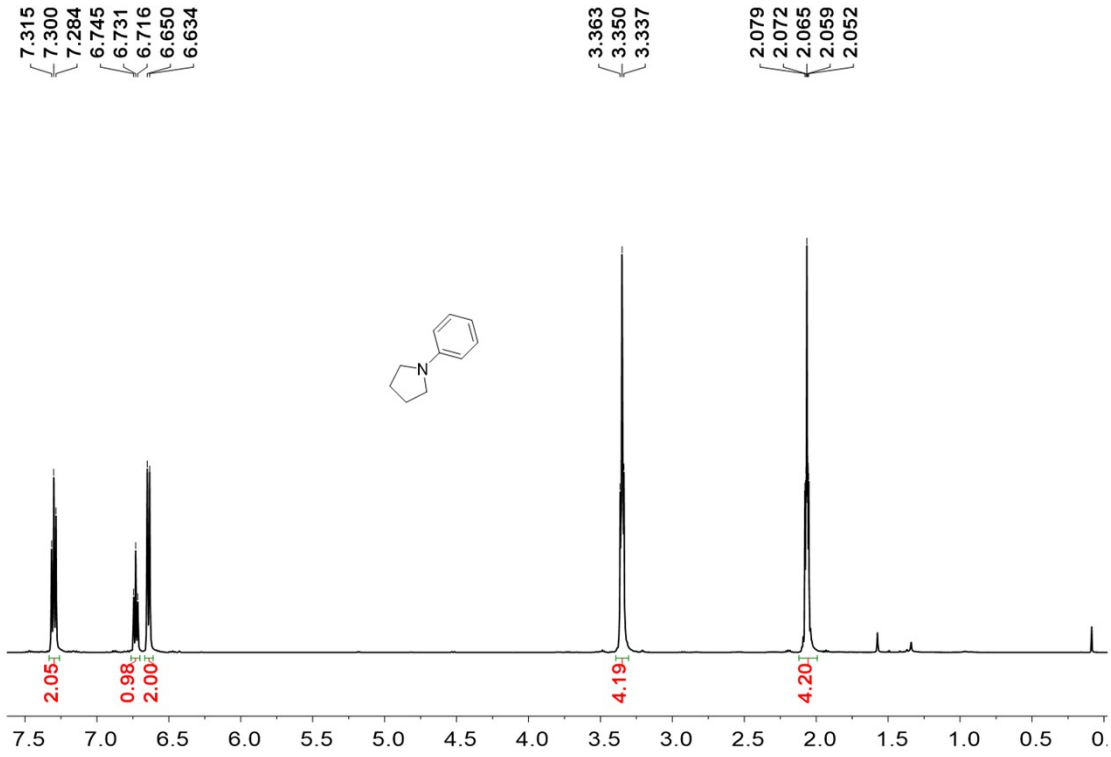


**$^1$H NMR of 8da**

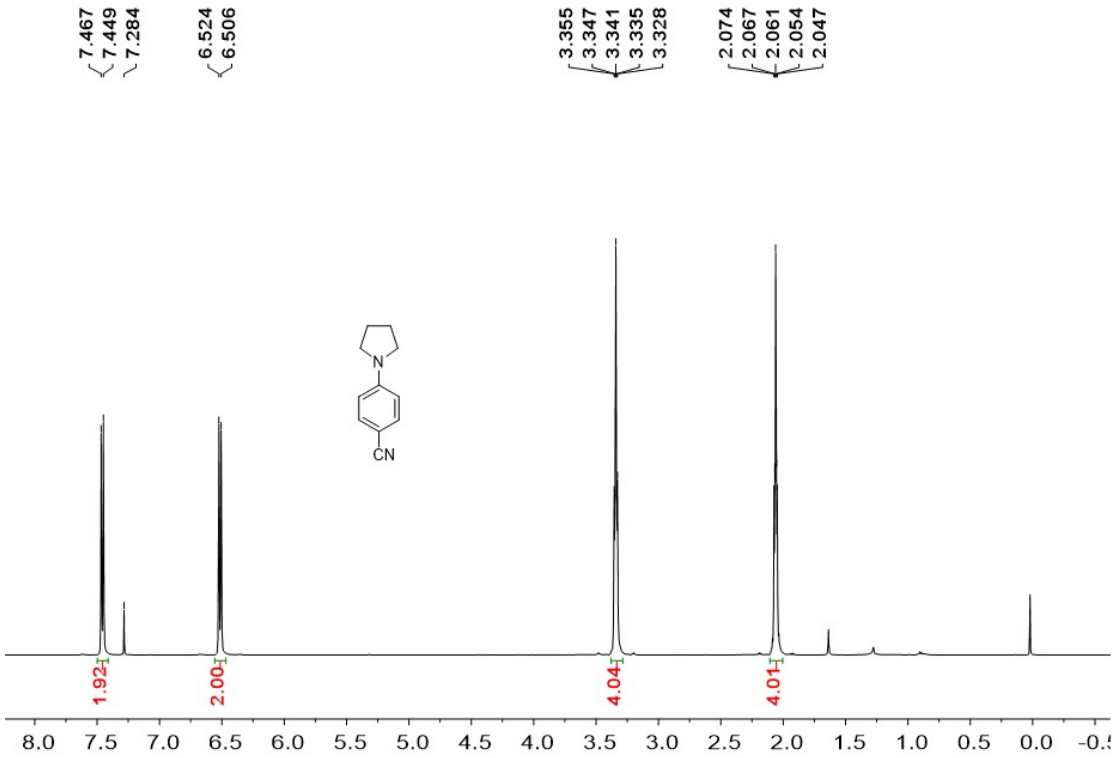

**$^{1}$H NMR of 8ea**

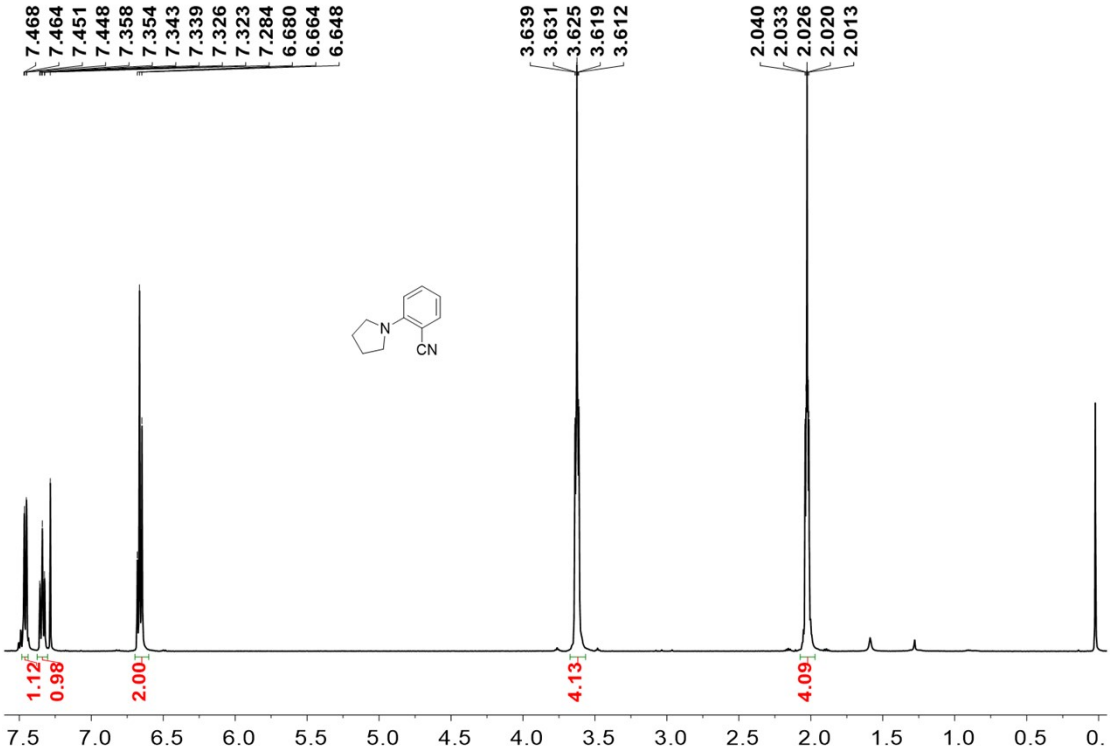
7.468
7.464
7.451
7.448
7.358
7.354
7.343
7.339
7.326
7.323
7.284
6.680
6.664
6.648
3.639
3.631
3.625
3.619
3.612
2.040
2.033
2.026
2.020
2.013
N
CN
1.12
0.98
2.00
4.13
4.09
7.5
7.0
6.5
6.0
5.5
5.0
4.5
4.0
3.5
3.0
2.5
2.0
1.5
1.0
0.5
0.

**$^{13}$C NMR of 8ea**

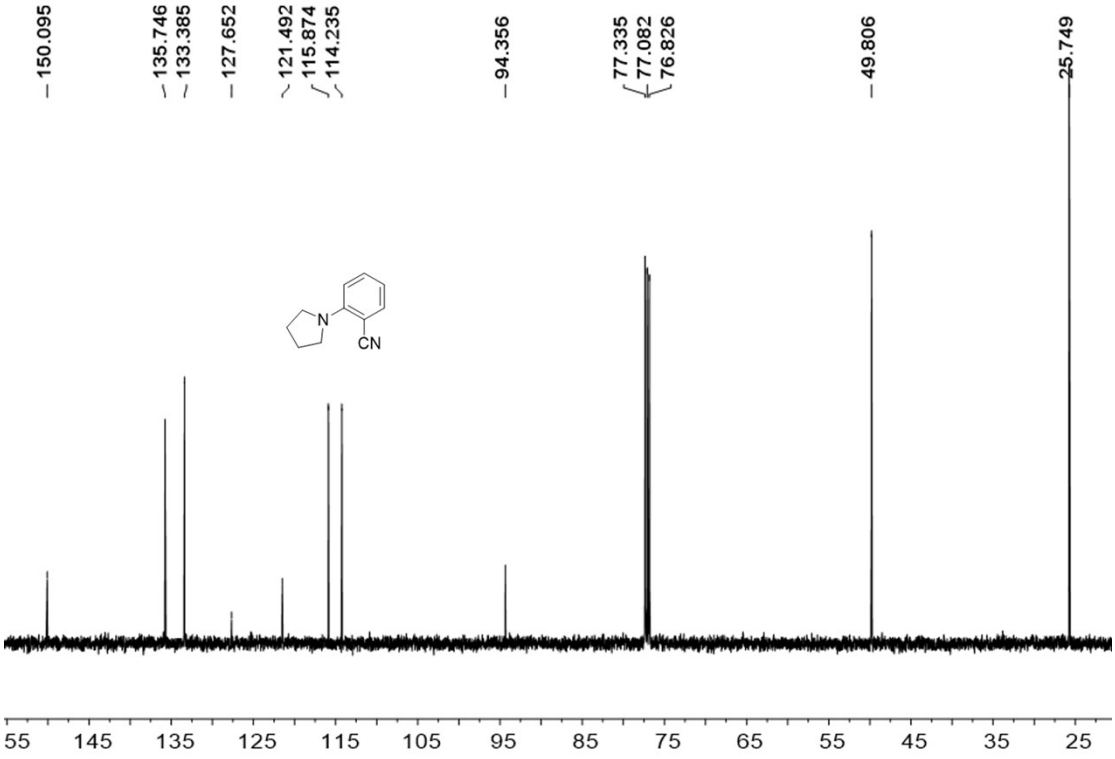


**$^{1}$H NMR of 8fa**

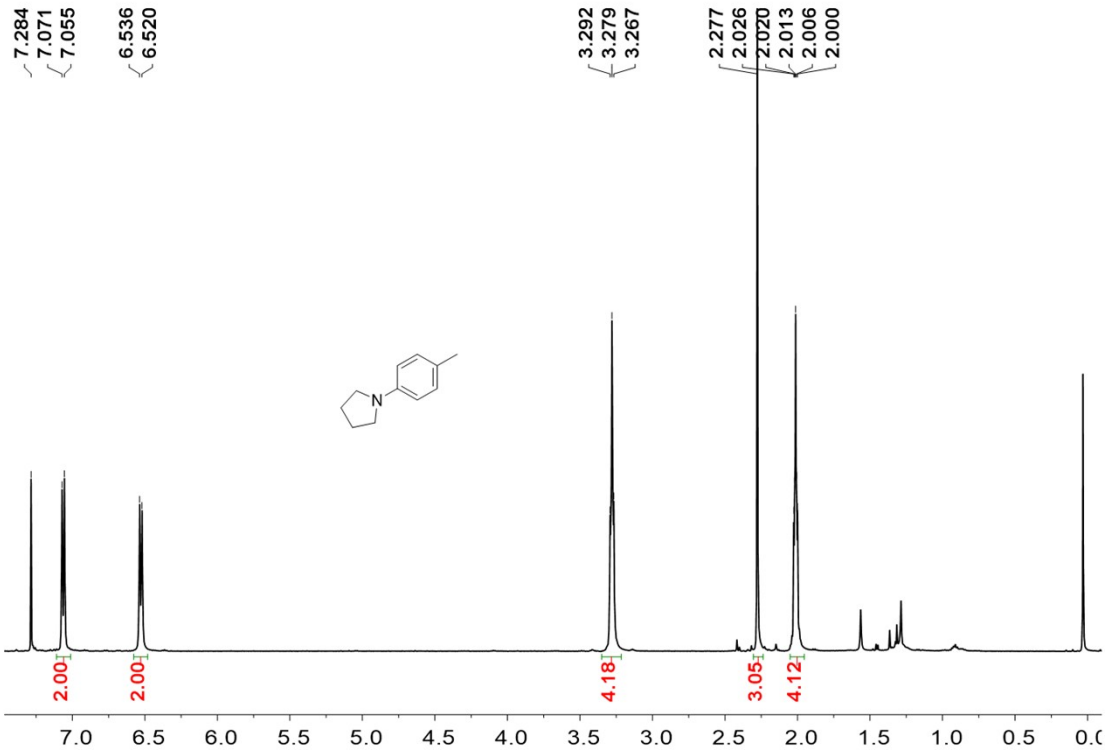

**$^{1}$H NMR of 8ga**

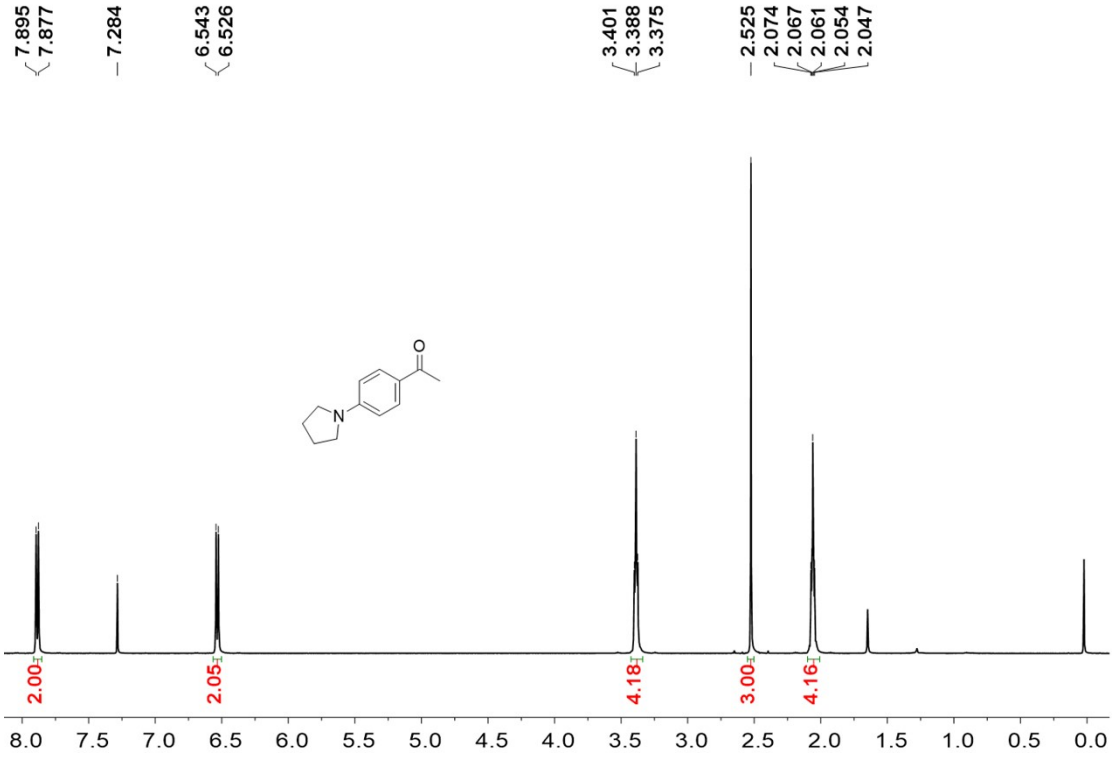
7.895
7.877
7.284
6.543
6.526
3.401
3.388
3.375
2.525
2.074
2.067
2.061
2.054
2.047
O
N
2.00
2.05
4.18
3.00
4.16
8.0
7.5
7.0
6.5
6.0
5.5
5.0
4.5
4.0
3.5
3.0
2.5
2.0
1.5
1.0
0.5
0.0

**$^{1}$H NMR of 8ha**

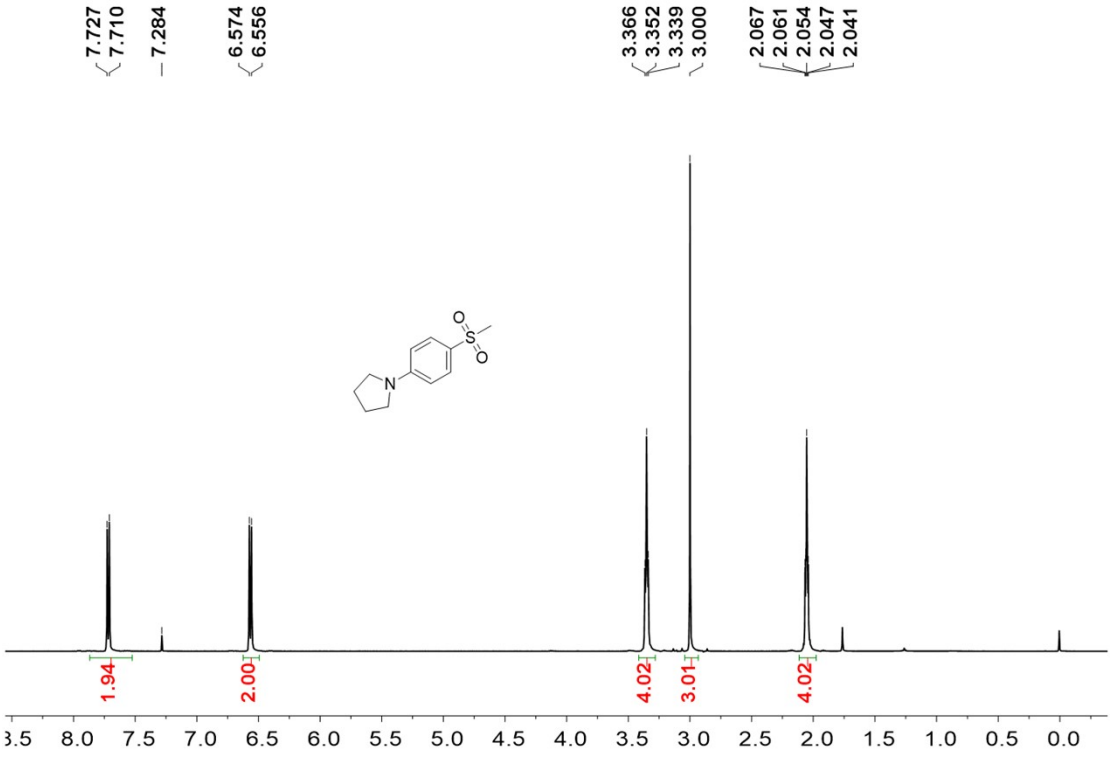


**$^{13}$C NMR of 8ha**

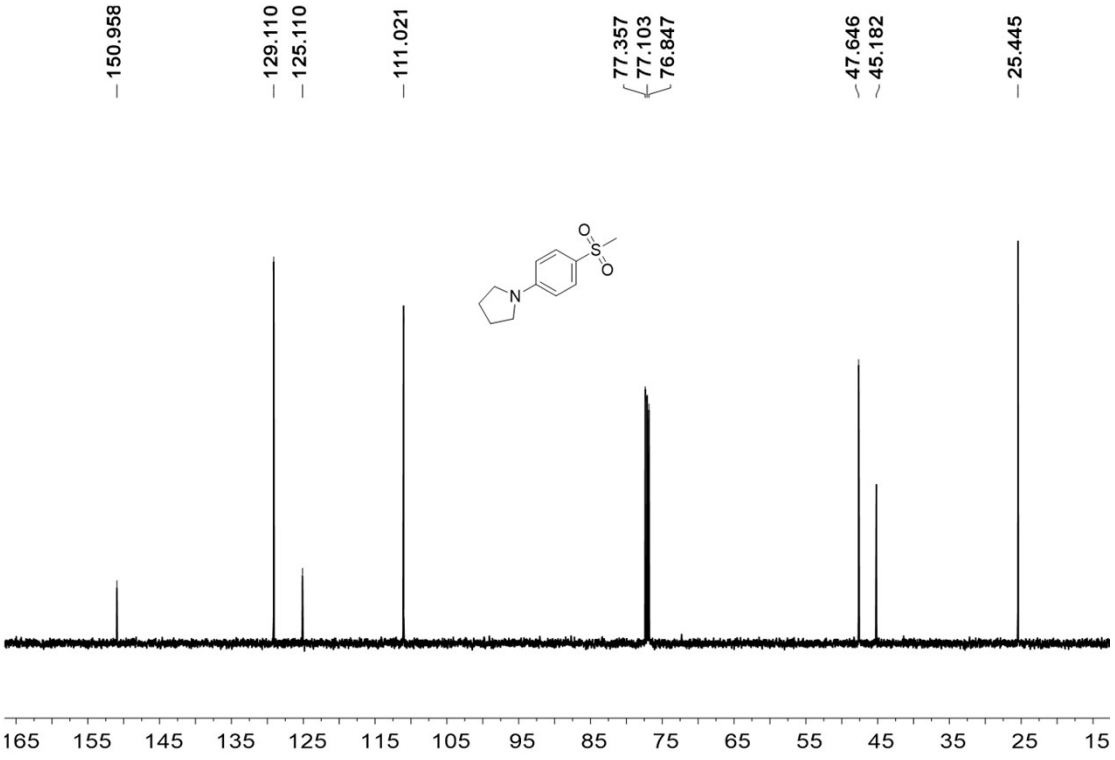

**$^1$H NMR of 8ia**

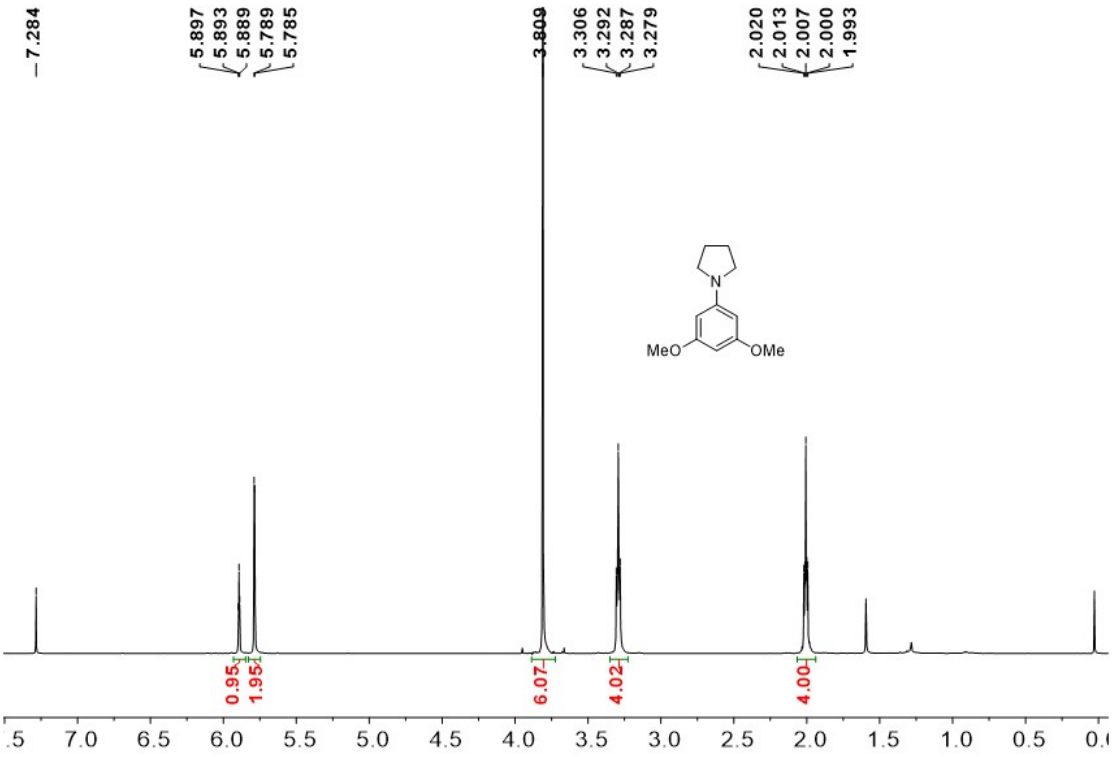


**$^1$H NMR of 8ja**

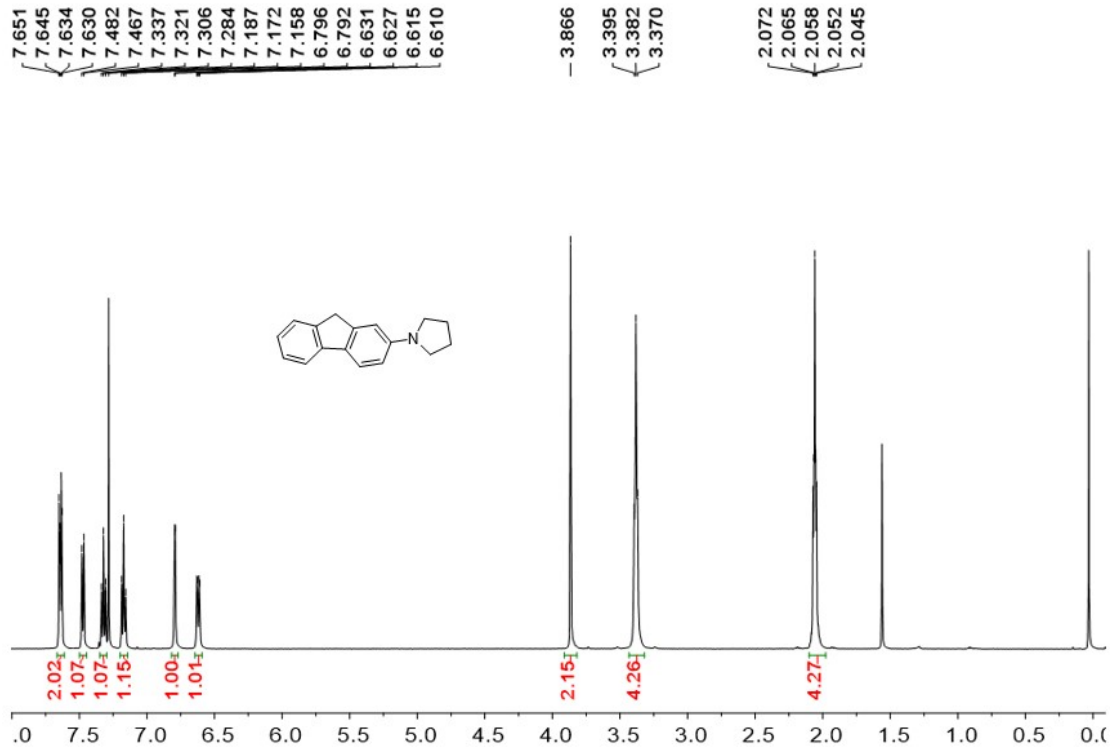

**$^{13}$C NMR of 8ja**

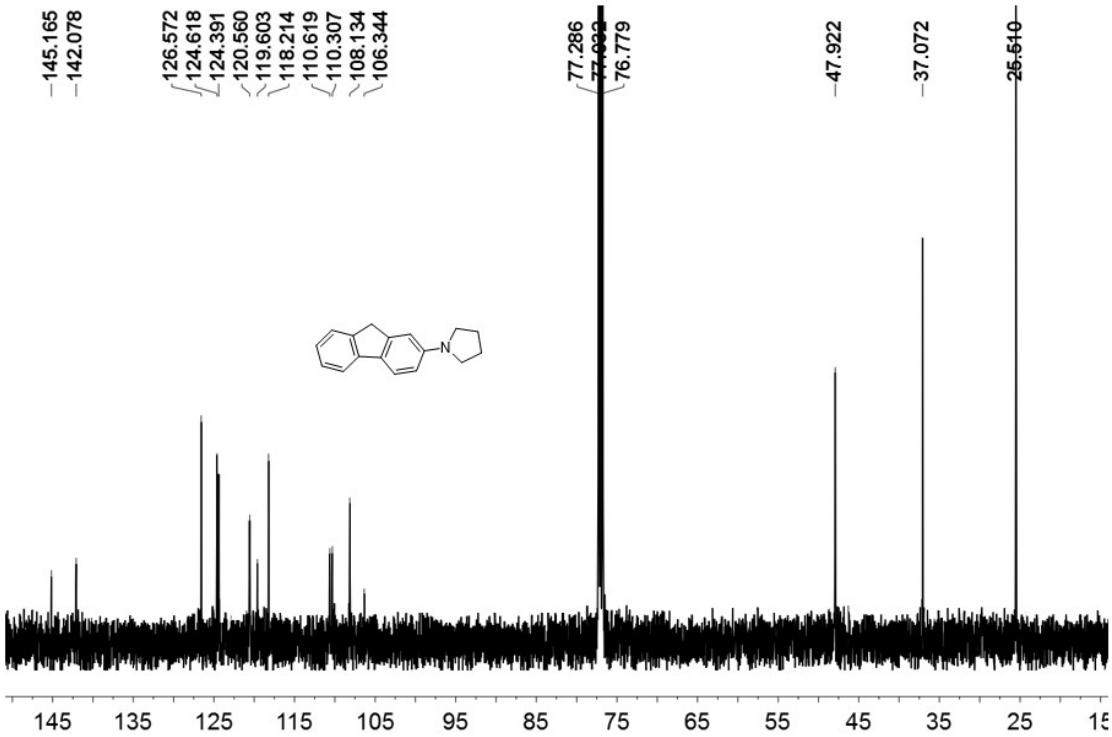


**$^{1}$H NMR of 8ka**

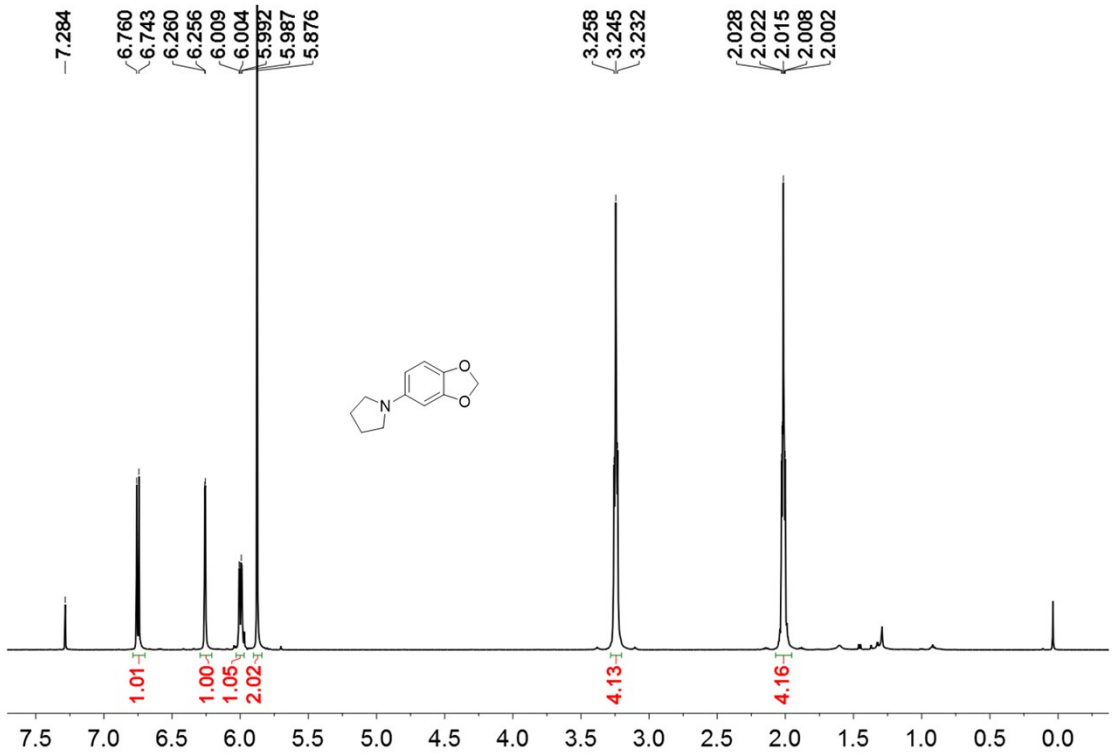

**$^{13}$C NMR of 8ka**

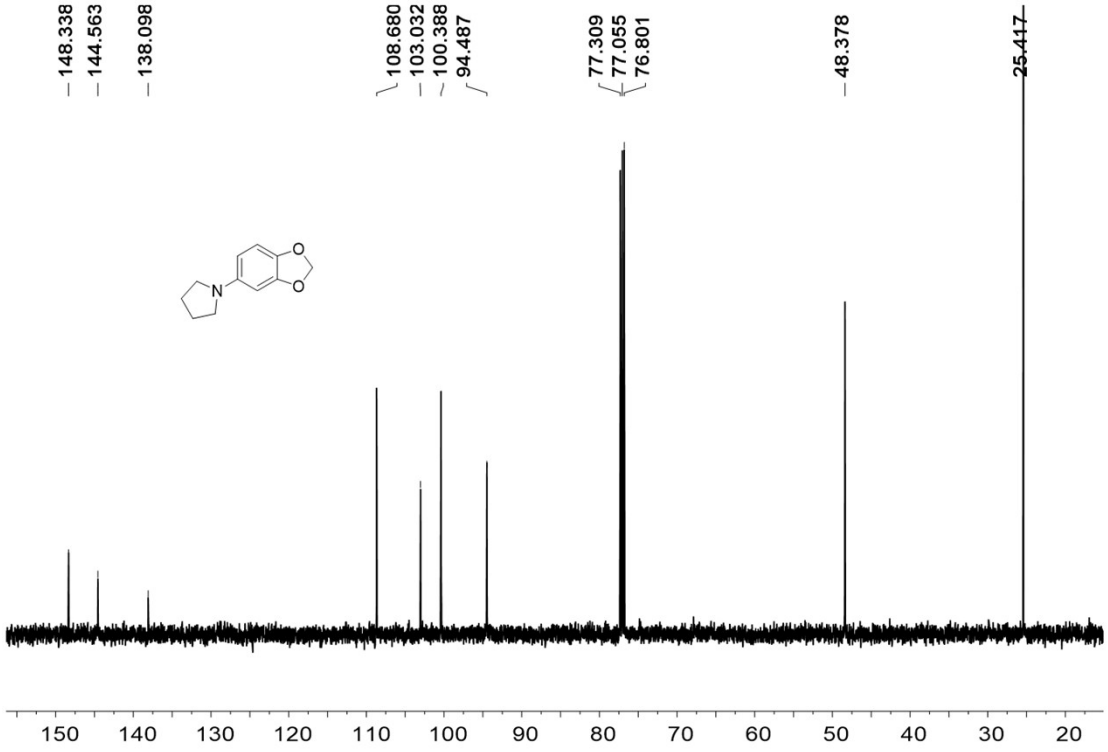


**$^{1}$H NMR of 8la**

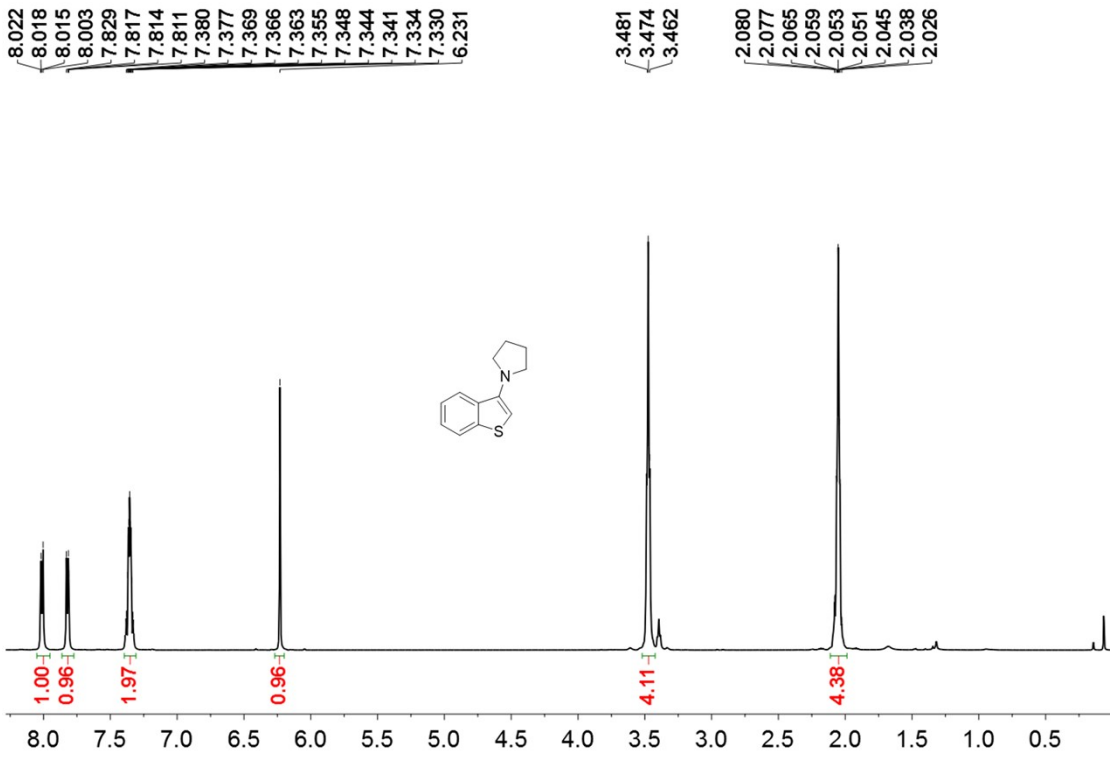

**$^{13}$C NMR of 8la**

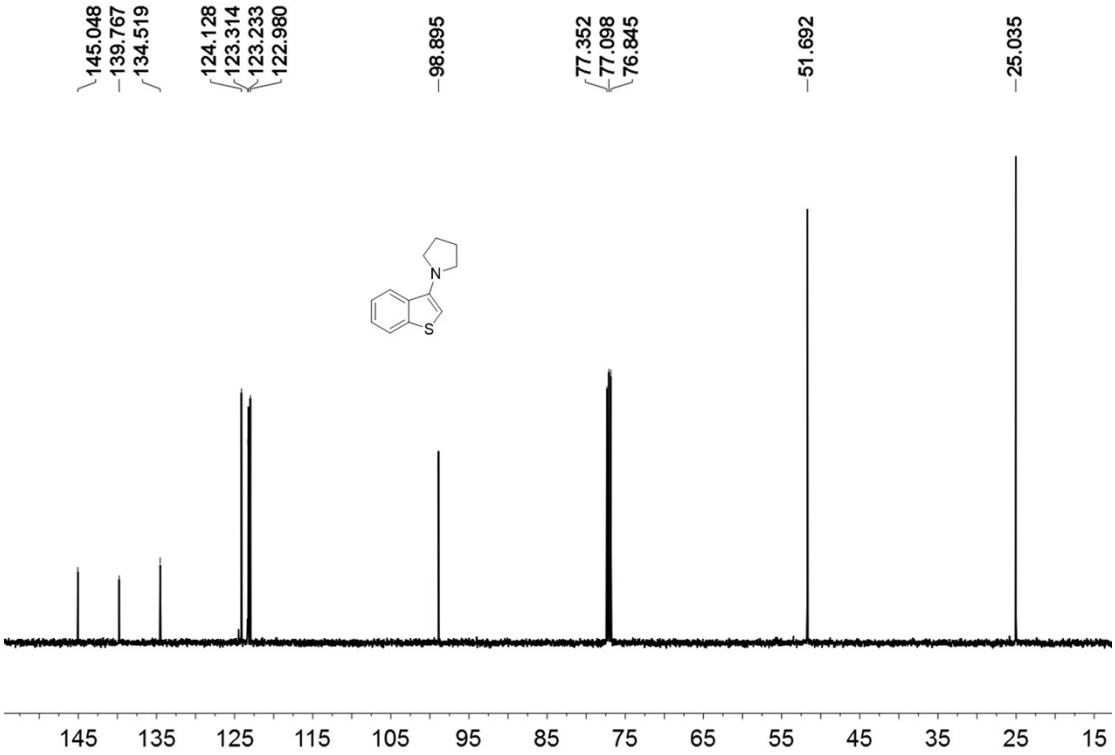


**$^{1}$H NMR of 8ma**

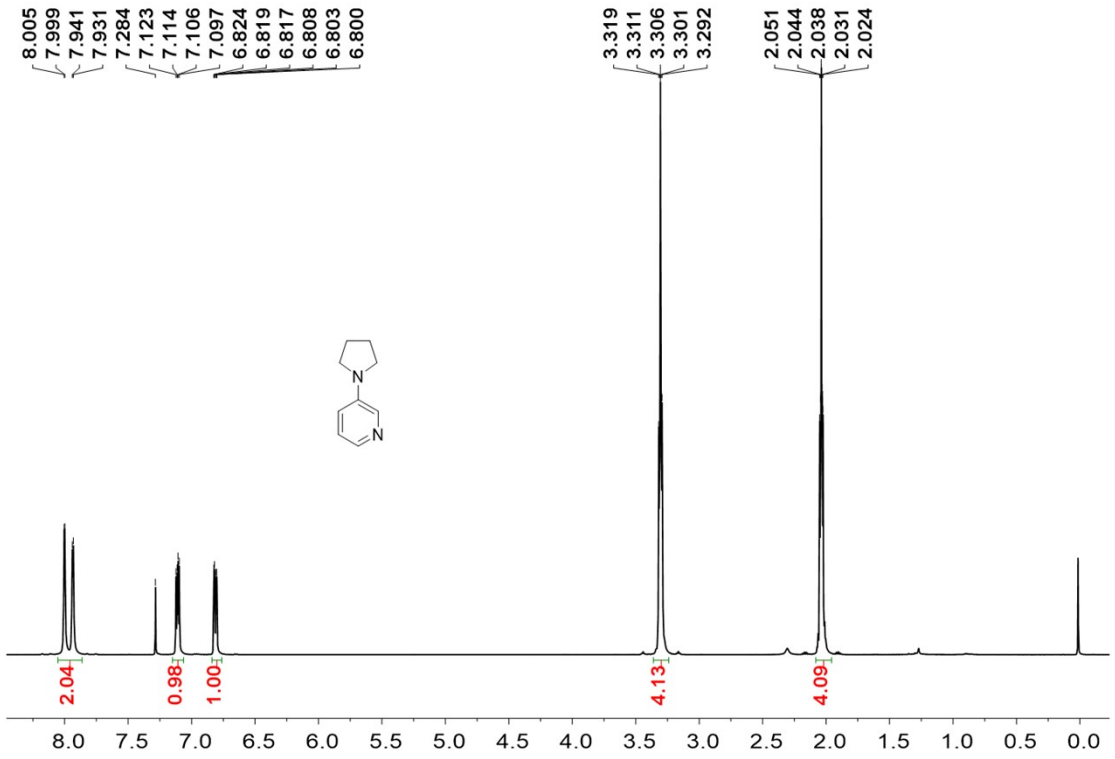

**$^1$H NMR of 8na**

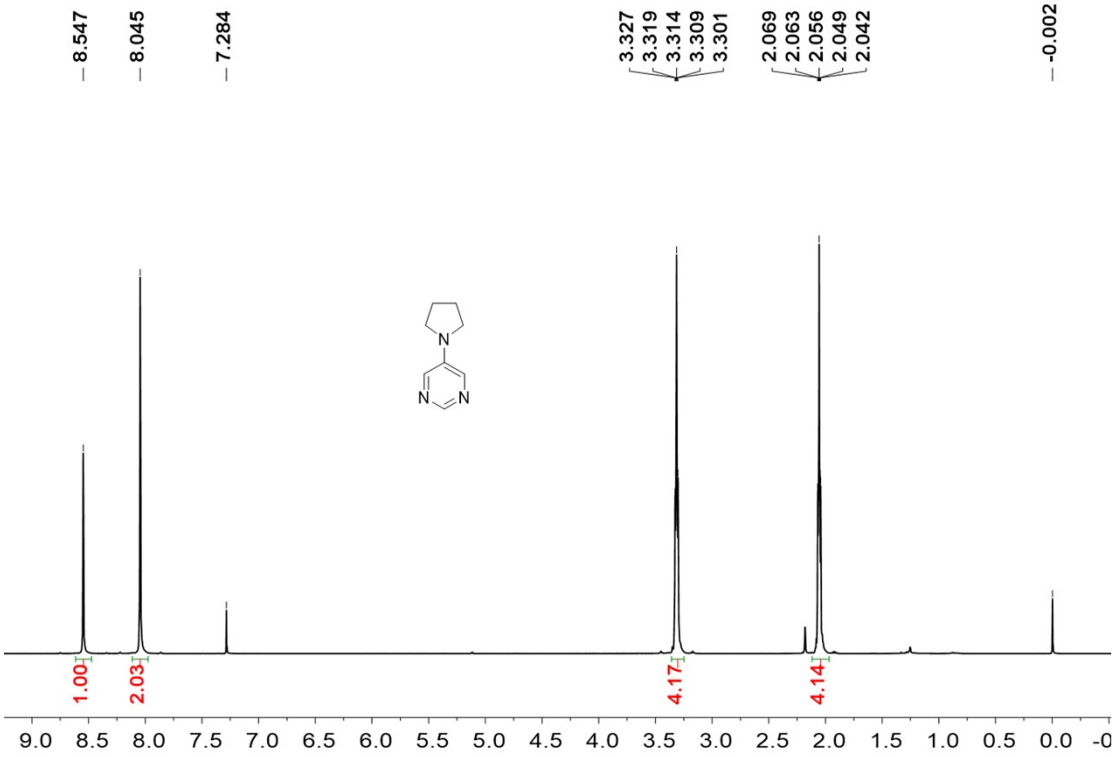


**$^1$H NMR of 8of**

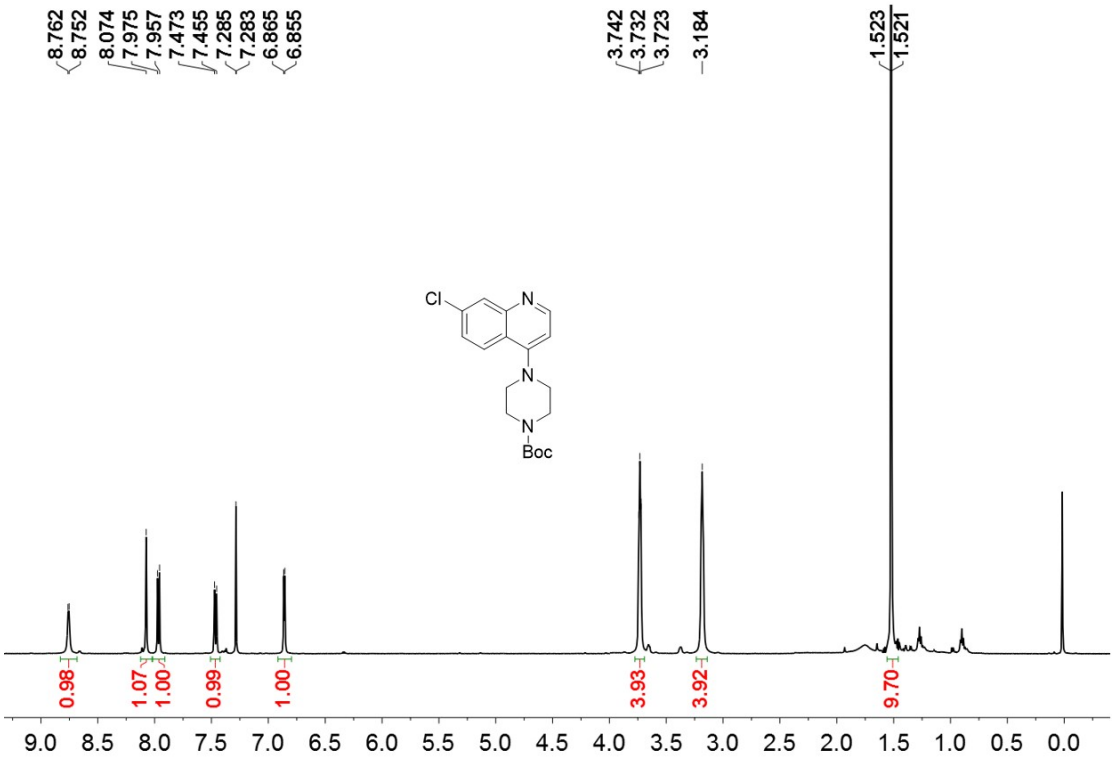

**$^{13}$C NMR of 8of**

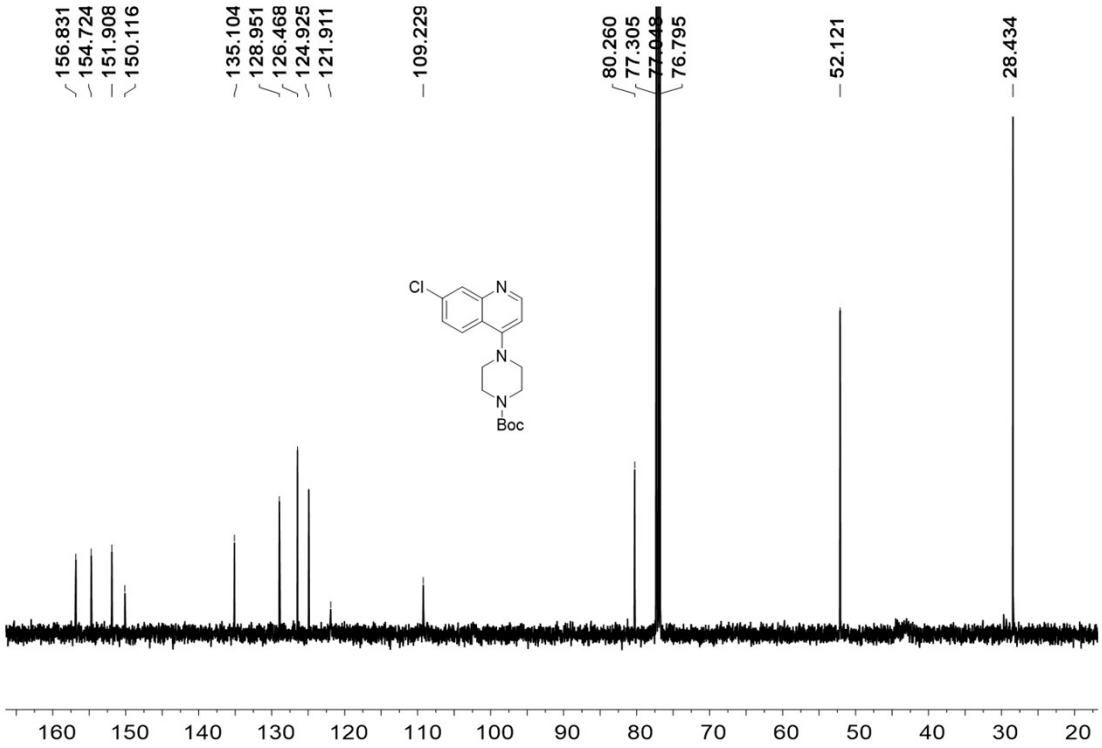

**$^1$H NMR of 10aa**

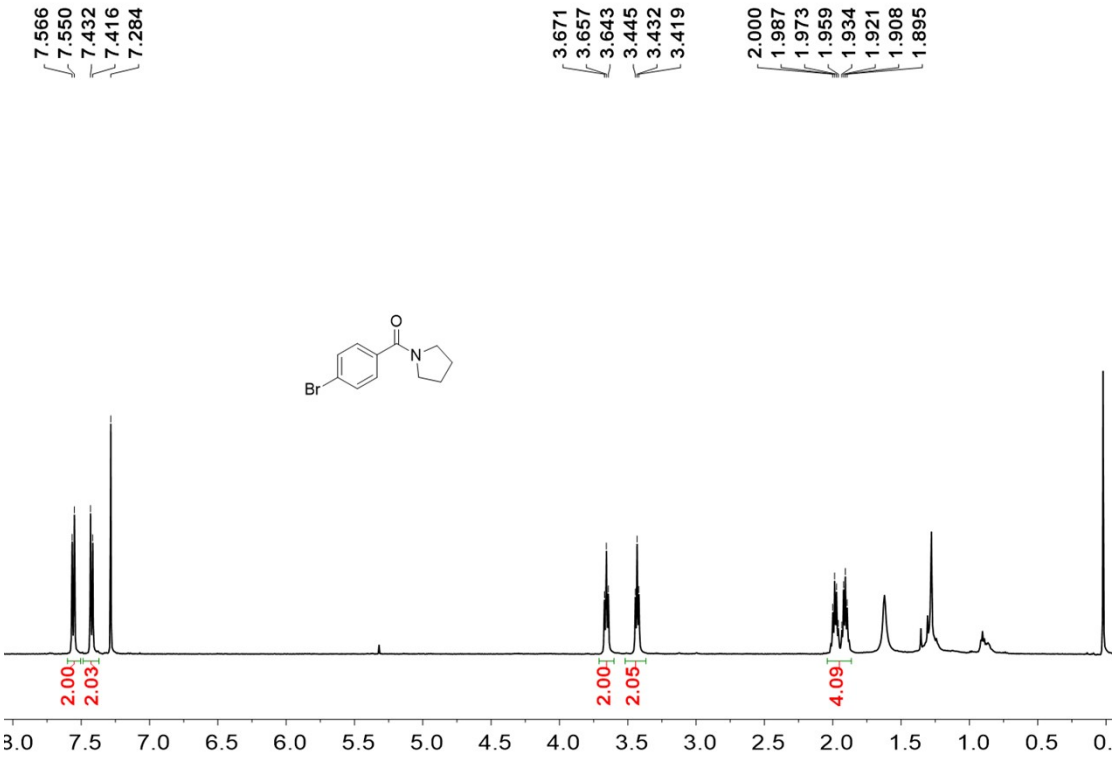


**$^1$H NMR of 10ab**

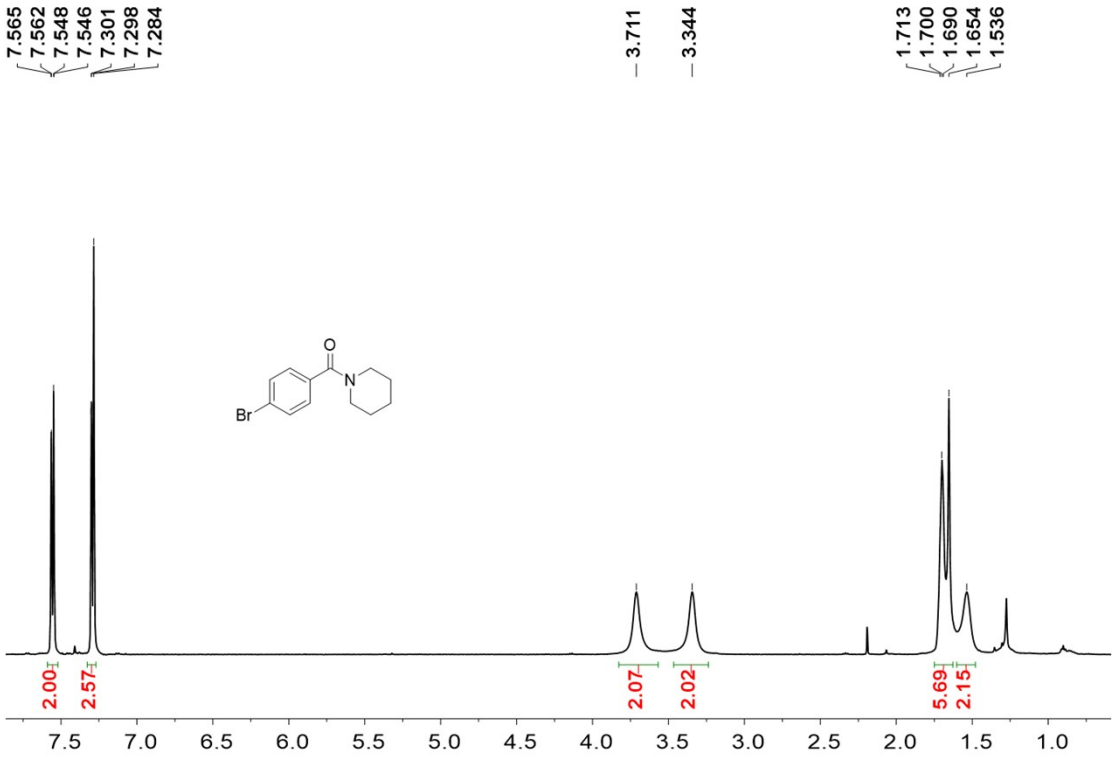

**$^{1}$H NMR of 10ba**

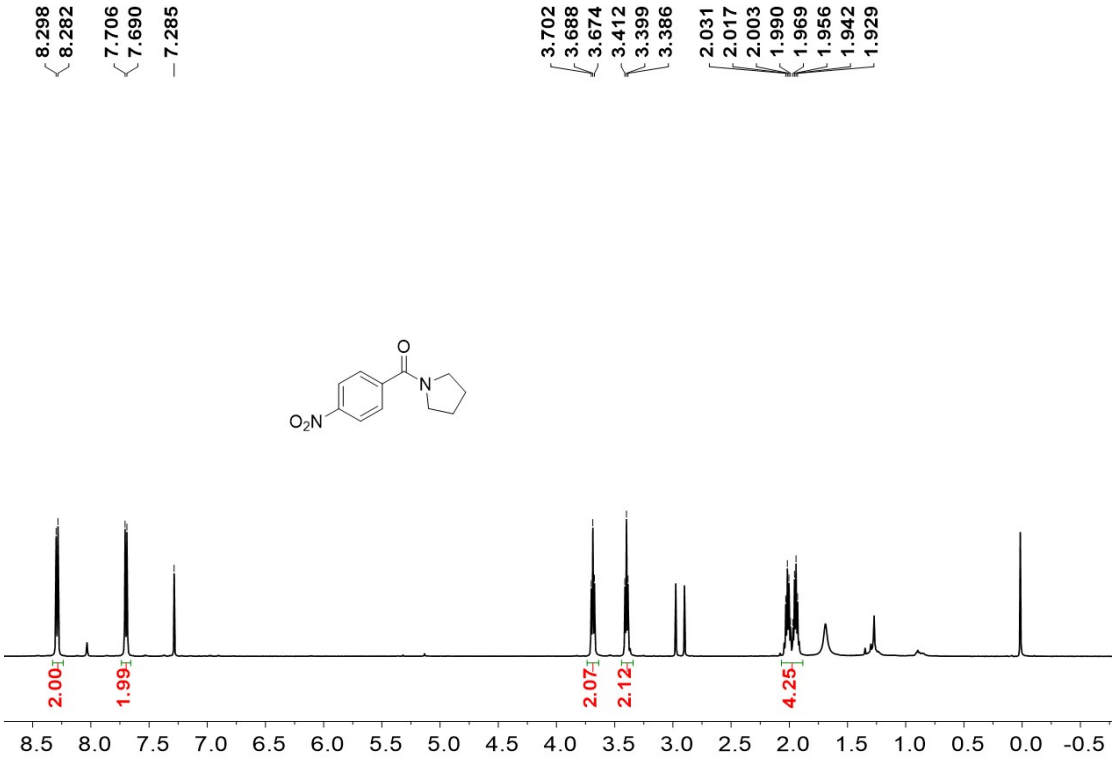


**$^{13}$C NMR of 10ba**

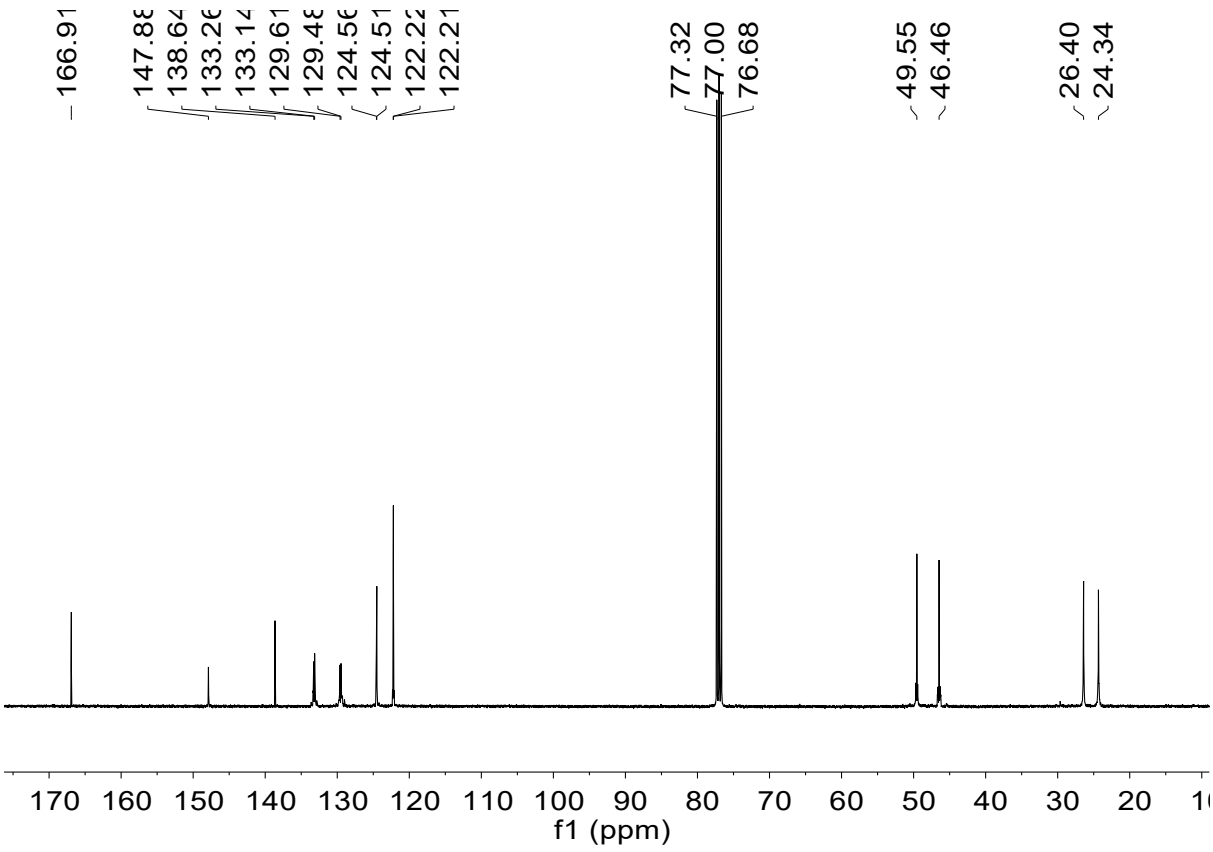

## $^{1}$H NMR of 10ca

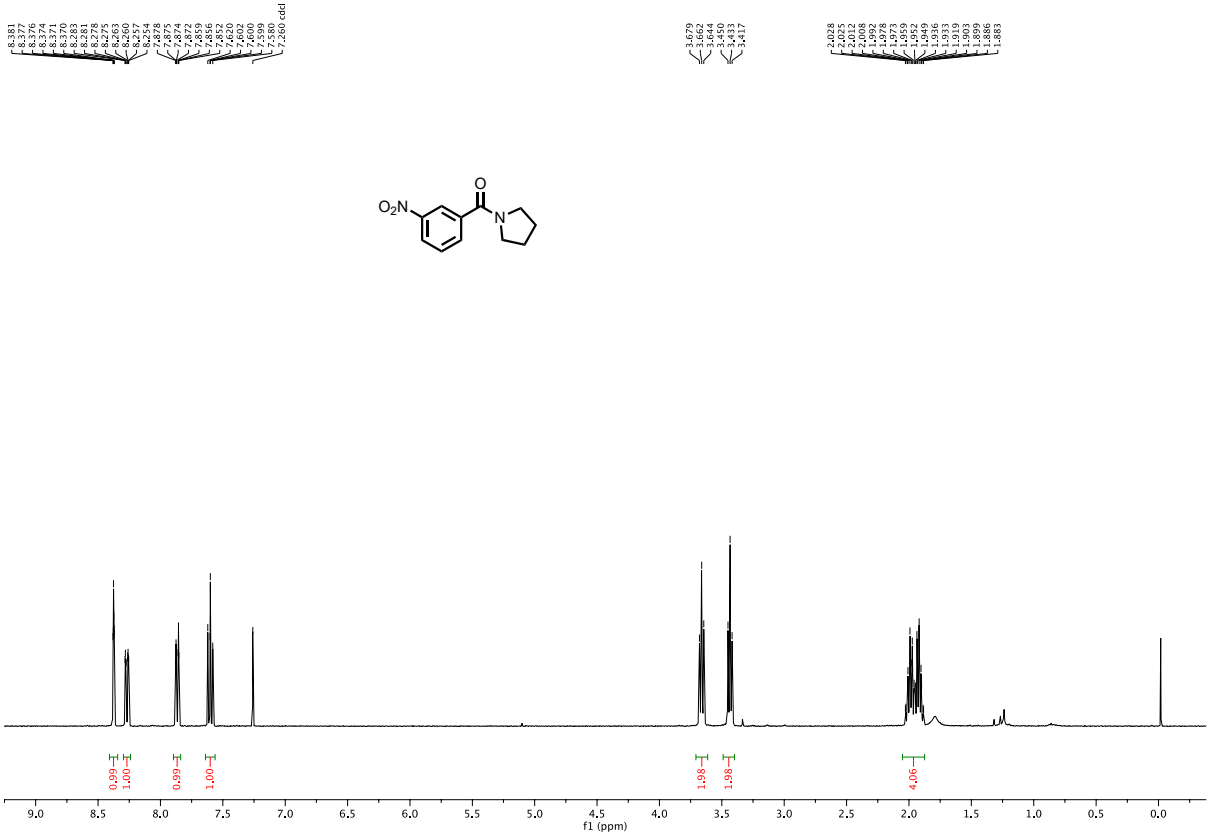


## $^{13}$C NMR of 10ca

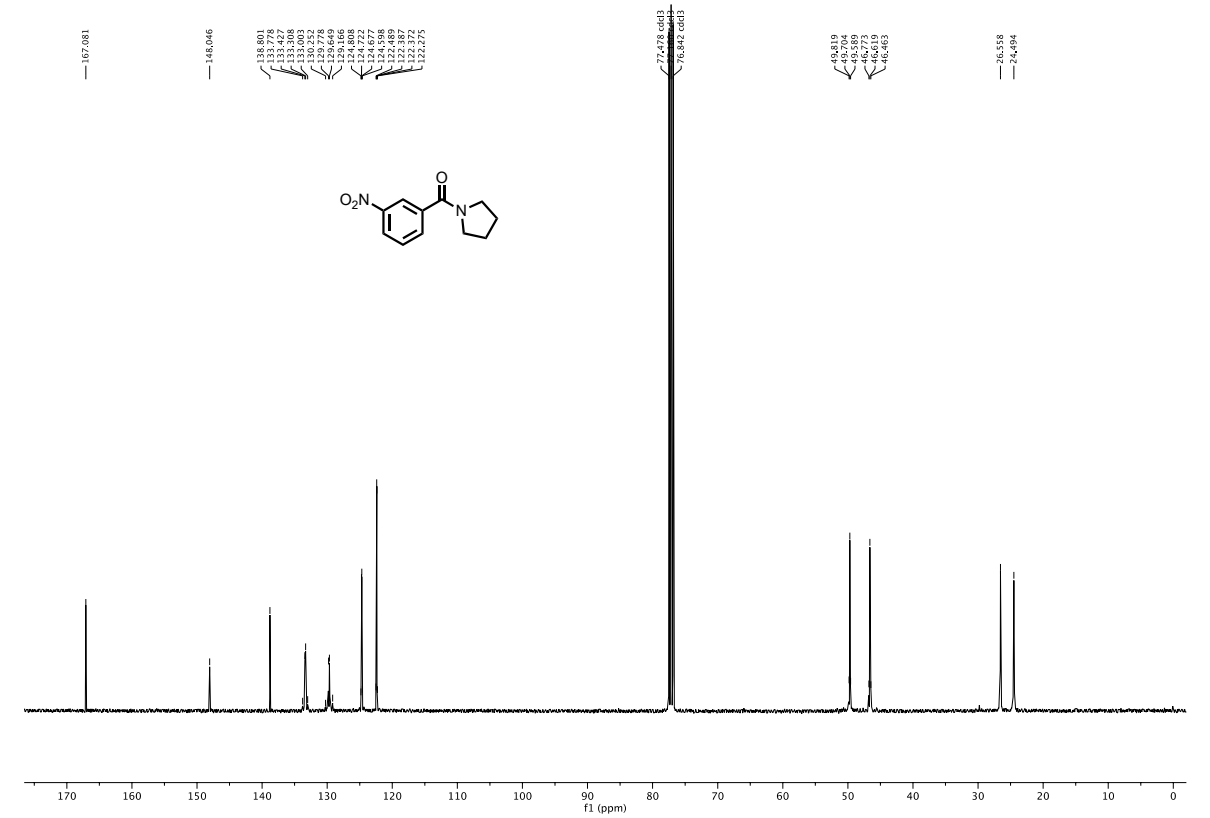

## $^1$H NMR of 10da

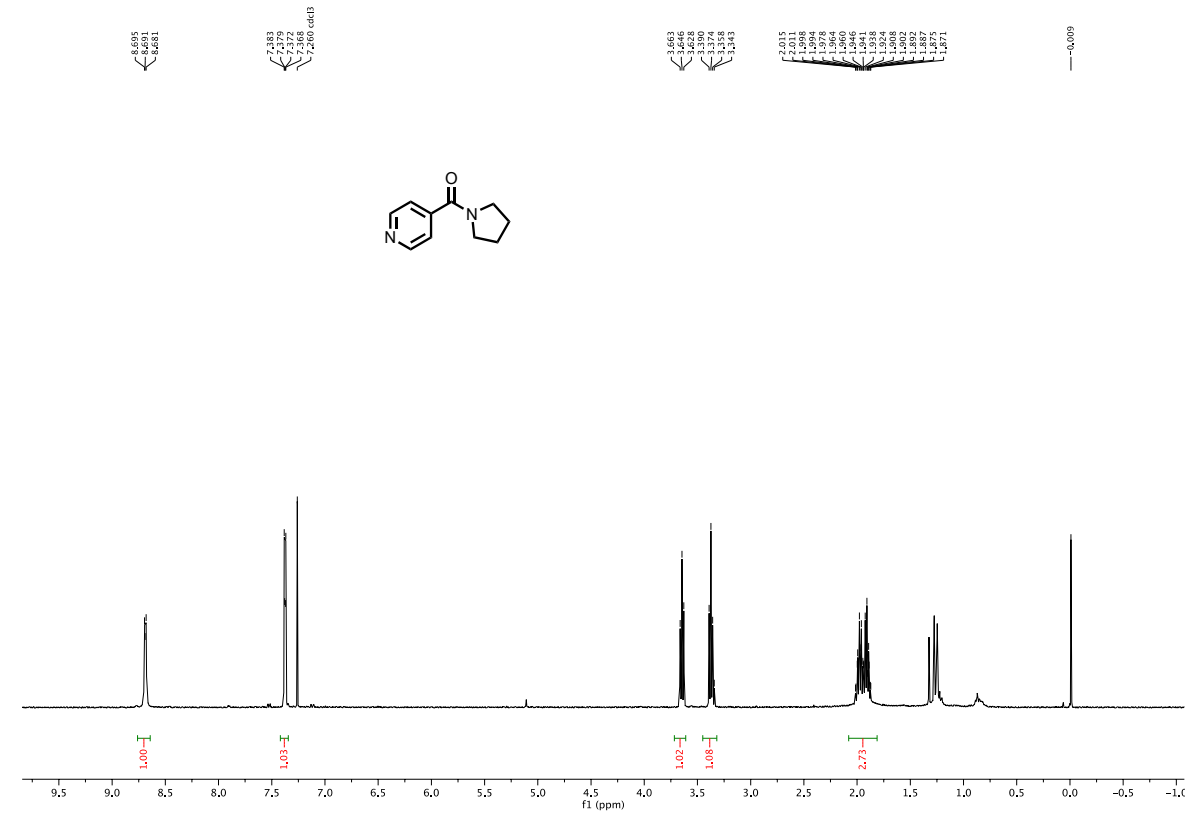


## $^1$H NMR of 10ea

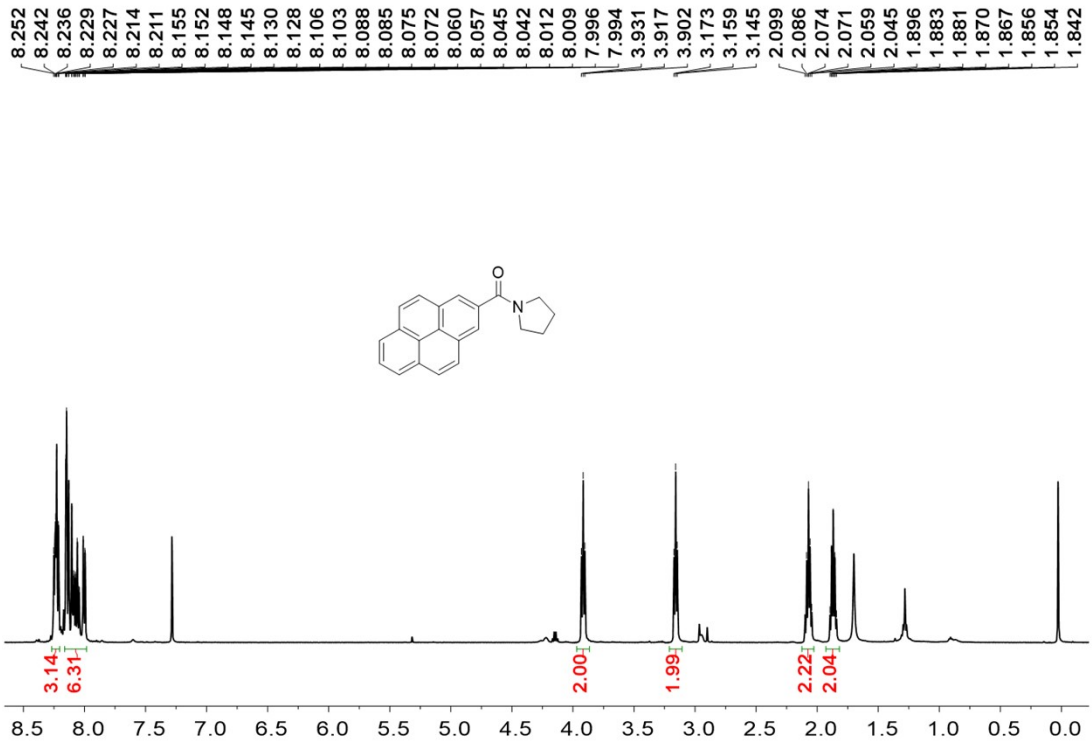

**$^{13}$C NMR of 10ea**

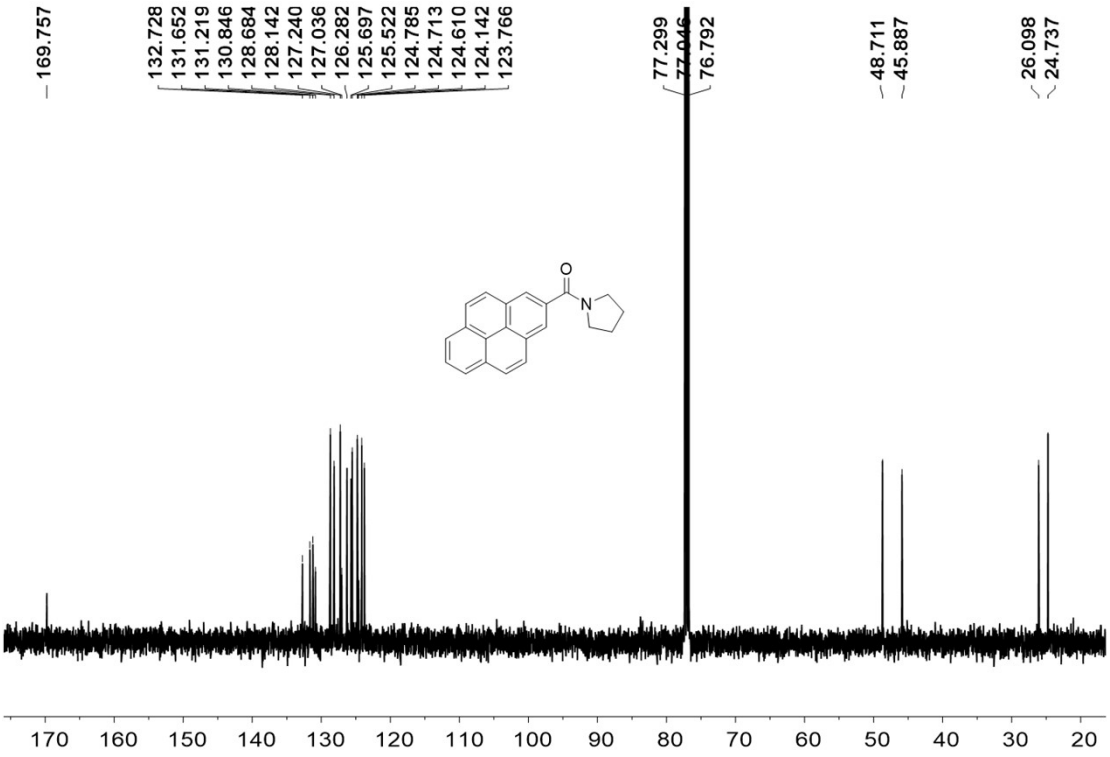


**$^{1}$H NMR of 10fa**

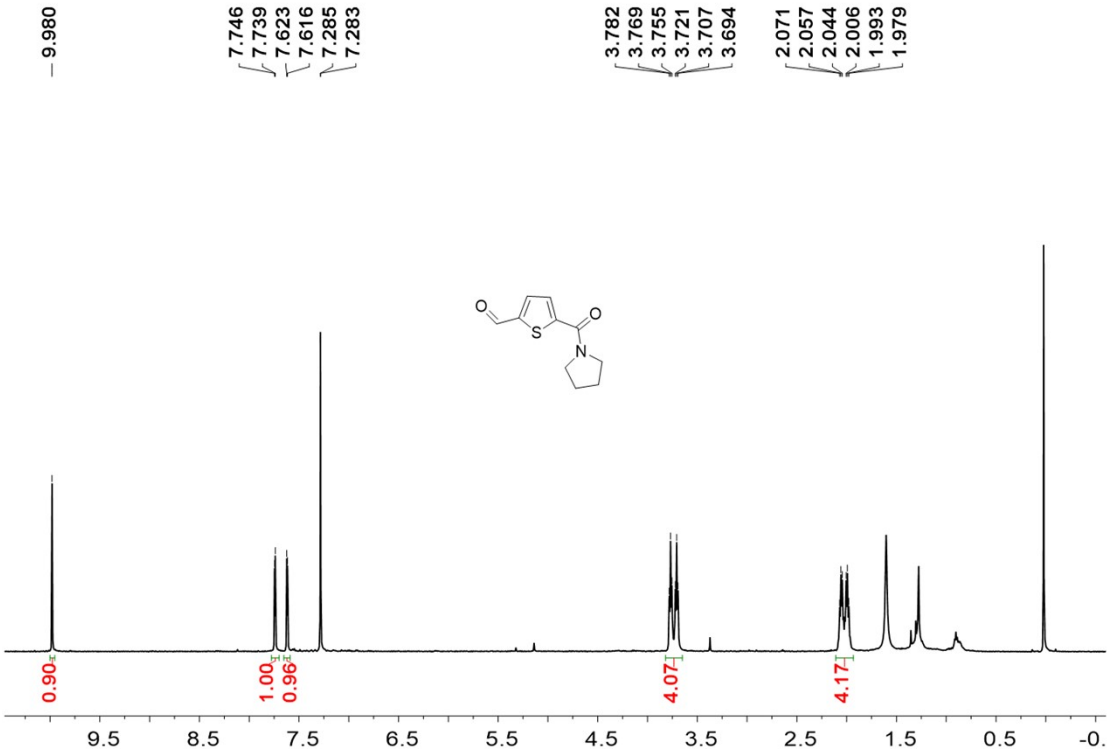

**$^{13}$C NMR of 10fa**

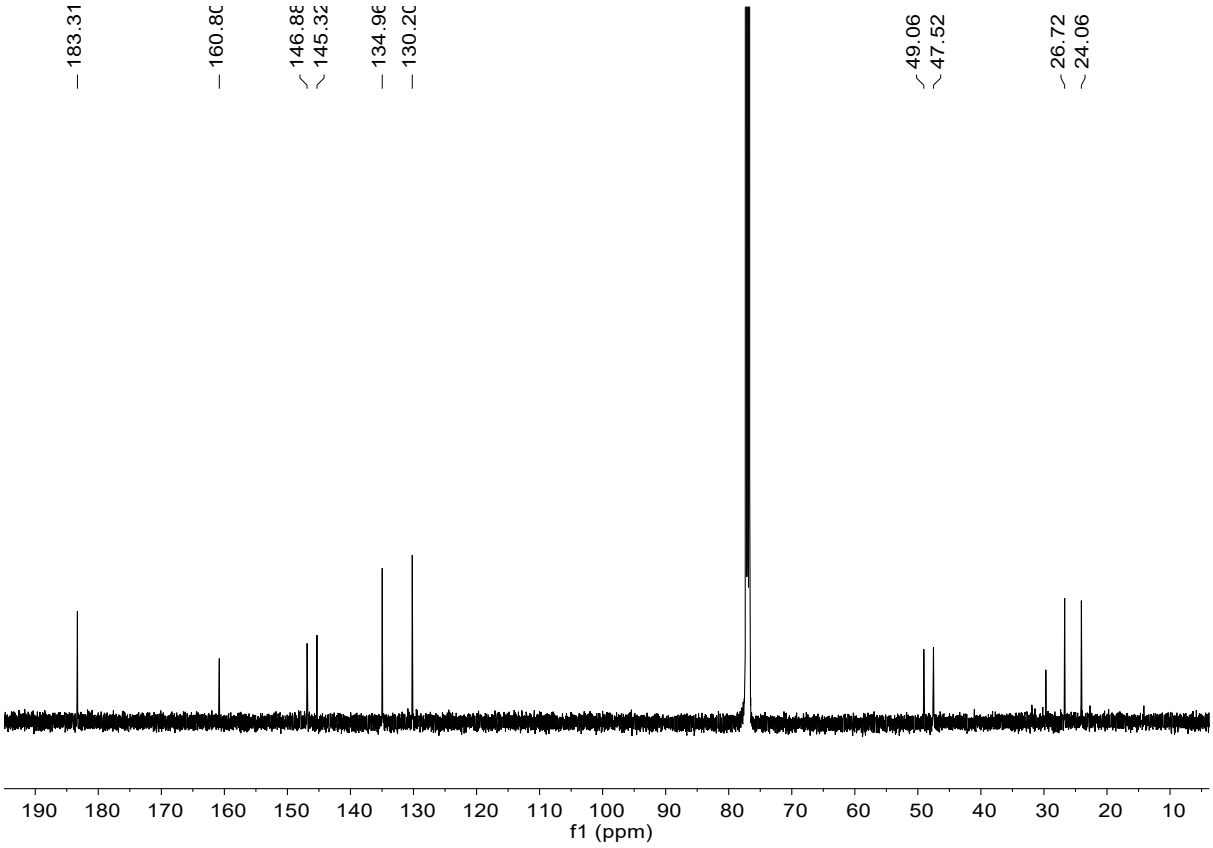


**$^{1}$H NMR of 10faa**

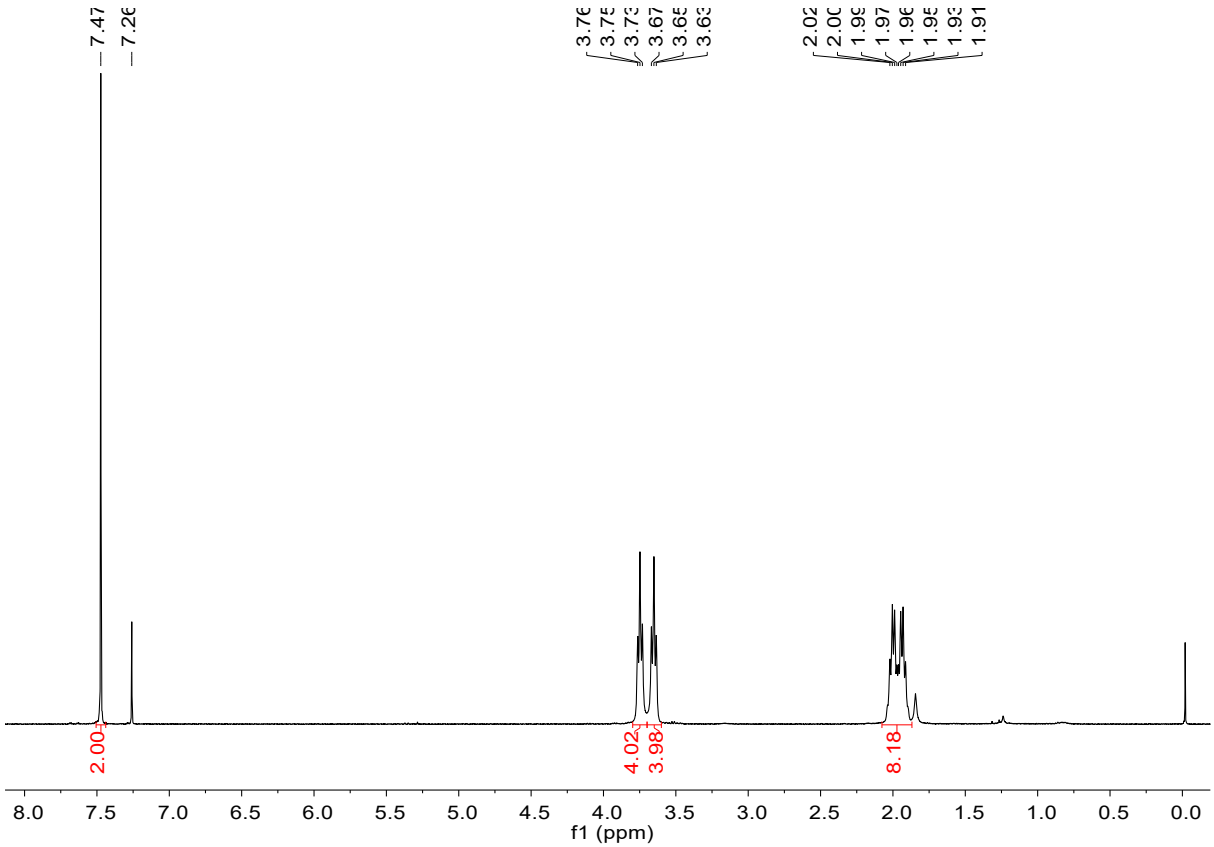


**$^{13}$C NMR of 10ea**